COMPUTATIONAL STUDY OF HISTO-ASPARTIC PROTEASE (HAP) AND ARTEMISININ-QUININE HYBRID-INTERACTION, MECHANISM AND ANTI MALARIAL ACTIVITY

A THESIS

SUBMITTED TO **SAMBALPUR UNIVERSITY**

FOR THE DEGREE OF

DOCTOR OF PHILOSOPHY

IN

SCIENCE

(Bioinformatics)

2012

BY

RAJANI KANTA MAHAPATRA, M.Sc, APGDBI

(Registration No.193/2010/Life. Sc.)

Dedicated

to

My Parents

CERTIFICATE

This is to certify that the thesis entitled as ***"COMPUTATIONAL STUDY OF HISTO-ASPARTIC PROTEASE (HAP) AND ARTEMISININ-QUININE HYBRID-INTERACTION, MECHANISM AND ANTI MALARIAL ACTIVITY"*** *submitted by Rajani Kanta Mahapatra to the School of Life Sciences, Sambalpur University in fulfilment of the requirement for the award of the degree of Doctor of Philosophy in Science (Bioinformatics) is a record of bona fide research work carried out by him under our joint supervision and guidance. The thesis or any part thereof has not formed the basis for the award of any degree or diploma.*

To the best of our knowledge and conviction Mr. Mahapatra holds an excellent conduct and moral character.

Dr. Pradeep Kumar Naik
Co-Supervisor

Prof. Niranjan Behera
Supervisor

DECLARATION

*I, **Mr. Rajani Kanta Mahapatra**, hereby declare that the evaluation embodied in this thesis, **"COMPUTATIONAL STUDY OF HISTO ASPARTIC PROTEASE (HAP) AND ARTEMISININ-QUININE HYBRID-INTERACTION, MECHANISM AND ANTI MALARIAL ACTIVITY"** is the original work carried out by me under the joint supervision of Prof. Niranjan Behera, School of Life Sciences, Sambalpur University, Burla & Dr. Pradeep Kumar Naik, Department of Biotechnology & Bioinformatics, Jaypee University of Information Technology, Wakanghat and that the results or any part of results have not been submitted for any other degree or diploma.*

Date: **(RAJANI KANTA MAHAPATRA)**

Place: Burla.

ACKNOWLEDGEMENT

I would like to express my heartfelt gratitude to all those who have contributed directly or indirectly towards obtaining my doctorate degree. I am highly indebted to my esteemed supervisors, Prof. Niranjan Behera & Dr. Pradeep Kumar Naik who have guided me through thick and thin. Their positive attitude towards research and zest for high quality research work has prompted me for the timely completion of the work. I deem it a privilege to be a scholar doing research under them.

Also I feel indebted to Prof.D.C.Warhurst (Emeritus Professor, University of London), Prof.John Åqvist (University of Uppsala), Dr. Hugo Gutiérrez de Teran (University of Santiago de Compostela), Dr. Huogen Xiao, Research Associate (University of Guelph), Dr. A. Bell (Trinity College, Dublin) who have helped me by providing their expert opinion with invaluable suggestions for accomplishment of the PhD thesis.

Sincere thanks to Dr. Mrutyunjay Suar, Director of School of Biotechnology in KIIT University, Bhubaneswar for his encouragement and support during the course of study.

I shall remain ever grateful to Mr. R.Raghu, Schrödinger Inc. for providing trial license software for preparation of the thesis work. I would personally like to thank Mr.Hege S. Beard, Schrödinger Applications Scientist, Schrödinger Inc. for his technical help during the research work.

Finally, I wish to thank the respondents of my study and all the individuals whose comments, reviews and suggestions have helped my project in developing an informative insight. Lastly, I extend my apologies to anyone I failed to mention.

(RAJANI KANTA MAHAPATRA)

LIST OF TABLES

CHAPTER-4

CHAPTER-5

LIST OF FIGURES

ABBREVIATIONS

DHQ = Dihydroartemisinin

ACTs= Artemisinin based combination therapy.

CQ= Chloroquine

CHAPS=3-[(3-cholamidopropyl) dimethylammonio]-1-propanesulfonate

HAP= Histo-aspartic Protease

FePPIX= Ferriprotoporphyrin-IX

MDR= Multi Drug Resistant

$\mathbf{G}_{\mathbf{score}}$ = Relative docking score

$\mathbf{\Delta\Delta G}_{\mathbf{bind\text{-}cald}}$ =Calculated relative binding energy

BHIA= β-haematin inhibitory assay

Pf = *Plasmodium falciparum*

PMs= Plasmepsins

CONTENTS

Chapter-1

Introduction

1.1 Preamble

Malaria is undisputedly a disease of poverty. The most severe form of malaria is caused by blood borne malaria parasite *Plasmodium falciparum* as cerebral malaria with fever, multi-organs failure, coma and death may ensure in 72 hours; if the disease is not properly diagnosed and treated by rapid effective antimalaria drug. For several decades the gold standard for treatment of malaria was chloroquine (CQ), a 4-aminoquinoline since 1940. However, the continuous use of CQ as monotherapy, it was reported that CQ resistance strains of *P. falciparum* have developed and rendering this drug increasing ineffective. Inspite of the prevalence of CQ resistant *P. falciparum*, the drug continued to be widely used in India and other countries of the world. The combination drug treatment practices are now-a-days, common in treating many infectious diseases. A combination therapy of a new class of antimalaria drug, artemisinin-quinine hybrid compound is reported to be highly effective against cultured, asynchronous, blood-stage *P. falciparum* strains 3D7 and FcB1.

1.2 Epidemiology of malaria

Despite intensive international efforts, malaria still affects 5% of world population [Liwang *et al.*, 2009]. Every year about 12 lakhs people all over world died from this infectious disease. The severity of malaria in India in compare to other tropical countries is more and about 55% of reported cases are from India. Children are most affected and victims of death [WHO, 2011].

A major factor that severely hinders to 'roll-back malaria' is the emergence and spread of parasite resistant to affordable antimalarial agents. The situation is particularly grave in south-east Asia, where the prevalence of multidrug resistant (MDR) parasites has become the great challenge for management of malaria [Olliaro *et al.*, 2005], leading to major changes in the treatment policy of the WHO [Bosman *et al.*, 2007].As a result, WHO sponsored campaign for prevention and more effective treatment, however the disease is not been controlled. The disease is estimated to be responsible for an average annual reduction of 1.3% in economic growth for countries with the heaviest malaria burden [Sachs *et al.*, 2002].

1.3The cause of the disease

Malaria results from the infection caused by four species of the protozoan parasite *i.e. Plasmodium falciparum, Plasmodium vivax, Plasmodium ovale* and *Plasmodium malariae*. The life cycle of *Plasmodium* parasite is complex and requires two different hosts, a vertebrate host (man) and an invertebrate host, the female *Anopheles* mosquito (vector) [White *et al.*, 1999].The infection may be acquired wherever there are human host carrying the parasites and sufficiency of suitable female anopheles mosquitoes together with condition of temperature and humidity which favour the development of the parasite in the mosquitoes. So malaria bears the list of mosquitoes borne disease.

While four *Plasmodium* species commonly infect humans, the two that causes most morbidity and mortality are *Plasmodium falciparum* and *Plasmodium vivax*. Besides, *P. malariae* is the cause of most deaths, which occurs mainly in children and pregnant woman in sub-Saharan Africa. So *P. falciparum* is selected as the main target of drug intervention with the following special features [Dame *et al.,* 2003]

1. *P. falciparum* digests up to 80% of host cell haemoglobin during the erythrocytes phase of its asexual life cycle consuming ~10 g of haemoglobin per day.
2. Malaria death is high and almost all malaria death is due to *P. falciparum* with cerebral malaria.
3. *P. falciparum* is most prevailing parasite in tropical country in compare to the other three species.
4. The appearance of drug resisistance mutation in *P. falciparum* is high in compare to other species.
5. Four plasmepsins resided at a time in digestive vacuole of *P.falciparum* but departure in number of plasmepsins are noticed in other three species.
6. *P.falciparum* HAP is the most divergent vacuolar plasmepsin with no counterpart with other characterized species of *Plasmodium*.

1.4 Pathogenesis

Life cycle of *Plasmodium* is completed with two hosts, human serve as the primary host and mosquito, a secondary host (Fig.1.1). The life cycle of *Plasmodium* can be divided into four phases.

1.4.1 Exo-erythrocytic cycle

1.4.2 Eryhrocytic cycle

1.4.3 Post eryhrocytic cycle

1.4.4 Sexual reproduction

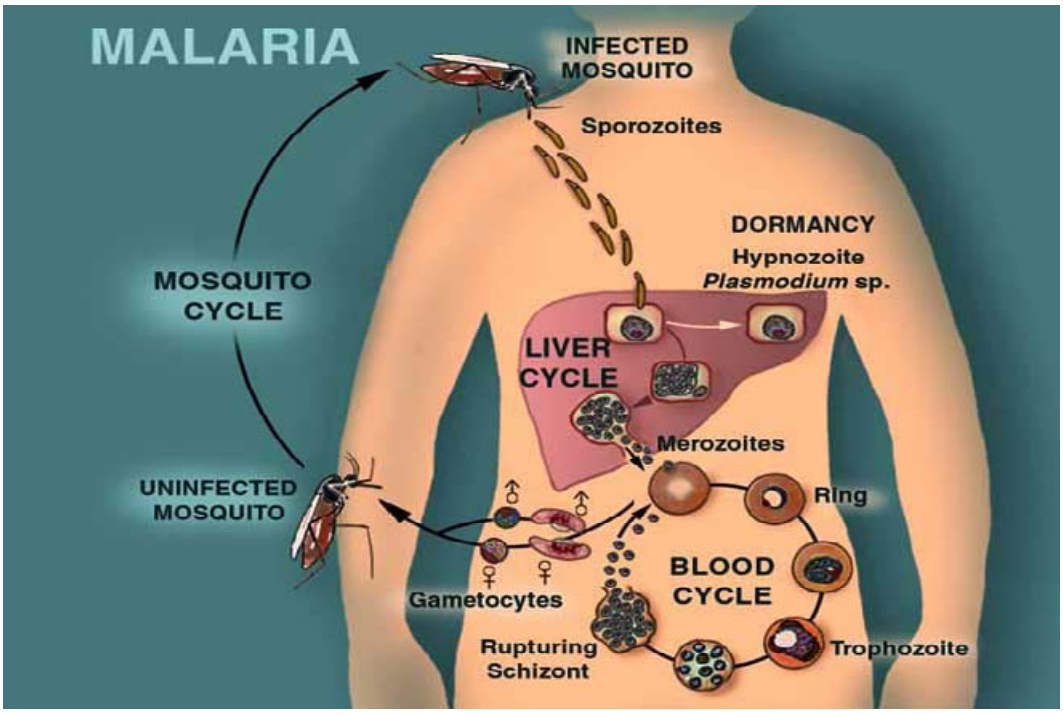

Fig1.1. Life Cycle of *Plasmodium falciparum* in two hosts

1.4.1 Exo-erythrocytic cycle

The cycle in man begins with the bite of a female *Anopheles* mosquito harbouring sporozoites in its salivary gland during its blood meal. The sporozoites travel through the punctured skin into the blood stream. The sporozoites in the blood stream travel to the liver and invade hepatocytes within 30 minutes of being released by the mosquito. In the liver cells they reside for 9-16 days and then start multiplying

asexually within the cells. Asexual reproduction (exoerythrocytic schizogony) in the liver releases thousands of merozoites, which are the first stage of the 48-hour asexual reproduction cycle in the red blood cells (eryhrocytic schizogony).

1.4.2 Erythrocytic cycle

The merozoites that enter the R.B.C are called metacryptozoites. Inside the R.B.C each becomes rounded and then starts grow in size. They absorb food by surface of the body. It enters a corpuscles and non contractile vacuoles developed in his body which give it a ring like appearance. As a result of further growth the vacuoles disappears and pseudopodia extend and ingest the cytoplasm laden with haemoglobin. The haemoglobin is break down into its protein component and haematin. The protein portion is used as food, while the haematin form a pigment known as haemozoin. It further grows to spherical shape and occupies almost entire corpuscle. After this it is ready for sexual reproduction. Its reproduction is called eryhrocytic schizogony and it takes place by multiple fission. The nucleus divides repeatedly till there are 12-24 nuclei. In this way a small oval cell known as micromerozoite is formed. The outer wall of the corpuscles now burst and a number of micromerozoites escape into the plasma. Each merozoite now enters a fresh and healthy RBC and the above is repeated [Bannister *et al.,* 2000]. The erythrocytic schizogony is the time when the human host suffers periodic cycles of clinical symptoms like fever and chills due to toxic effect of haemozoin granules

1.4.3 Post-eryhrocytic schizogony

The erythrocyte merozoites may again go from the blood stream to the liver cell in order to carry on another cycle of asexual multiplication where these merozoites are released into the blood stream. They cause relapse, often months after the primary attack.

1.4.4 Sexual reproduction

While the merozoites continue invading fresh RBCs and continue asexual reproduction, some of them exit the asexual reproduction cycle and mature to male and female gametocytes by a process known as gametogenesis. Finally they become free

from the corpuscles and float in the blood stream. The further development of the gamete does not take place in human body. When the mosquito sucks the blood from a malaria patient the blood contains gametes, the tropozoites and micomerozoites. In case of female *Anopheles*, a cold-blooded mosquito further development of gametes takes place within the mosquito [Sherman, 1998].

1.5 Clinical feature

The interval from the time of biting by the infected mosquito to the onset of detectable fever varies but is often about a weak or 10 days for *P.falciparum* infection and somewhat longer for the other species. *P.falciparum* infections are more insidious and more dangerous than other forms of malaria. Fever in this variety is prolonged and irregular and does not usually rise to quite so high. A severe haemolytic anaemia develops often with haemolytic jaundice. A patient with falciparum malaria, apparently not seriously ill, may suddenly develop complication which renders his condition grave. Children may die rapidly without any special symptoms [Macleod, 2010].

1.6 The present study

The structural parameter of recombinant HAP enzyme has been determined by X-ray crystallography (Bhaumik *et al.*, 2009). The antimalarial activity of artemisinin-quinine hybrid compound against *P.falciparum* has been studied *in vitro* [Walsh *et al.,* 2007]. With these two plus points; molecular modeling study has been implemented to determine the antimalarial activity of artemisinin-quinine hybrid targeting *P. falciparum* vacuolar plasmepsins. HAP enzyme has been considered as a primary target in this study. Similarly interaction mechanism of artemisinin-quinine hybrid and its structural derivatives has been analyzed with Fe-protoporphyrin-IX as a putative receptor through docking molecular mechanics study. So the project is entitled as **"COMPUTATIONAL STUDY OF HISTO-ASPARTIC PROTEASE (HAP) AND ARTEMISININ-QUININE HYBRID-INTERACTION, MECHANISM AND ANTI MALARIAL ACTIVITY".**

1.7 Selection of antimalaria drug

For the selection of anti malaria drug, following criteria have been taken into consideration.

(a) Malaria is a blood-borne disease and host haemoglobin is degraded by parasite to use as their nutrient in the food vacuole for their survival. So a fast acting blood schizontocide drug against multi drug resistant strain of *P.falciparum* is the prime consideration for selection of anti-malaria activity.

(b) The second aspect is toxicity; two principles should guide the selection of chemotherapeutic drug. Firstly, a chemotherapeutic agent must have a selective affinity for the protoplasmic constituent of the parasite, but not for the tissues of host. Secondly the agent should be selectively toxic to the parasite, but not to the host.

(c) Last but not the least; Malaria is a poor man's disease. Low cost-of-goods for antimalarial drug is the necessity for medical success. The drug should be safe, affordable and can be orally used.

1.8 Quinine

Quinine is first natural antimalaria drug isolated from Cinchona bark in 1820, replaces the crude preparation and continued to be the major antimalaria drug till 1942 [Wallace *et al.*, 1996]. Quinine is a laevorotatory alkaloid. The molecular formula is $C_{20}H_{24}N_2O_2$.The structure of quinine is presented below:

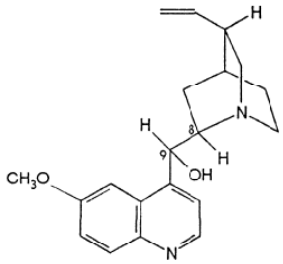

Fig.1.2. Chemical structure of quinine

Quinine is the drug of choice for cerebral malaria. Quinine has rapid schizonticidal action against intraeryhrocytic malaria parasites. It belongs to the aryl amino alcohol group of drugs. It is an extremely basic compound and is, therefore,

always presented as a salt. The dissociation constant pK*a* is 8.58 and the partition coefficient (LogP) value of unionized Quinine is 2.79. Quinine is rapidly absorbed both orally and parenterally, reaching peak concentrations within 1-3 hours [Salako *et al.*, 1998]. It is distributed throughout the body fluids and is highly protein bound, mainly to alpha-1acid glycoprotein. The half-life of quinine ranges between 11-18 hours [White *et al.*, 1983]. Over the years, malaria parasites have developed resistance to a number of commonly used anti-malarial drugs. However the development of resistance to quinine has been slow. Although its use started in the 17th century, resistance to quinine was first reported in 1910 [Peters, 1982]. Findings from a recent systematic review of about 435 clinical trials published between 1966 and 2002 showed that the recrudescence rates for quinine reported over these past 30 years remained roughly constant [Myint *et al.*, 2004].These findings are encouraging and suggest that efficacy of quinine has been preserved.

1.9. Artemisinin

Artemisinin is an oxidant, a natural drug extract of Quinghao named Quinfgaosu, a weed like plant growing over large part of China. It is an endoperoxide a sesquiterpene lactone [Klayman, 1985]. The active principle of this herb called artemisinin ($C_{15}H_{22}O_5$) [Liu JM, 1992]. The compound showed good *in vitro* and *in vivo* antimalarial activity. Several studies showed artemisinin to be an exceptional antimalarial agent with negligible toxicity and high efficacy against human malaria parasites. This also includes that malaria, resistant to conventional antimalarial [Li *et al.*, 1994]. The structure of artemisinin is presented below:

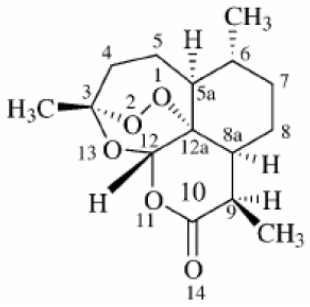

Fig.1.3 Chemical structure of artemisinin

Artemisinin has a peroxide group. The lactone ring has a trans-configuration. It has an unusual 1, 2, 4-trioxane ring, a bridging peroxide group [Lee and Hufford, 1990, Luo and Shen, 1987]. The white needle crystals of artemisinin are hardly soluble in

water or oil therefore formulations other than oral and rectal are not in clinical use. However, since the peroxide bridge is stable under certain chemical reactions, several more soluble artemisinin derivatives, arteether, artemether (oil soluble), sodium artesunate (water soluble) and dihydroartemisinin (DHQ) have been synthesized for the treatment of malaria. DHQ is the first metabolite of artemether, arteether and artesunate. DHQ is the most effective compound of this class [Janse *et al.*, 1994]. Artesunate can be regarded as a pro-drug of DHQ.

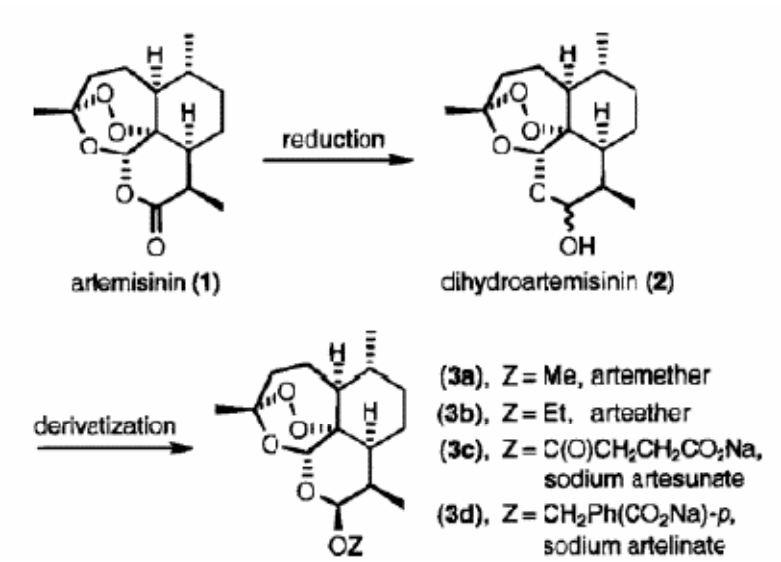

Figure 1.4. Artemisinin and its derivatives

1.9.1 Antimalaria activity of artemisinin

Although artemisinin has been on the market for more than 30 years, little is known about its biological targets till date [Wu, 2002]. Presence of the endoperoxide moiety is the key to its antimalarial activity [Brossi *et. al*., 1988; Klayman, 1985; Lee *et. al*., 1990; Luo *et. al.,* 1987].One of the main reasons is that artemisinin does not exert its lethal effect through the whole intact molecule, but rather, through some transient species generated after cleavage of the peroxy bond [Wu, 2002]. Being hydrophobic in nature, artemisinin passes biological membrane easily [Augustijns *et al*., 1996]. In vitro studies have suggested an uptake of artemisinin by both healthy and malaria infected red blood cells [Asawamahasakda *et al*., 1994]. During the blood stage phase of the parasite, more than 70% of the haemoglobin within the infected erythrocyte is digested [Francis *et al.*, 1997]. Haeme is released which is toxic for the

parasite and neutralized by polymerization into haemozoin or "malaria pigment" in the form of a crystalline, insoluble, black-brown pigment. The haeme polymerization pathway is specific to the malaria parasite and offers a potential biochemical target for the design of antimalarial. Haeme or iron (II) salts triggers reductive cleavage of the peroxide bond in artemisinin to form oxygen centred radicals. Oxy radicals then form carbon centred radicals [Kamchonwongpaisan *et al.,* 1996] (Figure 1.5). These radicals cause oxidative stress and damage the parasite's membrane systems such as mitochondria, rough endoplasmic reticulum and plasma membranes [Asawamahasakda *et al*., 1994, Cumming *et al.,* 1997, Maeno Y *et al*., 1991]. Recent studies have shown that artemisinin taken up by the malaria parasite growing in vitro was selectively concentrated in the parasite food vacuole and was associated with haemozoin [Hong *et al*, 1994]. Artemisinin also interacts with haeme, forming covalent adducts [Hong *et al*., 1994, Meshnick *et al.,* 1991]. However, it has also been reported that the artemisinin haeme complex does not possess any antimalarial activity [Meshnick *et al.,* 1991]. Further studies related to structural and mechanistic aspects of the interaction of artemisinin with haeme may yield important information for the design of better antimalarial.

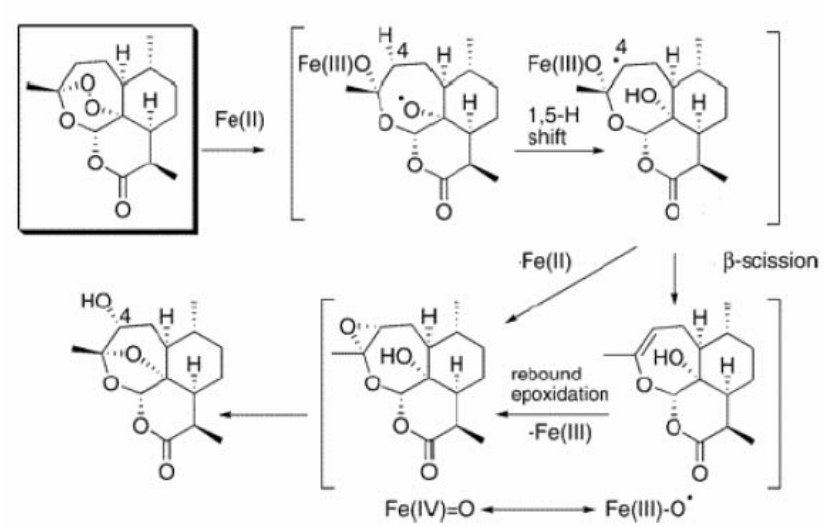

Fig.1.5. Mechanism of action of artemisinin through formation of free radicals

1.10 Need of drug combination: artemisinin-quinine hybrid compound

Drug combination potentially offers a number of important advantages over monotherapy. Appropriately chosen combination must be super-additive and might provide synergistic activities. Drug combination increase the likelihood that in the setting of drug resistance, combination might offer additional advantage if the separate agents are active against different parasite stages and if they provide opportunity to decrease dosage of individual agent thereby reducing cost and/or toxicity.

In order to overcome the limitations, disadvantages and deficiencies of individual use of quinine and artemisinin against malaria, artemisinin-quinine hybrid has been selected and analyzed to design a complete antimalaria drug (Fig 1.6). Quinine and artemisinin are the alkaloids, from natural source of plant kingdom. The linkage of dihydroartemisinin and quinine in a single hybrid molecule retains and possibly enhances the antimalaria activities of both artemisinin and quinine. It also increases the potency of compound of hybrid which enhanced the cellular uptake over that of the individual components. So quinine and its analogue structure and artemisinin with its derivatives with suitable combination have many advantages like quick reduction of fever, fast cleaning of parasite in the blood and no significant side effects. Quinine has drug resistance problem where as artemisinin being newly introduced drug with no resistance problem but suffers as monotherapy from late recrudesces due to its short half life period. So Artemisinin based combination therapy (ACTs) with quinine has more advantages than the individual components.

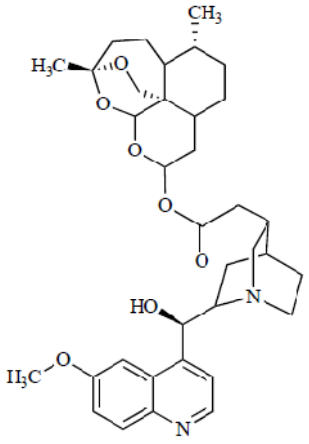

Fig.1.6 Dihydroartemisinin-quinine hybrid structure

Additionally, this new hybrid may act as a 'mutual prodrug' in the case where ester group is hydrolyzed to the individual component and thus act as a unique way of delivering the anti-malaria agents to protozoan site of action. Also the combination might be expected to show a decrease in the duration of the side effects that are often associated with quinine regimes and additionally offer the possibility of a new antimalaria drug with discrete activities in its own right.

Hybrid molecule also has advantages: (1) The phrmacokinematics of the hybrid molecule is more predictable. (2) It is possible to use the uptake capacity of one motif to boost the biodisponsibility of the second entity. (3) As both components of the hybrid have independent mechanisms of action, resistance to a drug of this type may be less likely.

1.11 Properties of dihydroartemisinin-quinine hybrid compound

1. The dihydroartemisinin-quinine hybrid obtained showed superior antimalarial activity over quinine, artemisinin and a 1:1 mixture of artemisinin and quinine both in cultures of *P. falciparum* 3D7 and the chloroquine-resistant strain FcB1 [Walsh *et al.*, 2007].
2. The compound has both the characteristic feature of hybrid as well as prodrug since the ester bond can easily be hydrolyzed and dihydroartemisinin is more potent than artemisinin itself.
3. The hybrid compound has higher potency because enhanced cellular uptake over the individual parent compounds.
4. This compound is expected to readily form soluble salts in the same way as quinine so may offer an improvement in formulation and allow for shorter treatment with enhanced compliance.
5. The combination might be expected to show a decrease in the duration of the side effects that are often associated with quinine regimens and additionally offer the possibility of a new antimalarial drug with discrete activity in its own right.

6. Artemisinin-quinine hybrid compound has higher half life than its lipophilic, fast-acting artemisinin entity with the coupling of the slow-acting, polar quinine derivative.
7. As both components of the hybrid have independent mechanisms of action, resistance to a drug of this type may be less likely.
8. An interesting feature of the artemisinin–quinine hybrid was that the two drugs had been reported to be synergistic with FIC (Fractional Inhibitory Concentration) is less than 0.5 [Bell, 2005].
9. In artemisinin-quinine hybrid the recrudescence rate is reduced significantly usually associated with artemisinin monotherapy at rate of around 10%.
10. The hybrid drugs may be less expensive since, in principle, the risks and costs involved may not be different from any other single entity.
11. The hybrid antimalaria drug is effective against MRD (multi-drug resistant) parasite because the chance of parasites simultaneously developing resistance as a result of genetic mutations to two drugs with different modes of action is much lower than the chance of parasite developing resistance to single drug.

1.12 Experimental study

The hybrid structure of artemisinin-quinine has superior activity to that of artemisinin alone, quinine alone, or a 1:1 mixture of artemisinin and quinine. The artemisinin–quinine hybrid had potent antimalarial activity in culture (Table 1.1)

Table 1.1 Fifty percent inhibitory concentration (IC_{50}) of the artemisinin-quinine hybrid compared with the individual drugs

Compound	3D7 (48 hrs)	3D7 (72 hrs)	FcB1 (48 hrs)	FcB2 (72 hrs)
	IC_{50}/nM/Final/Initial	*IC_{50}/nM/Final/Initial*	*IC_{50}/nM/Final/Initial*	*IC_{50}/nM/Final/Initial*
	Geometric mean IC50/nM (95% confidence limit)			
Quinine	149 (95.1, 232)	73.5 (57.0, 94.6)	96.8 (74.5, 126)	75.3(59.0, 96.1)
Artemisinin	89.4 (40.7, 60.0)	45.5 (35.3, 58.6)	50.0 (43.7, 57.3)	55.0(39.0, 77.4)
Art-Qui-OH	8.95 (6.59, 12.2)	10.4 (6.06, 17.9)	9.59 (7.06, 13.0)	10.2 (4.73, 21.9)
Quinine+ Artemisinin	31.8 (27.4, 37.0)	28.6 (21.5, 38.2)	27.9 (26.5, 29.5)	26.3 (24.7, 28.0)

P. falciparum 3D7 was inhibited by much lower concentrations of the hybrid than of quinine or artemisinin alone, suggesting that the actions of both quinine and artemisinin moieties were preserved. Moreover, when the activity of the hybrid was compared with that of a 1:1 mixture of quinine and artemisinin (on a mol quinine/mol artemisinin basis), the hybrid was about threefold superior. This suggested that the two molecules joined together were more active than the same two molecules administered separately. The higher activity of the hybrid may however be the result of its cleavage to form quinine and dihydroartemisinin, the latter compound being more active than artemisinin itself.

1.13 Additive/Synergistic study of hybrid molecule

The artemisinin-quinine hybrid compound with two individual components of artemisinin and quinine; the interaction with respect to additive or synergistic have been studied with experimental IC_{50} value of the individual compound in comparison to the concentration of hybrid. The fraction inhibitory concentration FIC has been calculated as follows [Bell, 2005]

FIC of hybrid molecule =Concentrations of the Inhibitor/IC_{50} of the Compound B+ Concentration of the Inhibitor/IC_{50} of the Compound A

'Cut-off' value of $\sum$ FIC = 0.5 has been widely used, such that $\sum$ FIC < 0.5 is regarded as synergistic and $\sum$ FIC > 0.5 not.

FIC for Chloroquine sensitive 3D7 strain:

After 48 hrs of incubation= 8.95/49.4+8.95/149=0.18+0.06=0.24 < 0.5

After 72 hrs of incubation=10.4/45.5+10.4/73.5=0.22+0.14=0.36 < 0.5

FIC for Chloroquine resistant FcB1 strain:

After 48 hrs of incubation=9.59/50+9.59/96.8= 0.19+0.09=0.28 < 0.5

After 72 hrs of incubation= 10.2/55 +10.2/75.3=0.18+0.13=0.32 <0.5

So from the above data a conclusion can be drawn that the linkage of artemisinin and quinine in a single molecule can possibly enhance the antimalarial activity of the parent compounds.

1.14 Structure-activity relationship (SAR) of artemisinin-quinine hybrid

In the stereochemistry of artemisinin-quinine hybrid, artemisinin and quinine naturally occurring alkaloids are two components of combination therapy of artemisinin. The chiral analysis of quinine is (-) 8(S), 9(R). The decision to modify the vinyl functionality of quinine was based on study with the compound which indicated that modification to other potential side have unfavourable effect on activities. Particularly the hydroxyl group (-OH) and the quinoline ring are essential for activities but the quinuclidine ring can be substantially modified without loss of activity [Walsh *et al*., 2007]. Alteration to the stereo chemical centres on quinine have mixed effect with erythro configuration at the C-8 and C-9 position of quinine analogous being more active than the stereoisomer's for some but not, all derivatives. With respect to artemisinin modification to the lactone functionally is well tolerated with dihydroartemisinin and artesunate all possessing potent antimalarial activity. The compound artemisinin-quinine hybrid which contains artemisinin like trioxanes (O1, O2 and O4) is not absolutely necessary however the sesquiterpene lactone bearing endoperoxide (O1 and O2) bridge is essential for antimalarial activity. The stereo chemical analysis of dihydroartemisinin and its structural study indicates, in general, ether, ester and carbonate derivatives of dihydroartemisinin demonstrate appreciable antimalarial activity. Also liphophility is an important factor in maintaining and increasing antimalarial activity. Dihydroartemisinin containing the easily esterifiable hemiacetal functionality is one of the principal artemisinin metabolite form *in vivo*; it was selected as the most appropriate artemisinin derivatives to form the artemisinin-quinine hybrid.

1.15 Experimental rationale

Despite the availability of effective anti malarial drugs, the prevention and treatment of malaria is progressively becoming more difficult due to the prevalence of multi-drug resistant (MDR) parasite. A number of hybrid agents have been designed and tested for antimalarial activity. Significant efforts also have been focused on identifying new analogues that have a similar mechanism of action yet superior in activity. This project work is the first approach of this kind of endeavour where

computational methodology is applied to predict the binding modes and anti malarial activity of artemisinin-quinine hybrid and its derivatives two putative bio systems; haeme polymerisation and vacuolar plasmepsins.

1.16 Objective of the present study

The drug artemisinin-quinine hybrid has experimentally proved to be a novel and potent antimalarial compound. So the objective of research work is to investigate the drug affinity and mode of binding with two separate receptors inside the food vacuole target.

The detailed objectives of the research work compiled in the thesis are as follows:

1. To study and analyze the interaction mechanism of artemisinin-quinine hybrid and its congeners complex with Fe-Protoporphyrin-IX.
2. To estimation of binding energy (ΔG_{bind}) by the method of docking molecular mechanics based on generalized Born/surface area (MM-GBSA) solvation model.
3. To study the mode of interaction of hybrid molecule with HAP enzyme.
4. To predict the binding mode & estimate the relative binding affinity of Art-Qui-OH with respect to two known inhibitors of HAP
5. To design an adaptive inhibitor of plasmepsins family of *P.falciparum* considering HAP as the primary structure.

Chapter-2

Literature Review

2.1 Epidemiology of malaria

2.2 Antimalaria drug

2.3 Drug-resistant *P. falciparum* malaria

2.4 Artemisinin and its derivatives as antimalarial drugs

- 2.4.1 Artemisinin derivatives
- 2.4.2. Antimalaria activity of artemisinin

2.5 Artemisnin based combination therapy (ACTs)

2.6 Next-generations antimalaria drug based on ACTs: hybrid drug

- 2.6.1 Artemisinin-based hybrid & derivates

2.7 New molecular targets with potential for antimalaria drug development

2.8 Histo-aspartic Protease of *Plasmodium falciparum*

- 2.8.1 Enzyme kinetics of HAP
- 2.8.2 Functional redundancy of aspartic protease in *P.falciparum*
- 2.8.3 Inhibitor of Histo-aspartic protease

2.9 Structure-based virtual screening methods for computer-aided drug discovery

2.10 Adaptive inhibitor for plasmepsins family

2.11 Conclusion

2.1 Epidemiology of malaria

The epidemiological study with respect to malaria has been well reported from different corners of the world [WHO, 2011].The situation is particularly grave in south east Asia, where the prevalence of multi-drug resistant (MDR) parasite has become great challenge for management of malaria. In this region *Plasmodium falciparum* parasite are resistant to many drugs commonly used to treat malaria, leading to major changes in the treatment policy of the WHO since 2006[Liwang *et al.*, 2009].Since then the WHO has advocated a policy of Artemisinin based combination therapy for treating *Plasmodium falciparum*.

2.2 Antimalaria drug

The intracellular trophozoite feeds on the haemoglobin of the red blood cell that serves as a source of amino acids. Digestion of the globin protein takes place inside the *Plasmodium* lysosome resulting in the generation of free haeme (Ferriprotoporphyrin-IX, FP). The latter is insoluble and precipitates in the form of a malaria pigment inside the lysosomes. Quinoline-containing compounds have long been used to combat malaria. The widely used quinoline drugs chloroquine, quinine, and mefloquine, as well as amodiaquine and the nonquinoline drugs such as halofantrine and lumefantrine are known to act against the blood stages of the infection by inhibiting detoxification of Fe (III) PPIX into haemozoin (Egan *et al.,* 2008). Quinine, the first quinoline antimalarial drugs were alkaloids extracted from the *Cinchona* tree [Wallace *et al*., 1996]. Quinine is lipophilic drug that bind tightly to serum components, including high-density lipoproteins [Mu *et al.*, 1975, Desneves *et al*., 1996]. Quinine has a pKa1 value of approximately 4.2 (Perrin, 1965) and a pKa2 value of 8.2–8.5 (Perrin, 1965, Mu *et al*., 1975). Quinine interacts weakly with haeme ($K_d = 2.6X10^{-6}$ M) [Chou *et al*., 1980] but has been shown to inhibit haeme polymerisation [Slater and Cerami, 1992, Chou and Fitch, 1993] and haeme catalase activity [Ribeiro *et al.,* 1997]. Quinine and other aryl amino alcohols concentrated in infected erythrocytes [Fitch,1970] as weak membrane-soluble bases, and are believed to accumulate in the acidic digestive vacuole contents where they undergo protonation [Homewood,1972] and cause the death of the intra-eryhrocytic malaria parasite by binding to toxic haematin [Macomber, 1967, Chou

et al., 1980] released during haemoglobin digestion, preventing its dimerisation to non-toxic malaria pigment (haemozoin, β-haematin) [Pagola *et al.*, 2000].

Over last few decades, different variants of quinine (very often, the structural analogues) such as chloroquine (4-amino-quinoline), mefloquine (quinoline methanol), primaquine have been used for malaria treatment [Surolia *et al*., 2002]. But the anti-malarial efficacy of each of these has been far from satisfactory due to mainly two major factors: (1) these drugs act on the targets whose biochemical structure/function overlaps with that of the human host [Milhous and Kyle, 1998]. (2) Evolution of resistant strains of the parasite within the last two decades due to indiscriminate usage of the drugs [Padmanaban and Rangarajan, 2001].

2.3 Drug-resistant *P. falciparum* malaria

Antimalaria drug resistance occurs when the drug concentrations are sufficient to reduce the susceptible parasite population [Chawira *et al*., 1987]. Resistance causes drug failures, because of reduced susceptibility; drug levels that would normally eliminate the infection can no longer do so. However, fully drug sensitive parasites can still cause a recrudescent infection if the plasma concentrations of the drug are insufficient [White, 1999a]. Increasing multidrug resistant *P. falciparum* in many parts of the world has aggravated the problem of deciding which antimalarial to use, particularly in countries where *P. falciparum* has developed resistance to chloroquine, mefloquine primaquine, antifolates such as Fansidar (Sulphadoxine-Pyrimethamine) and, to some extent, quinine which previously was effective in the treatment of severe and complicated malaria [Olliaro *et al*., 1995].

Multidrug-resistant *P. falciparum* malaria is prevalent in Southeast Asia and South America. Now Africa, with the highest burden of malaria, is also being affected [Wesdorfer *et al*., 1991]. Key factor contributing to the increasing malaria mortality and morbidity is the wide spread resistance of *P. falciparum* to the conventional antimalarial drugs such as chloroquine, sulfadoxine-pyrimethamine (SP) and mefloquine [Ridley, 2002, Ronn, 1996, Sowunmi *et al*., 1998, Agtmael *et al*., 1999]. Antimalarial drug resistance is usually a result either of changes in drug accumulation

or efflux (chloroquine, quinine, amodiaquine, mefloquine, halofantrine resistance) [White, 1998] or reduced affinity of the drug target resulting from point mutations in the respective genes encoding the target (pyrimethamine, cycloguanil, sulphonamides, atovaquone resistance) [Foote *et al.,* 1994, Ward *et al*., 1995].

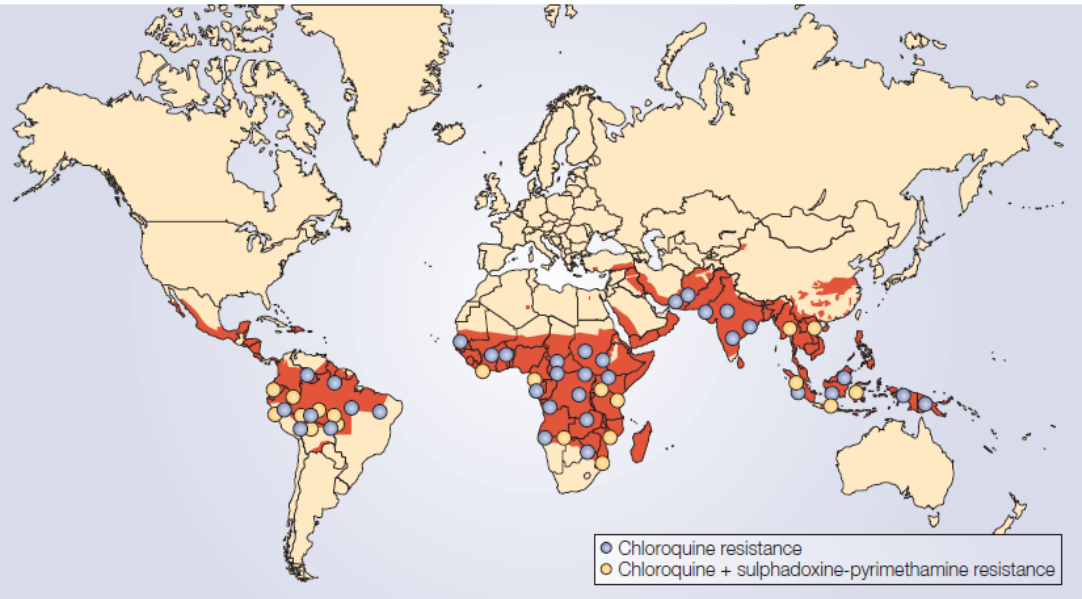

Fig.2.1. Illustrates the global distribution of malaria, showing areas where *Plasmodium falciparum* resistance to the most commonly used anti malaria drugs, chloroquine and sulphodoxine-pyremethamine has been documented.

2.4 Artemisinin and its derivatives as antimalarial drugs

The active moiety Artemisinin (qinghaosu) was isolated by Chinese scientists in 1972 from the aerial parts of *Artemisia annua* L. [Klayman, 1985, Liu, 1979]. The compound showed good *in vitro* and *in vivo* antimalarial activity. Several studies showed artemisinin to be an exceptional antimalarial agent with negligible toxicity and high efficacy against human malaria parasites, including those malaria resistant to conventional antimalarial [Li *et al.,* 1994].

2.4.1 Artemisinin derivatives

Representing a new class of anti malaria agents, artemisinin is a sesquiterpene lactones characterized by an endoperoxide bridge essential for its antimalarial activity.

Because the parent drug of Artemisinin is poorly soluble in water or oil, the carbonyl group of artemisinin was reduced to dihydroartemisinin (DHA) and its derivatives such as water soluble artesunate and oil soluble artemether and arteether. All these derivatives show greater antimalaria activity.

2.4.2. Antimalaria activity of artemisinin

Artemisinin is now being considered as the most potent anti malaria agents, effective against nearly all asexual and sexual parasite stages [Skinner *et al.*, 1996, Chen *et al.*, 1994]. It can kill malaria parasite within minutes with a parasite reduction ratio of approximately 10,000 per eryhrocytic cycle, resulting in a rapid clinical response [White, 2008, Woodrow *et al.*, 2005]. Moreover, the availability of suppository formulation of artemisinin provides additional advantage for easier administration, when oral therapy for malaria patients is precluded by vomiting, prostration and impaired consciousness. [Karunajeewa *et al.*, 2007, Gomes *et al.*, 2008].

2.5 Artemisnin based combination therapy (ACTs)

Despite being the fastest drug against all eryhrocytic stages of malaria parasite, artemisinin has a very short elimination half life (~1 hr), which precludes their use for malaria prophylaxis. In humans, artemisinin derivatives are rapidly bio-transformed to their bioactive metabolite DHA, which is later eliminated by glucoronidation [Lee *et al.*, 1990, Grace *et al.,* 1998, Ilett *et al.*, 2002]. The rapid elimination of artemisinin in human is advantageous in preventing the selection of resistant parasite by the residual concentration of drug. On the other hand the short, half life of artemisinin is also attributed to poor cure rate and high rate of recrudescence (> 25%) for short course of artemisinin therapy (3-5 days). Even 7 day regime of artemisinin monotherapy only cures 80-90% of uncomplicated falciparum malaria. This is one of the reasons that ACTs particularly combination of artemisinin with a long-lasting drug are recommended for treating falciparum infections [Ashley *et al.*, 2005, Davis et *al.*, 2005].

The rationale behind ACT is that the chance of parasites simultaneously developing resistance as a result of genetic mutation of two drugs with different modes of action is much lower than the chance of parasites developing resistance to a single drug [Nosten, 2007, White, 1999]. Currently, there are a number of ACTs being used or tested in different *P.falciparum*-endemic regions [Kremsner *et al.*, 2004]. Artemether-lumefantrine (Coartem) is a fixed dose oral combination for treating uncomplicated falciparum malaria in adults and children [Kokwaro et *al.*, 2007]. Artemisinin and ACTs also work well against *Plasmodium vivax* malaria [Karunajewa *et al*, 2008, Phan, 2002, Hamedi, 2004]. When developing an ACT, the partner drugs should ideally be structurally unrelated, most slowly eliminated *in vivo* and should target those parasite that are yet to develop resistance. The effectiveness of ACTs might be compromised with the use of an inappropriate drug. Therefore the partner drug selections are important taking into account of dosage compliance, minimized toxicity, and cheaper preclinical evaluation.

2.6 Next-generations antimalaria drug based on ACTs: hybrid drug

A recent rational approach of antimalarial drug design characterized as ‘‘covalent biotherapy’’ involves linking two molecules with individual intrinsic activity into a single agent, thus packaging dual activity into a single hybrid molecule. Current research in this field seems to endorse hybrid molecules as the next-generation antimalarial drugs. Some of these hybrid drugs have been demonstrated to be potent antimalarial agents, possessing no or minimum toxicity [Benoit-Vical *et al*., 2007, Cosle´dan *et al*., 2008]. However, so far none of these hybrid antimalarials have reached clinical application.

2.6.1 Artemisinin-based hybrid & derivates

One of the challenges for future malarial chemotherapy is to develop compounds that are innovative with respect to the chemical scaffold and molecular target [Olliaro and Wells, 2009]. There appear to be unlimited possibilities in which the artemisinin pharmacophore can be exploited in covalent biotherapy by linking it to other drug pharmacophores. Although the addition of artemisinin derivatives can improve the efficacy of certain conventional antimalaria agents in areas where parasites

have developed high level of resistance, reintroduction of these conventional drugs in ACTs is questionable or controversial. Many approaches to antimalarial drug discovery include (a) optimization of therapy with available drugs including developing analogues of the existing drugs (b) evaluation of potent agents from natural products especially plants, and (c) use of compounds originally developed against other diseases. In view of this background and of the reported antimalarial synergism between artemisinin/other endoperoxide and quinine, Walsh *et al.*, (2007) synthesized a novel covalently linked artemisinin–quinine hybrid in which the vinyl functionality of quinine was modified to allow the attachment of dihydroartemisinin.

There is paucity of literature on the structure-optimization and structure–activity relationship study of artemisinin-quinine hybrid. But progresses were made in the past decade pertaining to the development of anti-parasitic agents based on artemisinin derivatives. There have been a number of approaches to identify new artemisinin analogues with superior therapeutic profiles through chemical derivatization at positions such as C-10, C-3, C-9 and O-11 [Avery *et al.*, 2002].Similarly structure-activity relationship study were done in B-quinoline ring of quinine with diverse substitutions at the C-5, C-6, C-7, and C-8 positions on antimalarial activity against drug-resistant parasite strains [Madrid *et al.*, 2004]. In additional, there are also changes to the ring system affect the pK_as of the quinoline ring nitrogen and the side-chain nitrogen, physical parameters such as lipophilicity, sterics, and electro negativity.

2.7 New molecular target with potential for antimalaria drug development

The complete sequencing of *Plasmodium falciparum* genome has allowed the identification of new molecular targets within the parasite that may be amenable to chemotherapeutic intervention. Despite the growing appreciation of the need to target additional life cycle stages of parasite development, most of the currently available anti malaria drugs and the majority of the drug development activities now underway focus on the asexual blood stages of the parasite development [Fidlock *et al.*, 2008, Rosenthal *et al.*, 2003].

During its erythrocytic growth phase, the parasite degrades most of the host cell haemoglobin [Francis *et al.*, 1997] and utilizes the amino acids obtained through this mechanism for biosynthesis of its own proteins [Sherman *et al.*, 1970]. The parasite also reduces the colloid–osmotic pressure within the host cell to prevent its premature lysis [Esposito *et al.,* 2008]. The degradation process that takes place in the food vacuole of the parasite, involves a number of Plasmepsins (PMs), enzymes belonging to the pepsin family of aspartic proteases [Coombs *et al.*, 2001].

The *P.falciparum* genome encodes 10 aspartyl proteases [Bhaumik *et al.,* 2009]. Four of these Plasmepsins are located in the food (digestive) vacuole (DV: I, II, IV and the histo-aspartic protease) and are involved in the haemoglobin digestion [Banerjee *et al.*, 2001]. PM I, II, and IV and HAP encoding genes lie in a cluster on chromosome 14. The genes span a region of 20 kb, with ~4 kb separating one ORF from the next. The predicted coding sequences are 50–79% identical with each other at the amino acid level [Bhaumik *et al.*, 2009]. Two homologous aspartic proteases, plasmepsins I and II (PM I and II) initiate the degradative process by cleaving the native haemoglobin molecule in a highly conserved hinge region. Inhibitors of these proteases kill parasites in culture and animal models, suggesting that haemoglobin-degrading proteases are valid targets for chemotherapy [Olson *et al.*, 1999, Holland *et al.*, 1993].

2.8 Histo-aspartic protease of *Plasmodium falciparum*

P. falciparum HAP is the most divergent vacuolar plasmepsins with no counterpart in other characterized species of *Plasmodium* [Banerjee *et al.*, 2001]. The mature enzyme exhibits 60% overall sequence identity compared to PMII, but only 39% identity in the active site region [Nezami *et al.*, 2003]. The crystal structures of HAP complexed with Pepstatin-A, KNI-10006, and KNI-10395 have been determined [Bhaumik *et al.*, 2009]. The active site of HAP contains several significant deviations from the pepsin standard. In particular Asp32 which together with Asp215 creates the catalytic dyad (help to chelates the nucleophillic water molecule) in classic aspartic proteases is replaced by histidine, giving this enzyme its name. In addition, substitutions are found in functionally important flexible loop called the flap (residue 70-83), which changes its conformation upon ligand binding and thus participates in

catalysis. This substitution includes the strictly conserved Tyr75 and the highly conserved Val/Gly75, which are replaced by Ser and Lys respectively. Unexpectedly the active site of the apoenzyme contains a zinc ion tightly bound to Asp215 and His32 from one monomer and Glu278 A, from other monomer, with the coordination of zinc resembling that seen in other metal proteases. [Bhaumik *et al.*, 2009].

2.8.1 Enzyme kinetics of HAP

Molecular modelling has led to various proposed modes of action for HAP. Andreeva *et al,* (2004) suggested that HAP might act like a serine protease with a catalytic triad of Ser 37-His 34-Asp 214 and an oxyanion hole formed by Ser 38 and Asn 39. Alternatively, Bjelic and Aqvist have proposed that HAP functions through the direct participation of only Asp 214 with His 34 providing critical stabilization to the reaction [Bjelic *et al.*, 2004]. Using gel filtration chromatography as well as sedimentation velocity and equilibrium ultracentrifugation, it was shown that the recombinant mtHAP exists in dynamic monomer–dimmer equilibrium with an increasing dissociation constant in the presence of CHAPS. Enzymatic activity data indicated that HAP was most active as a monomer. The dominant monomeric form showed a Km of 2.0 μM and a turnover number, K_{cat}, of 0.036 s^{-1} using the internally quenched fluorescent synthetic peptide substrate EDANS–CO–CH2–CH2–CO–Ala-Leu-Glu-Arg-Met-Phe-Leu-Ser-Phe-Pro–Dap–(DABCYL)–OH (2837b) at pH 5.2.

2.8.2 Functional redundancy of aspartic protease in *P.falciparum*

Functional redundancy exists in the functions performed by the DV plasmepsins. Knocked out study on DV Plasmepsins I-IV indicates that no single DV plasmepsins is essential for *P. falciparum* intracellular growth [Omara-Opyene *et al.,* 2004]. Data from Bozdech *et al.*, 2003 and Le Roch *et al.,* 2003, indicate that PfPM1 and PfPM4 are transcribed early in the asexual cycle and the steady-state level of the mRNA falls during the latter half of the cycle, whereas for PfPM2 and PfHAP, the amount of transcript present is low in the first half of the cycle and rises prominently in the second half. This suggests that perhaps PfPM1 and PfPM4 could complement for each other, whereas PfPM2 and HAP could functionally complement as the other pair. This finding therefore provides a reasonable explanation for the fact that combination

of plasmepsins have been shown to be synergistic in haemoglobin cleavage. It is therefore probable that the different plasmepsins have evolved complementary roles in haemoglobin degradation that increase overall catalytic efficiency. Nevertheless, it is likely that the substantial redundancy in the food vacuole plasmepsins system will limit the utility of highly selective agents. Targeting a single plasmepsins is unlikely to result in an effective antiparasitic agent unless it fortuitously cross-reacts with multiple plasmepsins [Liu *et al.*, 2005]

2.8.3 Inhibitor of Histo-Aspartic Protease

Regarding inhibition of HAP, only one weakly active inhibitor, KNI-10006 has so far been reported while for Plm I and Plm II, a number of very potent inhibitor have been synthesized [Bjelic *et al*, 2004]. KNI-10006 is a peptidomimetic inhibitor with an IC_{50} of 0.69 μM [Nezami *et al.*, 2003] from a series of the so-called KNI compounds. The design of this series was based on the concept of substrate transition-state mimicry, with the central core made of α-hydroxyl-β-amino acid derivative, allophenylnorstatine, which contains a hydroxymethylcarbonyl isostere [Hidaka *et al.*, 2003]. The binding mode of KNI-10006 to HAP is drastically different from that of Pepstatin-A, as well as from a number of other KNI inhibitors bound to various aspartic proteases. The predominant interactions of KNI-10006 are within the flap [Bhaumik *et al.,* 2009].

HAP activity was completely inhibited by the aspartic protease inhibitor Pepstatin A (1 μM) [Banerjee *et al.*, 2002]. HAP apparently has high affinity for Pepstatin A, with a Ki value of (81pM) similar to those of other PMs. Pepstatin A is bound in extended conformation, with the statine hydroxyl positioned between Asp215 and His32. However, binding of the C-terminal half of the inhibitor it is oriented toward loop 287−292, making extensive interactions with the residues comprising this fragment. The flap is closed in the structure of the complex.

KNI-10395 is another potent inhibitor of HAP (99.2% inhibition at 5.0 μM). Recently the crystal structure at 2.5 Å resolutions revealed that although the central hydroxyl group of the inhibitor is bound close to the active site residues His32 and Asp215, it is not positioned directly between them but is hydrogen bonded to $O^{\delta 2}$ of

Asp215 via water molecule Wat243, as well as to the main chain carbonyl of Ala34. The flap assumes an open conformation, and the side chain of Trp39 is flipped away from the flap pocket. The structure of the HAP−KNI-10395 complex also revealed a novel mode of dimerisation involving domain swapping, previously not seen in any aspartic proteases [Bhaumik *et al.,* 2011].

2.9 Structure-based virtual screening methods for computer-aided drug discovery.

One of the major challenges in drug discovery is to identify novel compounds with biological activity. Computer-aided drug discovery technology has become an essential and powerful platform for the discovery of new lead compounds, as an alternative from, and complement to experimental approaches. As the number of high resolution structures of potential therapeutic targets and small molecules has grown, the significance of *in silico* experimental approaches has become increasingly important as demonstrated in recent studies by making use of public data [Cherkasov *et al.,* 2006, Cleves and Jain, 2006, Yoon *et al.,* 2005].

Virtual high throughput screening (Klebe, 2006, Oprea and Matter, 2004), which is a method to rapidly identify biologically active compounds *in silico*, can be roughly divided into two categories, ligand centric and receptor centric. Ligand centric methods essentially focus on the comparative analysis of the structural shapes and chemical complementarities between compounds and known ligands. Knowledge of the experimentally selected active compounds is a prerequisite when using this approach [Stahura and Bajorath, 2004]. Receptor centric methods predict the interaction of given compounds with a target receptor, and hence they do not require experimental data about the structure of the ligand. Molecular docking is one of the key methodologies for receptor centric virtual screening. It is a technique for predicting the best binding mode for a given compound that fits into a target receptor, and evaluating its binding affinity. The docking approach has become a primary technique used in many drug discovery programs [Kitchen *et al.,* 2004, Sousa *et al.,* 2006].

Once binding modes of the ligands have been predicted, the choice of method to estimate the free energies of binding is, in practice, determined by the number of compounds to be analyzed [Gohlke *et al.*, 2002]. Empirical [Bohm, 1994, Eldridge, 1997] and knowledge-based [Muegge I, 1997, Gohlke *et al*., 2000] scoring functions estimate the binding affinity from a single structure of the protein-ligand complex and can be used to filter out drug candidates from large databases of compounds ($\sim 10^7$). On the other hand empirical scoring functions are appealing for their speed, and their contributions to the binding free energy, e.g., entropy and solvation, in a very approximate fashion.

2.10 Adaptive inhibitor for plasmepsins family

Drug molecules with the ability to inhibit several members of a protein family with high affinity have been termed adaptive drugs [Velazquez-Campoy *et al.*, 2001, Nezami *et al.*, 2002]. Adaptive ligand need to be capable of presenting different interacting faces to variable regions in the binding site, a property that can be achieved by the presence of asymmetric functional groups and flexible elements [Velazquez-Campoy and Freire, 2001, Velazquez-Campoy *et al*.,2001a,b]. The amino acid are conserved across the malaria strain, but not in human aspartic proteases, suggesting that novel and selective antimalaria drug can be developed that can be better utilized these structural differences and may even allow the assembly of 'adaptive' drug molecule that have the ability to inhibit several members of a protein family at the same time. This has been realized to some extent in the systems described by Nezami *et al.,* (2003) who using computer modelling and docking techniques were able to rationalize the actual binding energies of a set of allophenylnorstatine based compound towards the four PM proteins.

2.11 Conclusion

The review points out that artemisinin based hybrid compound are the next generation anti malarial drug. Such drug can act as the last line of defense against multi drug resistant malaria parasite. In this connection experimental study have already revealed that dihydroartemisinin-quinine hybrid possess the superior anti malaria activity than the individual components. Such finding paves the way for investigating

the detail aspect of the molecular interaction of such hybrid drug with its target ferriprotoporphyrin-IX derived from hemoglobin digestion. The review also revealed that there is paucity of information about the possible molecular interaction of artemisinin based hybrid antimalarial with plasmepsins. Hence an *in silico* attempt can be made to study the binding affinity of the hybrid compound with the functionally redundant plasmepsins family of enzyme. Such attempt may lead to experimental verification and possible design of an adaptive inhibitor that can be of immense help in malaria prophylaxis.

.

Chapter-3

Molecular modeling evaluation of binding mode and affinity of artemisinin-quinine hybrid and its congeners with Fe-Protoporphyrin-IX as a putative receptor

3.1 Introduction

Malaria is a blood borne disease. The major function of the food vacuole of *P.falciparum* is to degrade the host red cell haemoglobin sequestered through the cytostome machinery and provide amino acid which is essential to the survival of the intra eryhrocytic malaria parasite. Massive degradation of haemoglobin also leads to generation of a large quantity of haeme that is toxic to parasite, promoting membrane damage due to its peroxidative property. In particular; Fe (III) PPIX produced by autoxidation of haeme released from haemoglobin is known to be capable of causing lipid peroxidation [Egan, 2006] and to destabilize membranes through a colloid osmotic mechanism. The most important pathway of haeme detoxication in *P.falciparum* is the formation of haemozoin pigment.

3.2 Haemozoin: unique crystalline drug target

Haemozoin is produced as an end product of haeme released during the digestion of host haemoglobin by the malaria parasite and is believed to be a detoxification pathway in the parasite. Haemozoin is now known to be a crystalline cyclic dimmer of Fe (III) PPIX in which the propionate group of one porphyrin moiety coordinates to the Fe (III) centre of its partner and vice versa, while the second propionic acid group of each Fe (III) PPIX hydrogen bonds to a neighbouring dimer in the crystal [Egan, 2008]. The particular type of porphyrin found in the haemoglobin is called proto-porphyrin and it contains iron in the central part of the haeme molecule. It is called Iron protoporphyrin Fe (III) PPIX. So Fe-PPIX drug receptor of hybrid molecule instead of haeme comprising with haemoglobin.

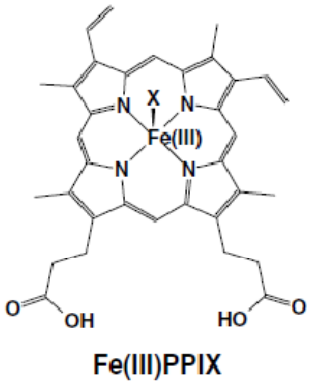

Fig.3.1. 2D structure of Fe (III) PPIX

3.3 Artemisinin based combination therapy

The widely used quinoline drugs chloroquine, quinine, and mefloquine, as well as amodiaquine and the nonquinoline drugs such as halofantrine are known to act against the blood stages of the infection by inhibiting the inclusion of Fe (III) PPIX into haemozoin, resulting in a build-up of toxic Fe (III) PPIX [Egan, 2008, Warhurst *et al*., 2003] and artemisinin cause a similar effect by reacting with haeme (Fe II-protoporphyrin IX) to give free radicals and adducts [Meshnick *et al*., 1993]. The artemisinin are the most effective antimalarial drugs with a remarkable therapeutic index. But with the prevalence of multidrug resistant (MDRs) *Plasmodium falciparum* parasite in south East Asia; lead to change in the treatment policy of World Health Organisation in 2006. Since then the WHO has advocated a policy of Artemisnin-based combination therapy (ACTs) for treating *P.falciparum* [Cui & Su, 2009]. The rationale for this combination is that the artemisinin derivative rapidly clears 95% of the parasites and the remaining 5% are cleared by the longer half-life partner drug and thus minimizes the risk of recrudescence.

3.4 Hybrid antimalaria drug

The combination of two separate pharmacological agents into a single molecule is an emerging strategy within medicinal chemistry and drug discovery. Paucity of promising novel antimalarial drugs under development and a fear of loss of the artemisinin to resistance, in malaria drug combination therapy, the current trend are to co-formulate two or more agents into a single tablet, termed as multicomponent drug [Morphy & Rankovic, 2005]. However, based on the wide interest in the hybrid molecules as well as numerous encouraging efficacy and toxicity reports, the next generation of antimalarial may as well be hybrid drugs as opposed to multicomponent ones. There are numerous advantages of employing hybrid molecules over multicomponet drugs in malaria therapy. Compared to the latter, hybrid drugs may be less expensive since, in principle, the risks and costs involved may not be different from any other single entity. Another advantage is that of the lower risk of drug–drug adverse interactions compared to multicomponent drugs [Muregi & Ishih, 2010].

3.5 Artemisinin-quinine hybrid- a novel and potent antimalaria drug

Quinine from Peruvian Cinchona trees provided the lead for the discovery and development of synthetic aminoquinolines [Warhurst *et al*., 2003]. Likewise, the discovery of artemisinin from the Chinese herb *Artemisia annua* has served as a template for development of semi-synthetic artemisinin including artesunate and artemether, which are being used extensively in ACT against drug-resistant malaria [Cui & Su, 2000].In view of this background and of the reported antimalarial synergism between artemisinin/other endoperoxide and quinine, a novel covalently linked artemisinin–quinine hybrid structure was synthesized in which the vinyl functionality of quinine was modified to allow for the attachment of dihydroartemisinin [Walsh *et al.,* 2007]. The rationale behind the design was to address the fact that artemisinin are lipophilic, fast-acting but quickly eliminated drugs. They are also associated with high rates of recrudescence when used in monotherapy [Walsh & Bell, 2009]. It was suggested that coupling of the slow-acting, polar quinine derivative might increase the half-life of the artemisinin moiety. Current research in this field seems to endorse hybrid molecules as the next-generation antimalarial drugs [Muregi & Ishih, 2010].

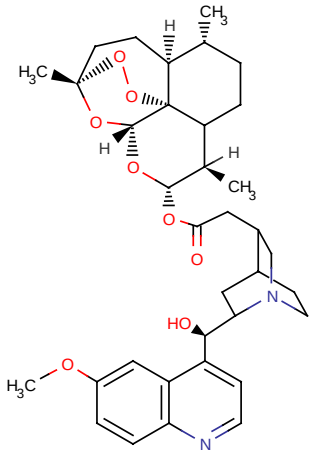

Fig. 3.2 Dihydroartemisinin-quinine hybrid

3.6 *In-vitro* drug resistance of *P.falciparum* to Art-Qui-OH

Drug resistance refers to the tolerance of pathogen/parasite to inhibitory action of antimalaria compound. The drug sensitivity pattern among the malaria parasites changed from time to time and place to place depending on the extent of usage of drug. The drug resistance value of dihydroartemisinin-quinine hybrid compound has been presented below in comparison to artemisinin alone, quinine alone and a 1:1 mixture of artemisinin-quinine in the chloroquine resistant strain FcB1 [Walsh *et al.,* 2007] (Table 3.1)

Table.3.1 In vitro drug resistance $IC_{50(R)}$ of *P.falciparum* to Art-Qui-OH

Compound	FcB1 (48 hrs)			FcB1 (72 hrs)		
	Conc. nM	Population (Final/Initial)	% of resistance	Conc. nM	Population (Final/Initial)	% of resistance
Quinine	96.8	74.5/126	59.12	75.3	59.0/76.1	60.25
Artemisinin	50.0	43.7/57.3	76.26	55.0	39/77.4	60.23
Art-Qui-OH	9.59	7.06/13	54.30	10.2	4.73/21.9	33.85
Quin+Art	27.9	26.5/29.5	89.80	26.3	24.7/56.28	43.8

3.6.1 Resistance index

The resistance index (RI) of Artemisinin,Quinine and Artemisnin-Quinine hybrid were calculated as IC_{50} nM of drug against CQ-R parasite/IC_{50} nM drug against CQ-S parasite [Kouznetsova *et. al.*, 2009].

Table 3.2. Resistance index value of Quinine,Artemisinin & Art-Qui-OH

Compound	IC_{50} nM (72 hrs) 3D7	IC_{50} nM (72 hrs) FcB1	Resistance Index
Art-Qui-OH	10.4	10.2	0.98
Quinine	73.5	75.3	1.02
Artemisinin	45.5	55.0	1.20

The Resistance Index (RI) of the drug was estimated to be 0.98 in comparison to 1.02 and 1.20 for quinine and artemisinin respectively. CQ-resistant parasites accumulate CQ in their acidic food vacuoles much less efficiently than CQ-sensitive

strains, suggesting that drug resistance results mainly from exclusion of the drug from the site of action rather than an alteration in the CQ target [Kouznetsova *et al.*, 2009]. The low value of drug resistance index as well as % of resistance leads to the suggestion that the hybrid is potent against multi drug resistant (MDR) parasite.

3.7 Artemisinin-quinine hybrid derivatives

In the design of Artemisnin-Quinine hybrid derivatives there are many physicochemical factors that need to be considered regardless of whether the molecular design under evaluation is targeting a single event or multiple biochemical events. The greatest design challenge to overcome when constructing hybrid molecules is for the ultimate design to fall within the appropriate number of hydrogen bond donor and acceptor sites, solubility characteristics and molecular weight to attain drug-like properties [Veber *et al.*, 2002, Lipinski *et al.*, 2001].

The following physiochemical parameters were calculated for Artemisnin-Quinine hybrid structure from commercial ACD software for Windows (Toronto, CANADA).

1. Molecular weight=622.74 g/mol
2. logP=5.57
3. pk_1=9.11
4. $pk_{2=}$ 4.77
5. $logD_{(7.4)}$= 3.85
6. $logD_{(5.2)}$= 1.52
7. $logD_{(4.8)}$= 0.97
8. VAR(Vacuolar accumulation ratio)= 213.79
9. LAR(Lipid accumulation ratio)= 7079.458
10. % of ionization with PH 7.4 and pK_1=98.04

In the design of Artemisinin-Quinine hybrid and its analogous the following physiochemical parameters were taken into consideration.

3.7.1 Log P (partition coefficient)

The entry of a basic drug through lipid membranes and its distribution into the aqueous compartments of an infected erythrocyte is determined by lipid–water partition coefficient (expressed as log P) interacting with pH through the ionization constant(s) (pK_a) of the basic centre(s) of the drug. The logP value of Artemisnin-Quinine-OH hybrid is estimated to be 5.57. In view of background; the logP value is set to be in the range of 4.5-6.10 [Warhurst *et al.*, 2007].

3.7.2 Molecular weight

The molecular weight of the hybrid molecule is estimated to be 622.74 g/mol. So the molecular weight kept below 650 g/mol to enhance the membrane permeability [Orrling *et al*., 2009]

3.7.3 H-bond donor and acceptor

In designing inhibitor with reference to hydrogen bond donor and acceptor we have refereed to '*Lipinski rule of 5'* which state that hydrogen bond donor and acceptor should not be more than 5 and 10 respectively [Lipinski *et al.*, 2001]

3.8 Automated docking and Prime-MM/GBSA energy scoring

The mechanism of action of any drug is very important in drug development. Generally, the drug compound binds with a specific target, a receptor, to mediate its effects. Therefore, suitable drug–receptor interactions are required for high activity. Understanding the nature of these interactions is very significant and theoretical calculations, in particular the molecular docking method, seem to be a proper tool for gaining such understanding. The docking results obtained will give information on how the chemical structure of the drug should be modified to achieve suitable interactions. Hence, this could bring about the development of new and more effective drugs. Thus, all possible configurations between Ferriprotoporphyrin-IX and artemisinin-quinine hybrid derivatives were explored by automated docking calculations to eliminate the bias in selecting preferred configurations (orientations).For the docked ligand the pose with the lowest Glide score was rescored using Prime/MM-GBSA approach. This approach is used to predict the free energy of binding for set of ligands to receptor.

3.9 Materials and Methods

3.9.1 Receptor preparation

Studies on the mode of action of artemisinin and its derivatives have shown that free haeme (Figure 3.2) could be the molecule targeted by artemisinin in biological systems and Fe ions interact with the peroxide when artemisinin react with haeme [Cheng *et al*., 2002, Jeffords, 2001, Wu *et al.,* 1998, Meshnick, 2002, Haynes *et al.*,2004]. Similarity spectrophotometric study revealed that quinine and related antimalaria drug interacts with haemin (Ferriprotoporphyrin-IX) [Warhurst, 1981].

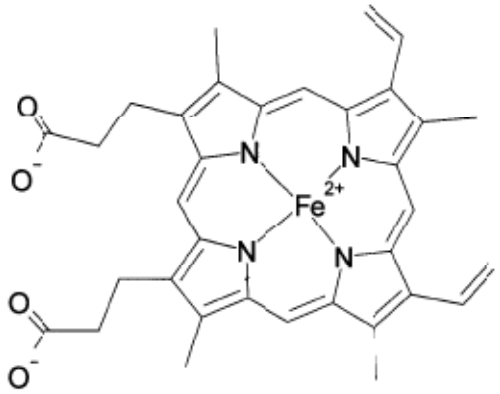

Fig.3.3. The structures of the haeme compound: Fe (II) PPIX

Studies on the mode of action of artemisinin and its derivatives have shown that free haeme could be the molecule targeted by artemisinin in biological systems. Similarly spectrophotometric study revealed that quinine and related antimalaria drugs interact with Ferriprotoporphyrin-IX.

So the X-ray structure of halofantrine-Ferriprotoporphyrin-IX (CCDC_659633) from the Cambridge Crystallographic Data Centre is used as initial structure in the preparation receptor binding site. Ferriprotoporphyrin-IX is a planar molecule with a strong positive charge on its central iron atom (Figure 3.3). After removal of halofantrine structure, the charge on the iron was assigned as +2 but the structure was kept the same. Hydrogen's were added to the model automatically via the Maestro

interface leaving no lone pair and using an explicit all-atom model. The multi-step Schrödinger's protein preparation tool (PPrep) was used for final preparation of receptor model. The complex structure was energy minimised using the OPLS-2005 force field and the conjugate gradient algorithm, keeping all atoms except hydrogen fixed. The minimisation was stopped either after 1000 steps or after the energy gradient converged below 0.01 KJ/mol.

3.9.2 Virtual library design

The virtual library of artemisinin-quinine analogues contains 34 compounds divided into nine sub libraries. All these compounds are taken from various sources belonging to different derivatives of artemisinin and auinine [Woolfrey *et al.,* 1998, Acton *et al*., 1993, Lin *et al,.* 1989, Posner *et al*., 1992, Avery *et al.,* 1995, Avery *et al.,* 1996, Madrid *et al.,* 2005].These molecules were rationally designed as functional mimics of natural artemisinin and quinine with the goal of simplifying the chemical synthesis and improving the antimalarial activity.

Sublib-I **-** *Dihydroartemisnin-Quinine Hybrid*-This library consists of only of one ligand. The structure is designed experimentally in which the vinyl functionality of quinine was modified to allow for the attachment of dihydroartemisinin.

Sublib-II **-** *Artemisinin-Quinine Hybrid* - This library consists of five ligands which are designed by attachment of Quinine moiety to the Artemisinin molecule at O-14.

Sublib-III- *C9 Artemisinin-Quinine Hybrid*- This library consists of two ligands in which the C9 substituted Artemisinin entity is attached to Quinine at O-14 position.

Sublib-IV- *C3 Artemisinin-Quinine Hybrid*- C3 substituted artemisinin derivatives are attached to Quinine moiety and two hybrids are present in this sub library.

Sublib-V- *C10 Artemisinin-Quinine Hybrid*- This library consist of five ligands in which the C10 carbon atom of artemisinin is modified and quinine molecule is attached to it at C9 carbon atom.

Sublib-VI- *Seco Artemisinin-Quinine Hybrid*-This library is having three ligands (16-18) with logP in the range from 5.22 to 5.79.The quinine molecule is attached to the seco artemisinin entity at C9 carbon atom.

Sublib-VII- *Miscellaneous Artemisinin-Quinine Hybrid*- This library consists of four ligand in which various substitution in different carbon atom of artemisinin molecule are attached to the quinine entity.

Sublib-IX- *Quinoline-Artemisinin Hybrid*- Quinoline-artemisinin sub library is having twelve ligands in which the various substitutions at quinoline ring of the quinine molecule is attached to artemisinin phramacophore.

We used ISIS Draw 2.3 software for sketching structure and converting it its 3D representation by using Chem Sketch 3D viewer of ACDLABS 12.0. LigPrep was used for final preparation of ligands from libraries for docking. LigPrep is a utility of Schrodinger software suit that combines tools for generating 3D structures from 1D (Smiles) and 2D (SDF) representation, searching for tatutomers and steric isomers and perform a geometry minimization of ligands.

3.9.3 Docking procedure

The mechanism of action of any drug is very important in drug development. Generally, the drug compound binds with a specific target, a receptor, to mediate its effects. Therefore, suitable drug–receptor interactions are required for high activity. Understanding the nature of these interactions is very significant and theoretical calculations, in particular the molecular docking method, seem to be a proper tool for gaining such understanding. The docking results obtained will give information on how the chemical structure of the drug should be modified to achieve of new and more effective drugs.

The Schrodinger Glide program version 4.0 has been used for docking. After ensuring that receptor and ligand are in the correct form for docking, the receptor-grid file was generated using a grid-receptor generation program. The default size was used

for the bounding and enclosing boxes. The grid box was generated at the centroid of the haeme. The ligands were docked initially using the 'standard precision' method. The best 10 poses and corresponding scores have been evaluated using Glide in single precision mode (Glide SP) .The pose with the lowest Glide SP score has been taken as the input for the Glide calculation in extra precision mode (Glide XP).

For each ligand, the pose with the lowest Glide score was rescored using Prime/MM-GBSA approach. The docked poses were minimized using the local optimization feature in Prime and the energies of complex were calculated using the OPLS-AA force field and generalized-Born/surface area (GB/SA) continuum solvent model. The binding free energy (ΔG_{bind}) is then estimated using equation:

$$\Delta G_{bind} = E_{R:L} - (E_{R+}E_L) + \Delta G_{solv+} \Delta_{GSA} \qquad (1)$$

Where $E_{R:L}$ is energy of the complex, E_R+E_L is sum of the energies of the ligand and unliganded receptor, using the OPLS-AA force field, ΔG_{solv} (ΔG_{SA}) is the difference between GBSA solvation energy (surface area energy) of complex and sum of the corresponding energies for the ligand and unliganded protein. Corrections for entropic changes were not applied in this type of free energy calculation.

3.10 Results

3.10.1 Docking of artemisinin-quinine hybrid derivatives

To better understand the mechanism of interaction and antimalarial activity of Art-Qui-OH & its structural derivatives, computer-aided docking procedures were performed between the drug and its putative receptor to identifying new analogues that have a similar mechanism of action yet superior activity. The XP score of the experimental structure; dihydroartemisinin-quinine compound is -7.485 kcal/mol. Out of 34 derivatives; seven ligands among the library; two from C3-Artemisinin-Quinine hybrid, three from C10-Artemisnin-Quinine hybrid and two from Miscellaneous Artemisinin-Quinine hybrid have more negative Glide score with values from -7.600 to -8.913 kcal/mol. [Table 3.3(a-h)].

Table 3.3(a): Dihydroartemisinin-quinine hybrid

Sl. No	Structure	LogP	Molecular Weight(g/mol)	XP Score (Kcal/mol)
1.	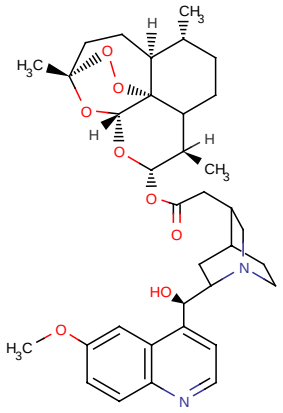	5.57	622.68	-7.485

Table 3.3(b)**:** Artemisinin-quinine hybrid derivatives

Sl. No.	Structure	LogP	Molecular Weight(g/mol)	XP Score (Kcal/mol)
2.	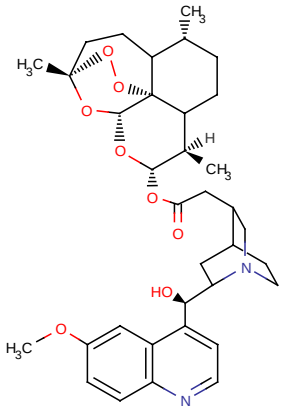	5.57	622.78	-6.802

3.	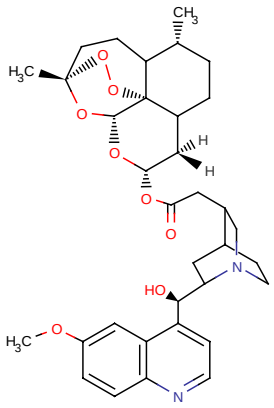	5.08	608.72	-6.914
4.	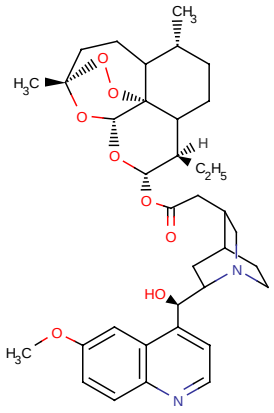	6.10	636.77	-6.950
5.	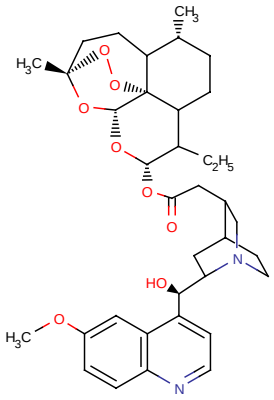	6.10	636.77	-6.932

6.	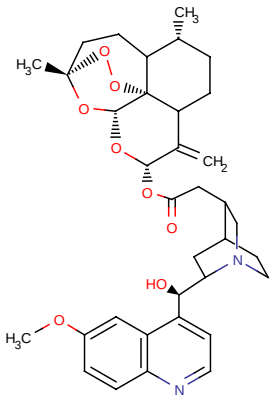	5.75	620.73	-7.241

Table 3.3(c): C9 Artemisinin-quinine hybrid derivatives

Sl. No	Structure	LogP	Molecular Weight(g/mol)	XP Score (Kcal/mol)
7.	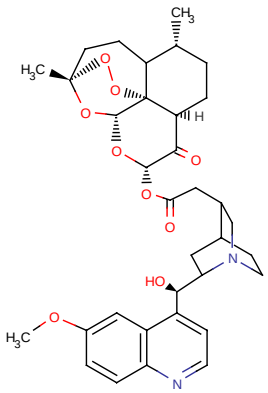	5.18	622.70	-5.310
8.	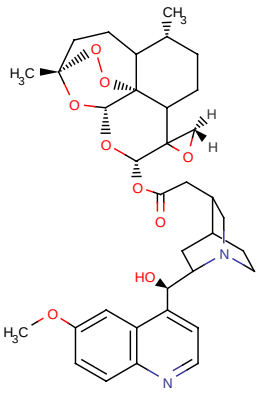	4.92	636.73	-5.450

Table 3.3(d): C3 Artemisinin-quinine hybrid derivatives

Sl. No.	Structure	LogP	Molecular Weight(g/mol)	XP Score (Kcal/mol)
9.	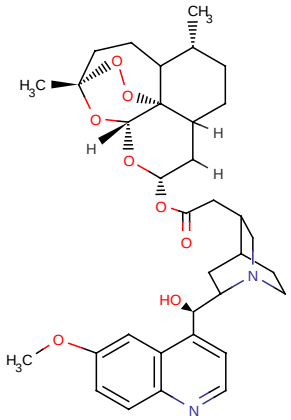	5.08	608.72	-7.673
10.	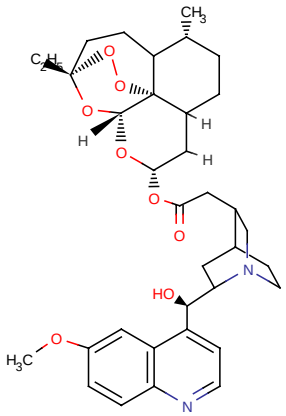	5.61	622.74	-7.620

Table 3.3(e): C10 Artemisinin-quinine hybrid derivatives

Sl. No.	Structure	LogP	Molecular Weight(g/mol)	XP Score (Kcal/mol)
11.	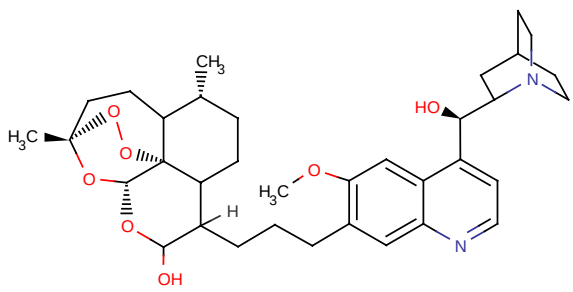	5.58	608.76	-7.722

12.	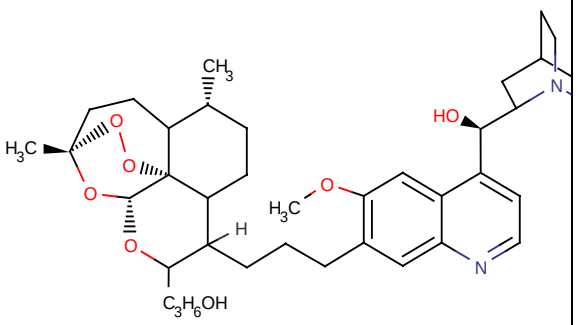	5.86	650.00	-7.815
13.	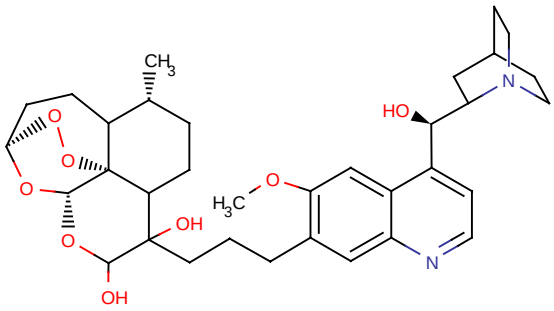	5.36	610.73	- 6.277
14.	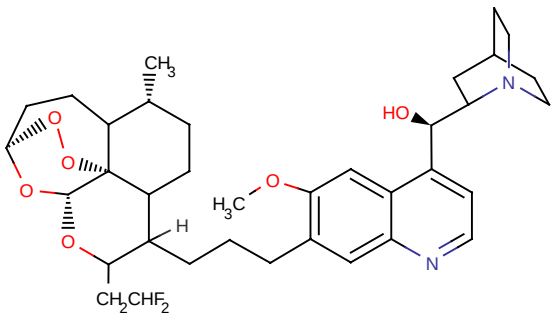	5.93	642.77	-7.622
15.	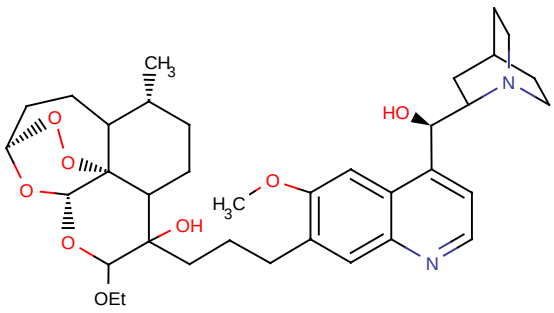	6.08	638.79	-6.283

Table 3.3(f): Seco-artemisinin-quinine hybrid derivatives

Sl. No.	Structure	LogP	Molecular Weight(g/mol)	XP Score (Kcal/mol)
16.	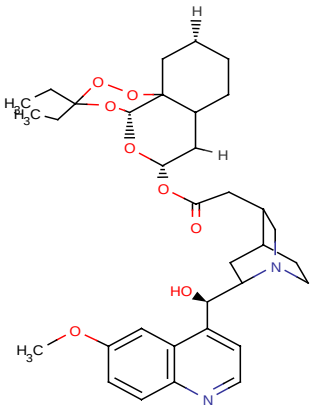	5.79	610.73	-7.070
17.	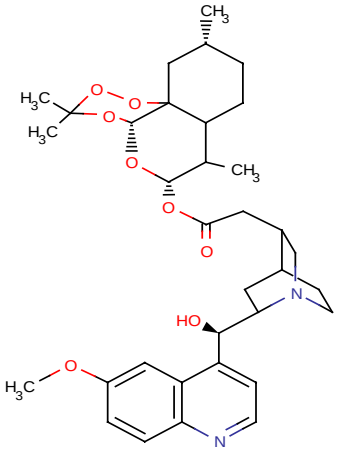	5.71	610.73	-5.586
18.	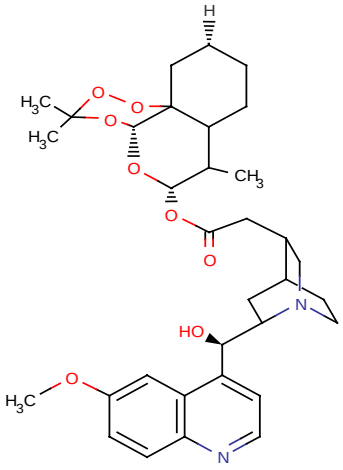	5.22	596.71	-6.914

Table 3.3(g): Miscellaneous Artemisinin-quinine hybrid derivatives

Sl. No.	Structure	LogP	Molecular Weight(g/mol)	XP Score (Kcal/mol)
19.	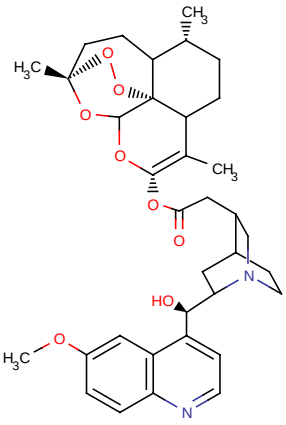	5.98	620.73	-7.600
20.	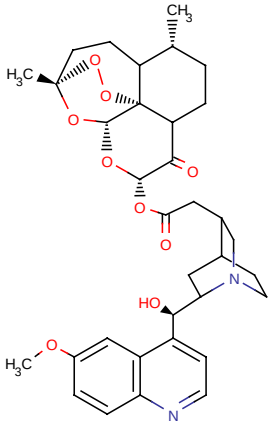	5.18	622.70	-6.768
21.	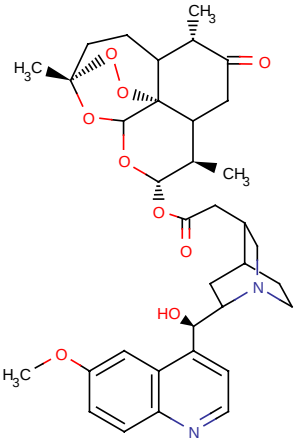	4.56	636.73	-8.913

Sl. No.	Structure	LogP	Molecular Weight(g/mol)	XP Score (Kcal/mol)
22.	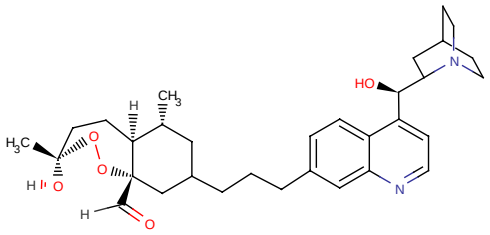	5.02	537.70	-6.671

Table 3.3(h):Artemisinin-quinoline hybrid derivatives

Sl. No.	Structure	LogP	Molecular Weight(g/mol)	XP Score (Kcal/mol)
23.	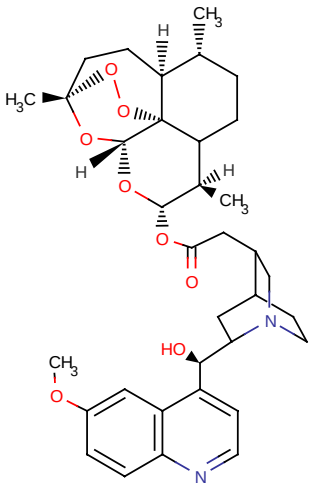	5.57	622.74	-5.83
24.	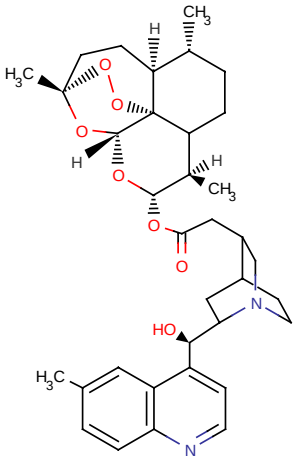	5.94	606.74	-7.02

25.	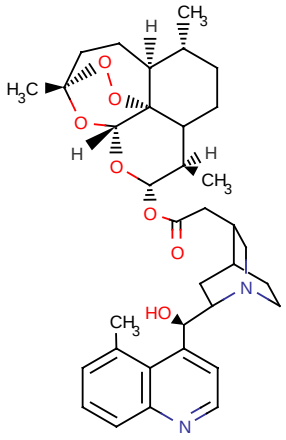	5.94	606.74	-7.30
26.	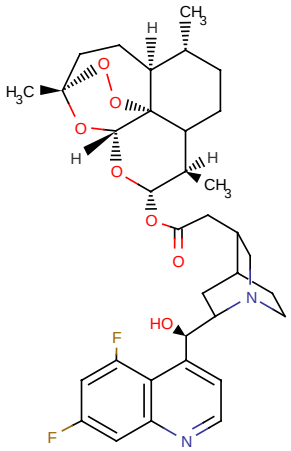	5.89	628.70	-5.79
27.	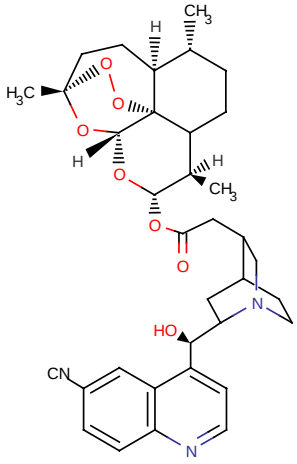	5.06	617.73	-6.64

28.	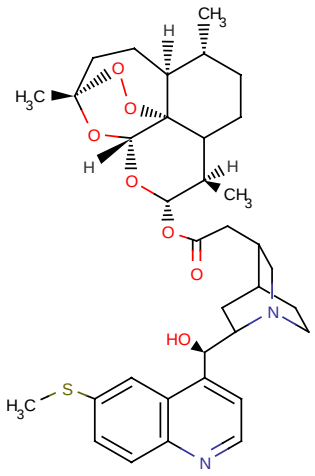	5.97	638.83	-6.77
29.	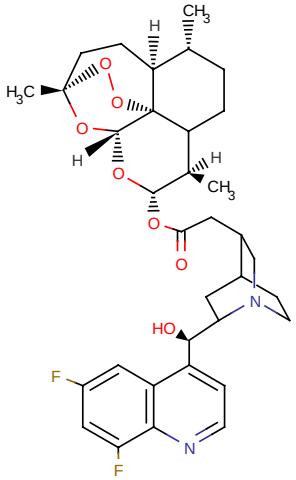	5.70	628.70	-6.56
30.	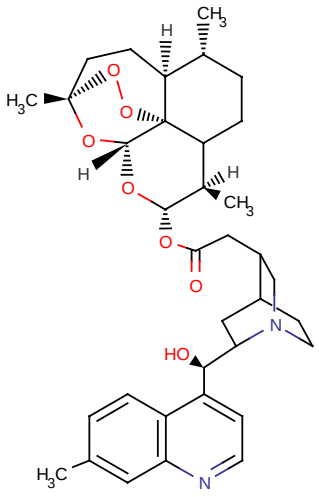	5.94	606.74	-6.69

31.	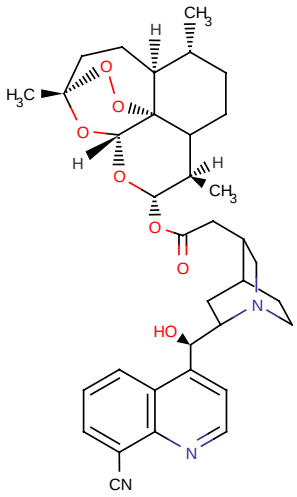	4.79	617.73	-6.53
32.	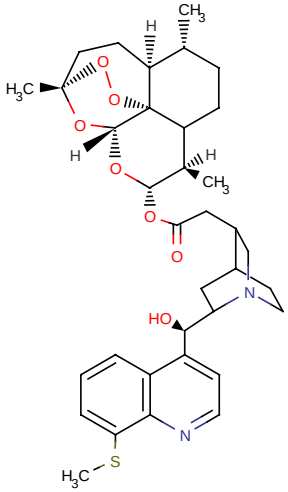	5.97	638.81	-6.58
33.	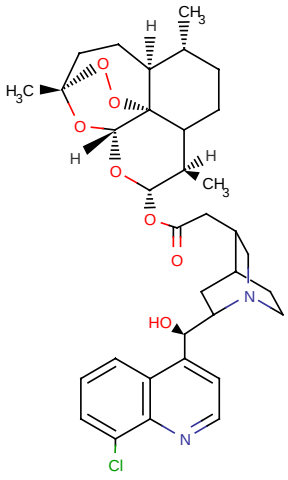	5.73	627.16	-6.54

34.	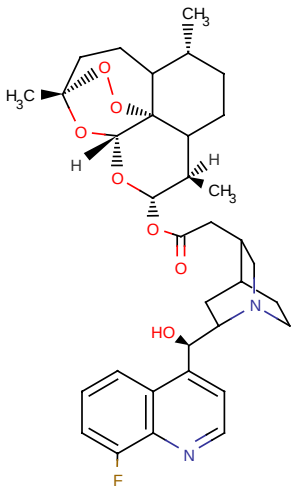	5.90	610.71	-6.54

For each of the seven ligands, the pose with the lowest Glide score was rescored using Prime/MM-GBSA approach. The ΔG_{bind} energies among these ligands vary in between -49.00 to -32.35 kcal/mol. The calculated relative binding energy ($\Delta\Delta G_{bind\text{-}cald}$) of the ligands was also obtained by using Art-Qui-OH as reference. The drop in calculated relative binding energy of the ligand provides a favourable energetic evaluation of the binding affinity. Interaction of Art-Qui-OH and its derivatives with Fe (II) PPIX (Iron (II)) involves binding between the endoperoxide bridges (O1 and O2) bridge of the hybrid to the front of the iron bridge of protoporphyrin-IX shown in **(**Figure 3.2**)**, therefore, distances between haeme iron and two peroxide oxygen's; O1, O2 as well as O11 and O13 and ΔG_{bind} of these derivatives were monitored (Table 3.4 & Table 3.5).

Table 3.4 G Score & ΔG_{bind} energy of Art-Qui-OH and its derivatives with Fe (II) PPIX

Ligand	G Score	ΔG_{bind}	$\Delta\Delta G_{bind\text{-}cald}$	Fe-O_1 (Å)	Fe-O_2 (Å)	Fe-O_{13} (Å)	Fe-O_{11} (Å)
1	-7.485	-32.35	0.00	3.273	2.817	5.149	5.071
19	-7.600	-34.38	-2.03	3.298	2.853	5.214	4.934
10	-7.620	-36.57	-4.22	3.282	2.825	5.172	4.951
14	-7.622	-37.43	-5.08	3.330	2.731	4.998	4.772
9	-7.673	-41.30	-8.95	3.281	2.817	5.125	4.867
11	-7.722	-42.48	-10.13	6.487	6.176	5.235	3.812
12	-7.815	-44.11	-11.76	3.276	2.833	5.083	4.639
21	- 8.913	-49.00	-16.65	3.317	2.817	5.120	4.786

All the energy parameters are expressed in kcal/mol

$\Delta\Delta G_{bind\text{-}cald} = \Delta G_{bind\text{-}ligand} - \Delta G_{bind\text{-}Art\text{-}Qui\text{-}OH}$

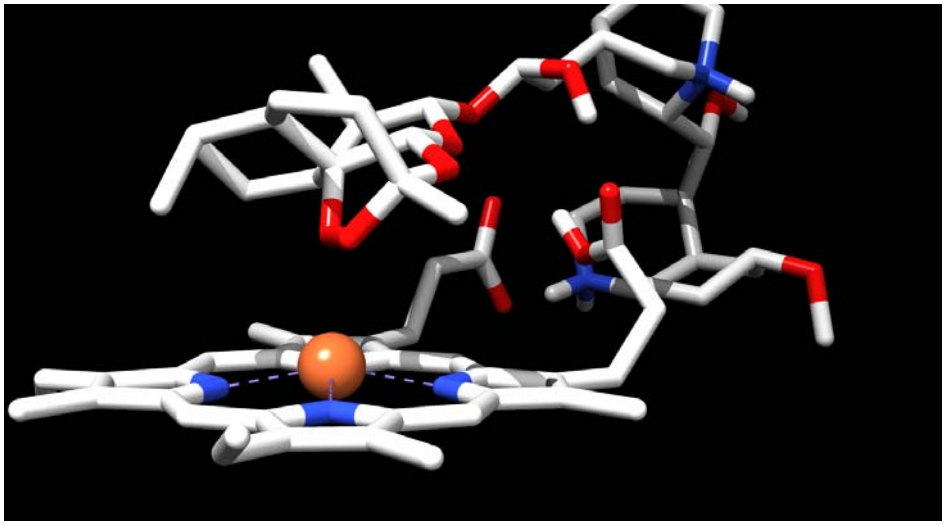

Fig3.2 Representative docking Fe-(O1-O2) interaction of hybrid Art-Qui-OH

Table 3.5(a) Dihydroartemisnin-quinine hybrid

Ligands	Fe-O_1distance (Å)	Fe-O_2 distance (Å)	Fe-O_{13}distance (Å)	Fe-O_{11} distance (Å)
1	3.273	2.817	5.149	5.071

Table 3.5(b) Artemisinin-quinine hybrid derivatives

Ligands	Fe-O_1distance (Å)	Fe-O_2 distance (Å)	Fe-O_{13}distance (Å)	Fe-O_{11} distance (Å)
2	3.409	2.824	5.040	6.435
3	3.282	2.888	5.279	5.514
4	3.455	2.852	5.126	6.554
5	3.317	2.817	5.120	4.786
6	4.104	3.791	6.091	5.456

Table 3.5(c) C9 Artemisinin-quinine hybrid derivatives

Ligands	Fe-O_1distance (Å)	Fe-O_2 distance (Å)	Fe-O_{13}distance (Å)	Fe-O_{11} distance (Å)
7	3.291	3.237	4.268	5.102
8	5.343	4.793	6.719	4.902

Table 3.5 (d) C3 Artemisinin-quinine hybrid derivatives

Ligands	Fe-O_1distance (Å)	Fe-O_2 distance (Å)	Fe-O_{13}distance (Å)	Fe-O_{11} distance (Å)
9	3.281	2.817	5.125	4.867
10	3.282	2.825	5.172	4.951

Table 3.5 (e) C10 Artemisinin-quinine hybrid derivatives

Ligands	Fe-O_1distance (Å)	Fe-O_2 distance (Å)	Fe-O_{13}distance (Å)	Fe-O_{11} distance (Å)
11	6.487	6.176	5.325	3.812
12	3.276	2.833	5.083	4.639
13	6.721	6.458	5.842	3.860
14	3.330	2.731	4.998	4.772
15	5.321	4.495	3.486	3.223

Table 3.5 (f) Seco-artemisinin-quinine hybrid derivatives

Ligands	Fe-O_1distance (Å)	Fe-O_2 distance (Å)	Fe-O_{13}distance (Å)	Fe-O_{11} distance (Å)
16	3.309	3.282	5.569	5.789
17	3.234	3.458	5.603	5.533
18	3.358	2.952	5.292	5.733

Table 3.5 (g) Miscellaneous artemisinin-quinine hybrid derivatives

Ligands	Fe-O_1distance (Å)	Fe-O_2 distance (Å)	Fe-O_{13}distance (Å)	Fe-O_{11} distance (Å)
19	3.298	2.853	5.214	4.934
20	3.317	2.817	5.120	4.786
21	3.323	3.208	5.482	4.704
22	4.283	3.265	3.793	4.014

Table 3.5 (h) Artemisinin-quinoline hybrid derivatives

Ligands	Fe-O_1distance (Å)	Fe-O_2 distance (Å)	Fe-O_{13}distance (Å)	Fe-O_{11} distance (Å)
23	3.405	2.820	5.401	6.444
24	3.401	2.825	5.406	6.435
25	3.390	3.085	5.329	6.541
26	3.294	3.115	5.488	5.553
27	3.440	2.847	5.111	6.527
28	3.399	2.818	5.056	6.443
29	3.460	3.086	5.336	6.579
30	3.312	2.817	5.043	6.439
31	3.406	2.822	5.041	6.439
32	3.367	2.924	5.307	5.528
33	3.399	2.830	5.062	6.451
34	3.405	2.819	5.044	6.436

3.11 Discussion

3.11.1 Interaction mechanism of artemisinin-quinine hybrid

Earlier reports [Walsh *et al.*, 2007, Walsh and Bell, 2009] have revealed that *P. falciparum* 3D7 strain growth was inhibited by much lower concentrations of the hybrid than of quinine or artemisinin alone, suggesting that the actions of both quinine and artemisinin moieties were preserved. Similar results were obtained with the chloroquine-resistant strain FcB1.

Seven novel ligands were identified with a favourable glide score (XP score) & binding free energy (ΔG) with reference to the experimental structure from a data set of thirty four hybrid derivatives. In any binding energy calculation, the correct binding structure of each ligand has to be determined first prior to binding energy estimation. Excluding only one structure from C10 artemisinin-quinine hybrid; in other docking configuration suggested that artemisinin moiety of the hybrid prefers to dock at endoperoxide oxygen's (O1 and O2), with O2–Fe as the shortest haeme–artemisinin distance and O1–Fe as the second shortest. Configuration of dihydroartemisinin-quinine hybrid had the peroxide oxygen O1 and O2 close to the Ferriprotoporphyrin-IX iron (3.273 Å & 2.817 Å) with O11 and O13 further removed (5.071 Å & 5.149 Å) (Figure 3.2) with a ΔG_{bind} value of -32.35 kcal/mol. Configuration of ligand 9 and 10 of C3-Artemisnin-Quinine hybrid series were almost identical. In both the cases O1 (3.281 and 3.282 Å) and O2 (2.817 and 2.825 Å) were closest, with other oxygen being further away: O11 (4.867 and 4.951 Å) and O13 (5.125 and 5.172 Å). Table 3.2 summarizes the results. Interesting configuration of ligand 11 of C10 Artemisnin-Quinine hybrid; the binding with the endoperoxide moiety of artemisinin is in a different configuration, and a stronger O11–Fe attraction is resulted (3.812 Å) than O1, O2 and O13 (6.487 Å, 6.176 Å and 5.325 Å) with a G score of -7.722 kcal/mol. The relative binding energy ($\Delta\Delta G_{bind\text{-}cald}$) of the ligand is calculated to be -10.13 kcal/mol. The possible explanation of such deviation may be explained based on the stereochemistry of artemisinin analogues, a mechanism that is controlled by steric hindrance. The analogues which approach the haeme-iron as close as possible will have better interaction and thus the good glide score. However, owing to the planar structure of the Ferriprotoporphyrin-IX, the repulsion between artemisinin and the protoporphyrin ring prevents artemisinin from approaching haeme-iron. Ligand 12 and 14 of this group produce final orientation with a relative binding energy $\Delta\Delta G_{bind\text{-}cald}$ of -11.76 kcal/mol & -5.08 kcal/mol. Both the configuration involved interaction with the peroxide-derived oxygen with the Fe atom of protoporphyrin-IX. In the most favourable configuration between Ferriprotoporphyrin-IX and miscellaneous artemisinin-quinine hybrid with G_{score} of -8.913 kcal/mol (the lowest), the O1-Fe & O2-Fe distance are 3.317 and 2.817 Å respectively. This structure has the lowest (ΔG_{bind}) score of -49.00 kcal/mol. From the docking simulation study it is revealed that the structure as well as orientation of

artemisinin-quinine hybrid with respect to haeme has a significant effect on drug action. It could then be concluded that iron in haeme interacts with O2 more preferably than O1, a preference which might arise from the more negative charge at O2 and the steric hindrance at O1. This observation is in agreement with docking results reported by Shukla *et al.,* (1995)

Artemisinin-quinine hybrid molecule is novel due to its modified structure and has potent anti malaria activities with presence of artemisinin consisting of endo peroxide bridge. Studies suggested that the antimalarial activity of artemisinin is due to the interaction of its peroxide group with the prosthetic haeme group of human haemoglobin. Reduction of the peroxide group may lead to cytotoxic free radicals and electrophilic intermediates, which may be able to react with specific malaria membrane associated proteins, leading to the parasite's death. Moreover, artemisinin could inhibit haemoglobin degradation, haeme polymerization, and interact with haemozoin, resulting in the split of the malarial pigment. As shown by Walsh *et al.,* their hybrid was highly active *in vitro* against the strains of *P. falciparum* 3D7 (with IC_{50} value 8.95 nM) and Chloroquine resistant strain *P.falciparum* FcB1 (IC_{50} value 9.59 nM).The reported results demonstrate a proof of concept for the linkage of artemisinin and quinine in a single molecule retains and possibly enhances the antimalarial activity of the parent compounds. It is likely that the hybrid can interact with haeme or its oxidation product haematin as a common target since these are both present in the eryhrocytic parasite.

3.12 The role of quinine

This novel artemisinin-quinine hybrid is active on the young eryhrocytic stages of *P. falciparum* with the presence of artemisinin derivatives, whereas quinine is active on the late stages. Presence of quinine entity in the hybrid structure helps to increase the potency of drug and enhanced the cellular uptake and simultaneously increase half life period of drug.

3.13 Biological significance

There is no doubt about the potent and novel anti malarial activity of the hybrid molecules. The next major steps, therefore, is to experimentally analyze the antimalaria activity by determining the IC_{50} value of Art-Qui-OH by BHIA (β-haematin inhibitory assay). Though the analogues ranged from poor to good binding affinity; the structures are not yet synthesized molecule. The information that we have obtained in this study may lead to the design and hopefully (synthesis) of more potent hybrid derivatives with receptor as haematin.

3.14 Conclusion

From the result, it can be concluded that the structure of artemisinin-quinine hybrid has a significant effect on the docking configuration. All the docking calculations indicate O2-Fe as the shortest haeme-artemisinin distance and O1-Fe as the second shortest. The steric hindrance at the Fe position plays an important role in the binding. The docking result revealed that the haeme-iron approaches the endoperoxide moiety at the O2 position in preference to the O1 position. Several sets of artemisinin analogues were studied in the docking simulations. The study conclusively indicates that magnitude of the binding affinity can be a key factor that decides the activeness of an individual inhibitor. In this chapter we propose a model for the binding mode and binding affinity of Art-Qui-OH and its derivatives with a putative receptor. This model will be of immense help for the rational design of new artemisinin based hybrid anti-malarial that can target the haemozoin formation.

Chapter-4

Molecular modeling and determination binding mode and relative binding affinity of artemisinin-quinine hybrid onto Histo-Aspartic Protease (HAP)

4.1. Introduction

4.2 Histo-aspartic Protease (HAP) of *P.falciparum* as a drug target

4.3 HAP enzyme classification

4.4 Substrate specificity of the enzyme

4.5 Structural feature of HAP enzyme

4.5.1 Flap region of HAP enzyme

4.6 Substitution in recombinant HAP enzyme

4.7 Apoenzyme active site

4.8 HAP enzyme activity

4.8.1 Role of PH in enzyme activity

4.9. Catalytic mechanism of HAP enzyme

4.9.1 Role of histidine in protonation for functionality of HAP

4.9.2 Auto-activation of Histo-Aspartic Protease (HAP)

4.10 HAP enzyme inhibitor

4.10.1 HAP-Pepstatin A complex

4.10.2 HAP - KNI-10006 complex

4.10.3 HAP - KNI-10395 complex

4.11 Urgency of new antimalarial

4.12 The need for drug combination

4.13 Hybrid antimalaria drug: Art-Qui-OH

4.14 Materials and Methods

- 4.14.1 Preparation of protein
- 4.14.2 Ligand preparation
- 4.14.3 Molecular docking of artemisinin-quinine hybrid
- 4.14.4 Post-scoring with MM-GB/SA

4.15 Result

- 4.15.1 Calculation of experimental binding energy (ΔG^{bind}_{exp})
- 4.15.2 Calculation of calculated binding energy (ΔG^{bind}_{cald})
- 4.15.3 Validation of the docking method
- 4.15.4 Calculation of Ki value

4.16. Discussion

- 4.16.1 Glide docking and rescoring using MM-GB/SA of ligands
- 4.16.2 Inhibitor (Art-Qui-OH) binding to HAP

4.17 Conclusion

4.1 Introduction

Plasmodium falciparum ingests and degrades up to 75% of the host cell haemoglobin during its intraerythrocytic stage [Loria, 1996].This is a massive catabolic process that takes place inside an acidic food vacuole and involves a pathway of proteolytic enzymes [Goldberg, 2005] both *in vitro* and *in vivo*, called Plasmepsins (PMs).These enzymes belonging to the pepsin family of aspartic proteases [Banerjee *et al.*, 2002, Coombs *et al.*, 2001]. The malaria genome project has revealed that there are 10 Plasmepsins in the *P. falciparum* genome [Shenai *et al.,* 2000]. Four of them, PM I and II, Histoaspartic protease (HAP, known previously as PM III), and PM IV reside in the food vacuole and can degrade haemoglobin or globin [Sijwali *et al.*, 2001] The four plasmepsins are highly homologous to each other, sharing more than 60% amino acid identity [Bhaumik *et al.*, 2011]. HAP is unique in that it has a histidine in place of the first canonical aspartic acid [Bhaumik *et al.*, 2009] but is an active protease that may function by an aspartic [Bjelic *et al.*, 2004] or serine protease mechanism [Andreeva *et al*., 2004].

4.2 Histo-aspartic Protease (HAP) of *P.falciparum* as a drug target

P. falciparum HAP is the most divergent vacuolar Plasmepsins [Banerjee *et al*., 2002] with no counterpart in other characterized species of *Plasmodium*. The unique properties of HAP make it an especially attractive protein for the development of novel antimalarial drugs.

The unique features of HAP are as follows

(i) HAP is novel due to its unique structure of active site (39% identity with Plm II) with several significant deviations from the pepsin standard. In particular, Asp32, which together with Asp215 creates the catalytic dyad in classic aspartic proteases, is replaced by a histidine, giving this enzyme its name, **Histo-aspartic protease**.

(ii) In the apoenzyme crystal HAP forms a tight dimmer not seen in any aspartic protease I, II and IV.

(iii) A zinc ion present in the active site is tetrahedrally coordinated by His32 and Asp215 from one molecule, Glu278A located in the intruding loop of the other molecule and by a water molecule.

(iv) The presence of water molecule in active site helps to form hydrogen bond in the interaction of enzyme substrate catalysis in mechanism of action of HAP.

(v) Substitution are found in the functionality important flexible loop called the "flap" (residues 70-83) which changes its conformation upon ligand binding and thus participate in catalysis.

(vi) The structure of the HAP−KNI-10395 complex crystals indicates the presence of a domain-swapped dimer. The type of domain swapping reported here has not been seen in any other plasmepsins, or indeed in any other aspartic proteases.

4.3 HAP enzyme classification

According to International Union of Biochemistry (IUB), the present system of classification of enzyme is based on reaction specificity. Accordingly the EC number of Plasmepsins III (HAP) is 3.4.23.23B. Recombinant HAP enzyme structure has 328 amino acid residues. To identify the position of amino acid in the structure pepsin numbering has been followed.

4.4 Substrate specificity of the enzyme

The recombinant HAP enzyme reacts on haemoglobin which is represented as fluorescent synthetic peptide substrate EDANS-CO-CH_2-CH_2-CH_2-CO-Ala-Leu-Glu-Arg-Met-**Phe-Leu**-Ser-Phe-Pro-Dap-(DABCYL)-OH(2837b) with a cleavage site of Phe-Leu at PH 5.2.[Xiao *et al*., 2010] The flexible pentapeptide substrate; Met-**Phe-Leu**-Ser-Phe (corresponding to residues 32-36 of human haemoglobin α-chain) binds into the surface of HAP enzyme. This fragment is located in the region joining two α helices. Upon haemoglobin dissociation, 32-36 fragments is exposed into solution and become available to the proteolytic enzyme.

4.5 Structural feature of HAP enzyme

The recombinant HAP protease structure contains 328 amino acid residues. The crystal structure of HAP apoenzyme was found to make a tight dimer involving very close contacts of the C-terminal domains, whereas the N-terminal domains are pointing away from each other [Bhaumik P *et al.*, 2009]. Because of formation of the dimer, the C-terminal helix (residues 225–235) and the loop (residues 238–245) are displaced from their position usually seen in pepsin-like aspartic proteases. As a result of formation of this tight dimer, the loop consisting of residues 276–283 of the second molecule is inserted into the putative active site of the first molecule. An unusual feature found in the crystals of unliganded HAP is the presence of a zinc ion in the active site of each monomer, interacting with His32 and Asp215. Two hydrophobic residues, Ile279A and Phe279B, from the same loop are packed inside a hydrophobic pocket formed by Phe109A, Ile80, Met104, Ile107, and Val120 of the first monomer. Four additional Zn ions are found on the surface of the HAP dimmer. Two of them are located in equivalent positions in each monomer and are coordinated to His204 and Asp202. The third Zn ion interacts with Asp 114 and His 193 of monomer A and water molecule, and the fourth one is coordinated by Glu54 and Glu57 of monomer A and by Glu57. It is unlikely that these additional Zn ions play any role in the mechanism of catalysis by HAP. Salt bridge formed at the interface between the monomeric forms is the major driving force for the formation of dimmer mediated by basic and acidic amino acid residues since the amino acid com position of HAP is rich in lysine, arginine, glutamic acid and aspartic acid, which accounts of 22.6% of the total amino acid (328aa).

4.5.1 Flap region of HAP enzyme

The most essential difference is noticed in flap region of HAP enzyme in compare to other three plasmepsins. The major peculiarity of HAP enzyme is the presence of free space under the flap which was formed due to replacement of bulk Try 77 by Ser 77 residue. The flap is closed in the structure of the Pepstatin-A complex, whereas it is open in the complex with KNI-10006. The flap pocket is predominantly hydrophobic in PMs and other aspartic proteases. However, an insertion of Phe109A in HAP and PMII or Leu109A in PMIV changes the architecture of this pocket and makes

it even more hydrophobic in PMs. Two hydrophobic residues Ile279A and Phe279B are packed inside a hydrophobic pocket. Another important residue, located at the entrance to the flap pocket, is Phe111 in HAP, substituted by threonine in PMII and by leucine in PMIV. These differences between PMs may bear on their specific ligand preferences. The conformation of the inserted residue changes in the complexes with different ligand in order to optimize the interactions with the moieties inserted in the pocket. The change, upon ligand binding, of the flap conformation from open to close is accompanied by a dramatic change in the conformation of Trp39 [P. Bhaumik *et al*, 2009].The flap is mobile structural element of all aspartic protease. The flap movement involves not only changes of the 'up and down' position but also shift from the flap plane due to alternation of torsion angles of the residues at the loop "root" [Popov *et al.*, 2008].

4.6 Substitution in recombinant HAP enzyme

The Plm-II is the first crystal structure development by x-ray crystallographic method in the plasmepsins family. The recombinant HAP enzyme structure was found out in latter stage incorporated with substitutions both in active and flap regions. The difference in amino acid sequence of Plm-II and HAP potentially important for catalysis is presented in Table 4.1

Table 4.1 Comparison of active site of Plasmepsins II and HAP

Plasmepsins II	HAP	Result of replacement
Asp34	His34	Hinders the general base catalysis
Gly36	Ala36	Unfavourable for the formation of a hydrogen bond between the NH of substrate residue in position *P2'* and CO of residue 36, which is inherent in pepsin-like enzyme
Flap region		
Glu74	Lys74	Substitution of a positive for a negative charge
Met75	Leu75	Leu is shorter than Met, which releases additional space under the flap
Tyr77	Ser77	Inactivates pepsin-like enzyme, releases extra space under the flap
Val78	Lys78	Additional positive charge
Tyr192	Met192	Excludes the formation of hydrogen bond between the CO of a substrate residue in position *P2'* and Tyr 192 OH, which is found in many pepsin-like enzymes
Gly216	Ala216	Unfavourable for the formation of a hydrogen bond between NH of the substrate residue in position *P1'* and CO of residue 216, which is formed in all pepsin-like enzymes

4.7 HAP enzyme active site

The active site of HAP is located in a large cleft formed by the N- and C-terminal domains of the protein. Whereas the overall architecture of the active site is preserved, a crucial difference in HAP is the replacement of the canonical aspartate from the N-terminal domain by His32. The other functionally important substitutions are found in the flap area, where the commonly conserved Tyr75 and Val/Gly76 residues are replaced in HAP by Ser and Lys, respectively. The two active sites in the dimeric apoenzyme are practically identical. Each of them contains a Zn ion bound to side chains that belong to both molecules of the dimmer. The Zn ion is tetrahedrally coordinated by the side chains of His32 and Asp215 from one HAP monomer, Glu278A from the other monomer, and a water molecule. The presence of Zn^{2+} cation in the HAP active site has disrupted the conserved catalytically important hydrogen bond between the side chains of Asp215 and Thr218. His32 is hydrogen bonded to the side chain of Ser35 which interacts with Trp39 via a water molecule.Glu278A is located in the loop consisting of residues 274−285, which is inserted into the partner active site, leading to the observed opening of the flap. Since the flap is in an open position in the apoenzyme, Ser75 and Lys76 are far away from the active site.

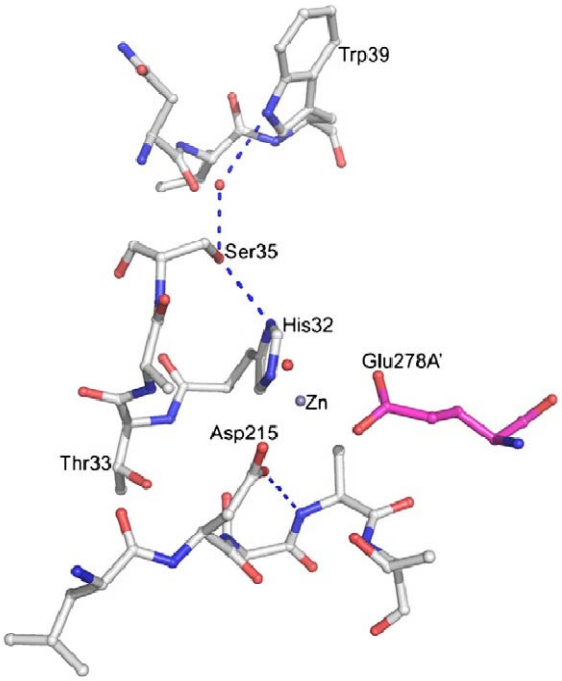

Fig: 4.1 Active site of recombinant HAP

4.8 HAP enzyme activity

The theoretical molecular mass of mature mtHAP monomer is 37.4 kDa. The experimental study of monomer-dimer equilibrium of recombinant HAP enzyme from enzyme-substrate reaction study shows that the recombinant HAP enzyme is more active as monomer. The HAP enzyme exists on dynamic monomer-dimer equilibrium at enzyme concentration 0.05mg/ml at PH 5.2. It was found from experiment that HAP easily formed a dimer or higher oligomeric form in concentration greater than 0.05 mg/ml while dimerisation results in loss of activity. Dimer formation may results in loss of enzyme activity due to the pronounced conformational changes in flap and loop regions, after formation of dimer, which also found in the structure of apoenzyme.

In order to determine the rates of substrate hydrolysis by mtHAP as a function of total enzyme, varying concentrations (0.05μM, 0.1μM, 0.2μM, 0.4μM, 0.8μM, 1.6μM, 3.2μM, 4.8μM and 6.4μM) of purified mtHAP were used in combination with 12μM of substrate [2837b] at pH 5.2 (100mM sodium acetate) at 25◦C. The dominant monomer form of recombinant HAP enzyme showed a Km value 2μM and turnover number, K_{cat} of 0.036 s^{-1}. The Km gives the measurement of affinity of enzyme and substrate. A low Km value indicates strong affinity between enzyme and substrate [Xiao *et al.*, 2010].

4.8.1 Role of pH in enzyme activity

HAP isolated from *Plasmodium*, the native HAP from food vacuole of malaria pathogen exhibits it maximum activity at PH (5.5-6.0) while the recombinant HAP enzyme is most active at pH5.2.The extent to which the flap opens at neutral PH, allowed the bulkier substrate to diffuse into the active site and provide best 'enzyme-substrate fit' for the specific substrate. In the acidic pH, there is a decrease opening of flap, thereby accommodating more substrate. It was suggested that a conformation changes in enzyme might lead to the increase activity.

4.9 Catalytic mechanism of HAP enzyme

The available structural & biochemical data do not provide an unambiguous answer about the exact nature of the catalytic mechanism of this unusual enzyme. The

unique nature of active site of HAP led to difficulties in elucidating its catalytic mechanism. Two different hypothesis have been developed (a) HAP is a serine protease with a catalytic triad of His 34, Ser 37 and Asp 215 [Andreeva *et al*., 2010] or (b) HAP is a novel protease with Asp214 acting as both the acid and the base during substrate catalysis with His34 providing critical stabilization [Bjelic *et al.*, 2004]. The recent structural study of HAP enzyme the hypothesis (a) is disproved. So the second hypothesis of catalytic mechanism proposed by Bjelic S *et al.,* now is in vogue with the Asp 215 and His 32 which is only stabilized in reaction pathway through a strong interaction with the developing positive charge, because its position is not optimal for functioning as either an acid or base catalyst.

4.9.1. Role of histidine in protonation for functionality of HAP

The enzymes require appropriate protonation of catalytic residues for optimal activity. In HAP, at pH optimum near 6, the active site histidine may function in the protonated state and acts as general acid, if its pK_a remains 6-7, the pK_a range of free histidine. Alternatively the pK_a of histidine may be lower in the micro environment of active site, causing histidine to be unprotonated at a general base near pH 6. A precedent exists for aspartic acid being sufficient for catalysis. Activity in basic pH range would also suggest that positive charge on histidine is not critical for HAP functionality because the residues would likely be neutral at PH 8.0, given that free histidine has free pK_a of 6.5.So the neutral state of histidine would, therefore, not be able to contribute a positive charge to substrate catalysis. So the mechanism takes place by aspartic acid residue with the substrate in presence of histidine, which only strengthens the catalytic action.

4.10 HAP enzyme inhibitor

The unique properties of HAP make it an especially attractive protein to target for antimalarial drug development. HAP apparently has high affinity for aspartic protease inhibitor Pepstatin-A [Banerjee *et al.*, 2002].

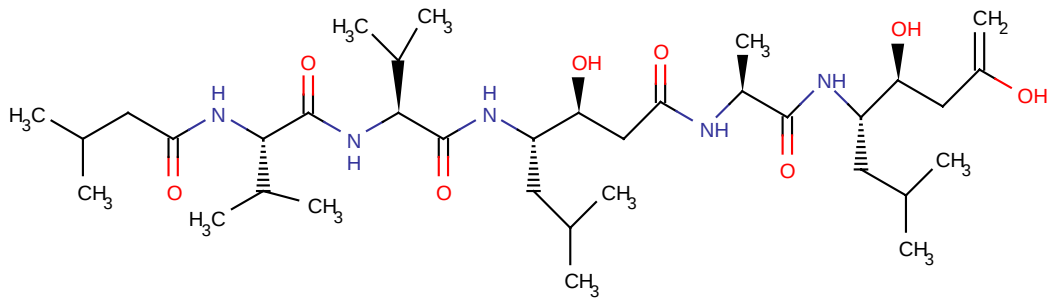

Fig.4.2 (a) 2D structure of Pepstatin-A

KNI compounds are peptidomimetic inhibitors containing flexible and asymmetric functional groups are proposed to be high affinity inhibitors of vacuolar Plasmepsins [Hidaka *et al,* 2003]. Many KNI compounds utilize a common molecular scaffold containing an allophenylnorstatine moiety followed by a thioproline ring. From the KNI series; KNI-10006 is the only one weakly active compound so far been reported as an inhibitor of HAP [Bjelic *et al.*, 2004]. KNI-10395 of this class is also a potent inhibitor of HAP [Bhaumik *et al.*, 2011].

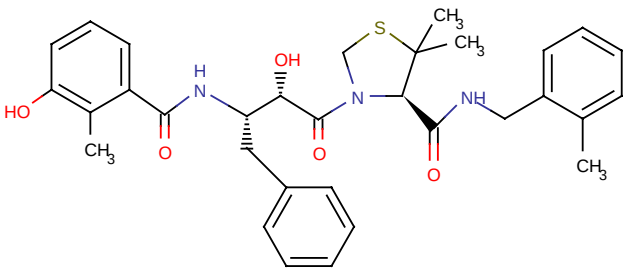

Fig.4.2 (b) 2D structure of KNI-10006

4.10.1 HAP-Pepstatin-A complex

HAP binds Pepstatin-A with a very high binding affinity (Ki=81pM). The binding mode of Pepstatin-A in HAP lies in an extended conformation, with the statine hydroxyl positioned between Asp215 and His32. However, binding of the C-terminal half of the inhibitor is distinctly different from that found in complexes with PMs and other pepsin-like proteases. The flap is closed in the structure of the complex.

4.10.2 HAP - KNI-10006 complex

KNI-10006 is a peptidomimetic inhibitor designed based on the on the concept of "substrate transition-state mimicry" with the central core made of allophenylnorstatine. KNI-10006 is a potent inhibitor of HAP with an IC_{50} of 0.69 μM. The binding mode of KNI-10006 to HAP is drastically different from that of Pepstatin A. The predominant interactions of KNI-10006 are with the flap, and this inhibitor does not make any contact either with loop 287−292 or with several other hydrophobic residues [Bhaumik *et al*, 2009].

4.10.3 HAP-KNI-10395 complex

The structure of the HAP−KNI-10395 complex was determined at 2.5 Å resolutions. The mode of binding of KNI-10395 in these sites is similar but differs substantially from the way in which other peptidomimetic inhibitors bind to aspartic proteases. The conformation of the inhibitor is considerably deformed, with the main chain turning back on itself, creating a U-shaped structure. This structure is internally stabilized by two hydrogen bonds, one between the peptide amino group of the 2-aminoindanol moiety and the peptide carbonyl of the methylthioalanine and the other between the peptide amino group of the methylthioalanine and the hydroxyl group of the 2-aminoindanol moiety. The inhibitor is bound to the enzyme by 25 hydrogen bonds, either direct or through water molecules [Bhaumik *et al.*, 2011].

4.11 Urgency of new antimalarial

Ideally, new drugs for uncomplicated *P. falciparum* malaria should be efficacious against drug-resistant strains, provide cure within a reasonable time (ideally three days or less) to ensure good compliance, be safe, be suitable for small children and pregnant women, have appropriate formulations for oral use and above all be affordable. Most antimalarial drugs that are now in use were not developed on the basis of rationally identified targets, but following the serendipitous identification of the antimalarial activity of natural products (for example, quinine and artemisinin). Alternatively, targets can be selected from enzymes or pathways that are present in the malaria parasite but absent from humans.

Older approaches to target validation include the demonstration that an inhibitor has potent antimalarial activity. This approach is limited, however, by the fact that it is often difficult to determine whether an inhibitor of a particular plasmodial target is exerting its antimalarial activity specifically by the predicted mechanism of action. This problem is partially solved by the repeated demonstration of antiparasitic activity of different inhibitors of a particular target, by the identification of very potent (generally low-nanomolar) activity.

4.12 The need for drug combination

There is a growing consensus that drug combinations are essential for the optimal control of malaria in developing countries. Combinations potentially offer a number of important advantages over monotherapy. First, they should provide improved efficacy. Appropriately chosen combinations must be at least additive in potency, and might provide synergistic activity. Second, drug combinations increase the likelihood that, in the setting of drug resistance, at least one agent will be clinically active. Third and probably most important drug combination should reduce the selection of antimalarial drug resistance.

4.13 Hybrid antimalaria drug: Art-Qui-OH

Art-Qui-OH (Fig.4.2) is a novel and potent anti malarial compound with an IC_{50} value of 8.95 nM and 9.59 nM after 48 hrs of incubation for chloroquine sensitive and resistant strain [Walsh *et al,* 2007]. Experimental reports revealed that there is paucity of information about the possible molecular interaction of artemisinin based hybrid antimalarial with plasmepsins [David A Fidock *et al.,* 2004]. Additionally artemisinin-quinine hybrid compound has higher half life than its lipophilic, fast-acting artemisinin entity with the coupling of the slow-acting, polar quinine derivative.So as a proof-of-concept we conceptualize to evaluate in silico the binding mode and relative binding affinity of Art-Qui-OH with the Histo-Aspartic Protease (HAP) of *P.falciparum.* The reason of choosing HAP as the drug target is that, HAP is the most divergent vacuolar plasmepsins, with no counterpart in other characterized species of *Plasmodium* [Bahumik P *et al.*, 2011].

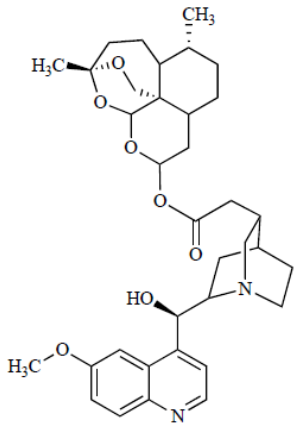

Fig.4.2(c) Dihydroartemisinin-quinine hybrid

4.14 Materials and Methods

4.14.1 Preparation of protein

The 3-D structure of HAP with two inhibitor Pepstatin-A (PDB ID: 3FNT) and KNI-100006 (PDB ID: 3FNU) have been used as receptor binding site. The presence of Zn ion and H_20 molecule along with His32, Glu 278A and Asp 215 residue in the active site claimed a unique and novel active site in compare to other classical Plasmepsins. The structure of recombinant HAP from malaria-causing parasite *P.falciparum* as an apoenzyme (3FNS) forms a tight dimmer not seen previously in any aspartic protease. Hydrogen atoms were added to the model using Maestro interface (version 8.5; Schrodinger LLC, New York) based on an explicit all atom model. Final preparation of was done using the multi step Schrodinger's protein preparation tool (PPrep) followed by energy minimization using OPLS 2005 force field with Polak−Ribiere Conjugate Gradient (PRCG) algorithm.

4.14.2 Ligand preparation

The two dimensional structure of artemisnin-quinine hybrid was collected from published data [Walsh *et al.*, 2007]. ISIS Draw 2.3 software has been used for sketching structure and converting it its 3D representation by using ChemSketch 3D viewer of ACDLABS 12.0. LigPrep was used for final preparation of ligands for docking. LigPrep is a utility of Schrodinger software suit that combines tools for generating 3D structures from 1D (Smiles) and 2D (SDF) representation, searching for

tatutomers and steric isomers and perform a geometry minimization of ligand. Ligprep utility produces a number of structures from each input structure with various ionization states, tautomers, stereochemistry, and ring conformations. The program automatically generated all possible stereoisomer's (default value of 32 was used) for each ligand. Furthermore, a unique low-energy ring conformation for each stereoisomer with correct chirality was generated with the help of Ligprep. All structures were subsequently subjected to molecular mechanics energy minimization using Macro Model with a convergence threshold of 0.05 and maximum iteration 500. These geometrically optimized structures were used for Glide (grid-based ligand docking with energetics) docking.

4.14.3 Molecular docking of artemisinin-quinine hybrid to HAP

All docking calculations were performed using the "Extra Precision" (XP) mode of Glide docking (version 4.5, Schrodinger Inc.) with the 2005 implementation of the OPLS-AA force field. Briefly, Glide approximates a systematic search of positions, orientations, and conformations of the ligand in the receptor binding site using a series of hierarchical filters. The shape and properties of the receptor are represented on a grid by several different sets of fields that provide progressively more accurate scoring of the ligand pose. The binding site is defined in terms of two concentric cubes: the bounding box, which must contain the mass centre of any acceptable ligand pose, and the enclosing box, which must contain all the atoms of a ligand pose for successful docking into the binding site. Glide also performed conformational searches for each input structure during docking process. A set of initial ligand conformations is generated through exhaustive search of the torsional minima and the conformers are clustered in a combinatorial fashion. Each cluster, characterised by a common conformation of the core and an exhaustive set of side-chain conformations, is docked as a single object in the first stage. The search begins with a rough positioning and scoring phase that significantly narrows the search space and reduces the number of poses to be further considered to a few hundred. These selected poses are energy minimized on pre computed OPLS-AA van der Waals and electrostatic grids for the receptor. In the final stage, the 5−10 lowest-energy poses obtained in this fashion are subjected to a Monte Carlo sampling in which nearby torsional minima are examined,

and the orientation of peripheral groups of the ligand is refined. The minimized poses are then rescored using the Glide Score function.

In this work the bounding box of size 10 Å×10 ×10 Å was defined Histo-Aspartic Protease and centred on the mass centre of the crystallographic KNI-10006 and Pepstatin-A to confine the mass centre of the docked ligand. The larger enclosing box with an edge length of 10 Å was also defined (which occupied all the atoms of the docked poses) in terms of the co-crystallized ligand. The scale factor of 0.4 for van der Waals radii was applied to atoms of protein with absolute partial charges less than or equal to 0.25. Five thousand poses per ligand were generated during the initial phase of the docking calculation, out of which best 1000 poses per ligand were chosen for energy minimization. Energy minimization protocol included dielectric constant of 4.0 and 1000 steps of conjugate gradient minimizations. Upon completion of each docking calculation, 100 poses per ligand were generated and the best docked structure was chosen using a Glide Score (G_{score}) function. Glide Score is a more sophisticated version of Chem Score with force field-based components and additional terms accounting for solvation and repulsive interactions.

4.14.4 Post-scoring with MM-GB/SA

The artemisinin-quinine hybrid, KNI-10006 and Pepstain-A that have been pre positioned with Histo-Aspartic Protease from Glide docking have been used to study the association of these ligands with the receptor using the automated mechanism of multi-ligand bimolecular association with energetic (Prime/MM-GBSA version 9.0; Schrodinger, LLC, New York).

For each ligand, the pose with the lowest Glide score was rescored using Prime/MM-GBSA approach. This approach is used to predict the free energy of binding for set of ligands to receptor. The docked poses were minimized using the local optimization feature in Prime and the energies of complex were calculated using the OPLS-AA force field and generalized-Born/surface area (GB/SA) continuum solvent model. The binding free energy (ΔG_{bind}) is then estimated using equation:

$$\Delta G_{bind} = E_{R:L} - (E_{R+}E_L) + \Delta G_{solv+} \Delta G_{SA}$$

Where $E_{R:L}$ is energy of the complex, E_R+E_L is sum of the energies of the ligand and unliganded receptor, using the OPLS-AA force field, ΔG_{solv} (ΔG_{SA}) is the difference between GBSA solvation energy (surface area energy) of complex and sum of the corresponding energies for the ligand and unliganded protein.

4.15 Result

4.15.1 Calculation of experimental binding energy (ΔG^{bind}_{exp})

The binding energy has been calculated with the following empirical formula.

ΔG^{bind}_{exp} = 2.303 RT log Ki where R=0.001986 kcal/mol & T=298 K

HAP-KNI10006 complex with Ki=0.028 nM*

*The Ki value of KNI-10006 against HAP was calculated as 0.028 nM; (Ki of PlmII/Ki of HAP) is 17.7 (Ki for Plm II=0.5 nM)

$\Delta G^{bind}_{exp} = 2.303 \times 0.001986 \times 298 \times \log (0.028 \times 10^{-9})$

ΔG^{bind}_{exp} = -14.38 kcal/mol.

HAP-Pepstain-A complex with Ki= 0.081nM

The Ki value of Pepstatin-A against HAP was calculated from the kinetic parameter as 81pM (0.081 nM).

So with the above empirical formula; ΔG_{exp} = -13.75 kcal/mol

4.15.2 Calculation of calculated binding energy ($\Delta G^{bind}_{cald.}$)

All docking calculations were performed using extra precision (XP) mode of Glide docking version 4.5 Schrödinger Inc with implementation OPLS-AA force field.

Table 4.2 ΔG_{score} for Pepstatin-A, KNI-10006 and Art-Qui-OH hybrid

Receptor	Ligand	Glide Score $_{(G\ score)}$	Glide energy	Glide E_{model}	ΔG_{score}
HAP	KNI-10006	-8.777	-40.436	0.000	1.317
HAP	Pepstatin-A	-8.758	-19.222	0.000	1.298
HAP	Art-Qui-OH	-7.460	-32.824	-44.216	_

$\Delta G_{score} = G_{score\text{-}Art\text{-}Qui\text{-}OH} - G_{score\text{-}Pepstain\text{-}A/KNI\text{-}10006}$

Table 4.3 ΔG^{exp}_{bind} & ΔG^{calc}_{bind} for Pepstatin-A, KNI-10006 and Art-Qui-OH hybrid

Receptor	Ligand	ΔG^{exp}_{bind} [a]	ΔG^{calc}_{bind}	$\Delta\Delta G_{bind\text{-}cald}$ (kcal/mol)
HAP	KNI-10006	-14.38 [b]	-14.10	3.44
HAP	Pepstatin-A	-13.75 [c]	-13.09	2.43
HAP	Art-Qui-OH	_	-10.66	_

All the energy parameters are expressed in kcal/mol

$\Delta\Delta G_{bind\text{-}cald} = \Delta G^{calc}_{bind\text{-}}$ *Art-Qui-OH* $- \Delta G^{calc}_{bind\text{-}}$ *Pepstatin-A/KNI-10006*

[a] ΔG^{bind}_{exp} is calculated using the relationship $\Delta G^{bind}_{exp} = 2.303$ RT log Ki

[b] Value from Ref [Nezami *et al*, 2003]

[c] Value from Ref [Banerjee *et al*, 2002]

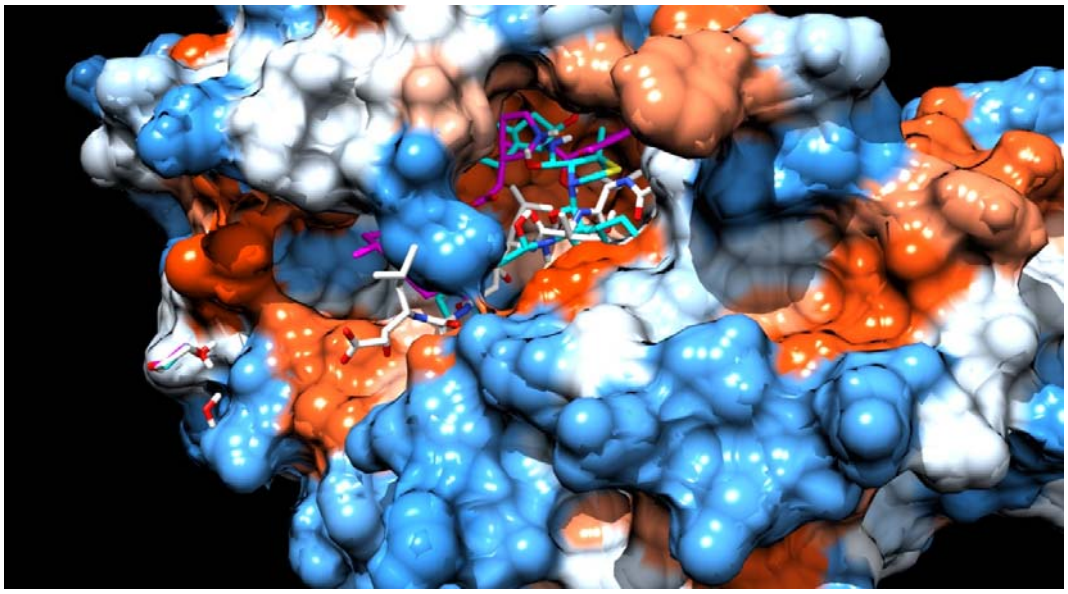

Fig.4.3 Overlapped docking poses of Pepstatin-A, KNI-10006 and Art-Qui-OH obtained from Glide docking in the active site of Histo-Aspartic Protease. (Magenta= Art-Qui-OH, Cyan=KNI-10006, Silver=Pepstatin-A)

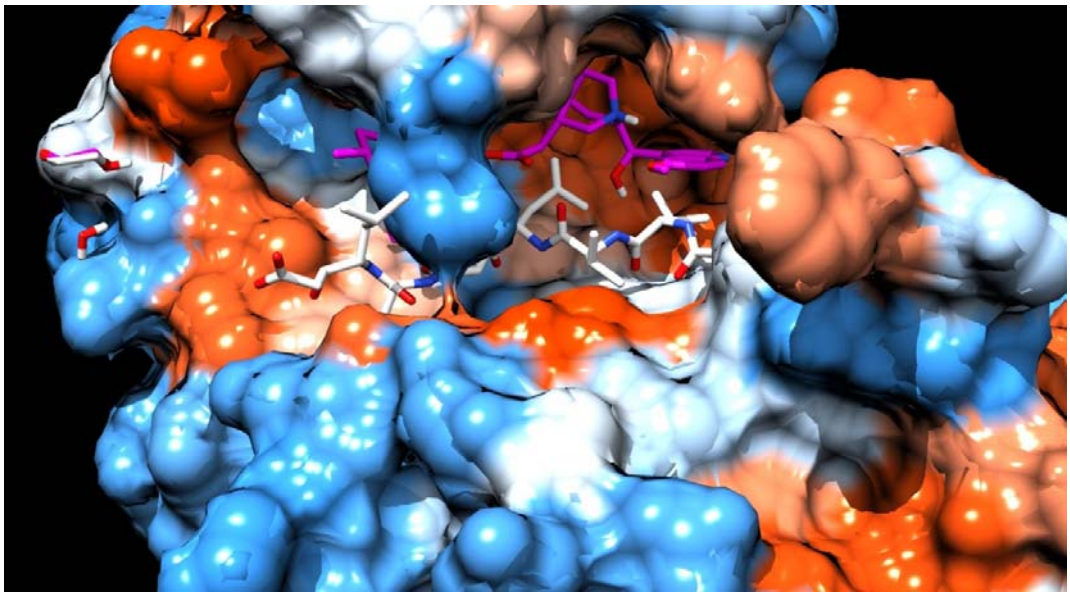

Fig.4.4 Overlapped docking poses of Pepstatin-A, and Art-Qui-OH obtained from Glide docking in the active site of Histo-Aspartic Protease (Magenta=Art-Qui-OH, Silver= Pepstatin-A)

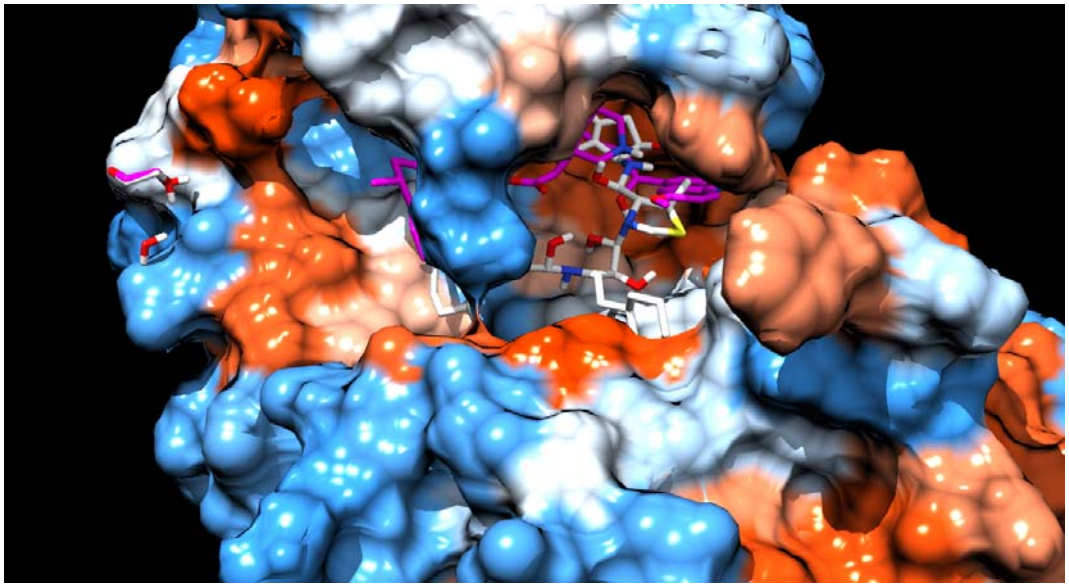

Fig.4.5 Overlapped docking poses of KNI-10006, and Art-Qui-OH obtained from Glide docking in the active site of Histo-Aspartic Protease (Magenta= Art-Qui-OH, Silver=KNI-10006)

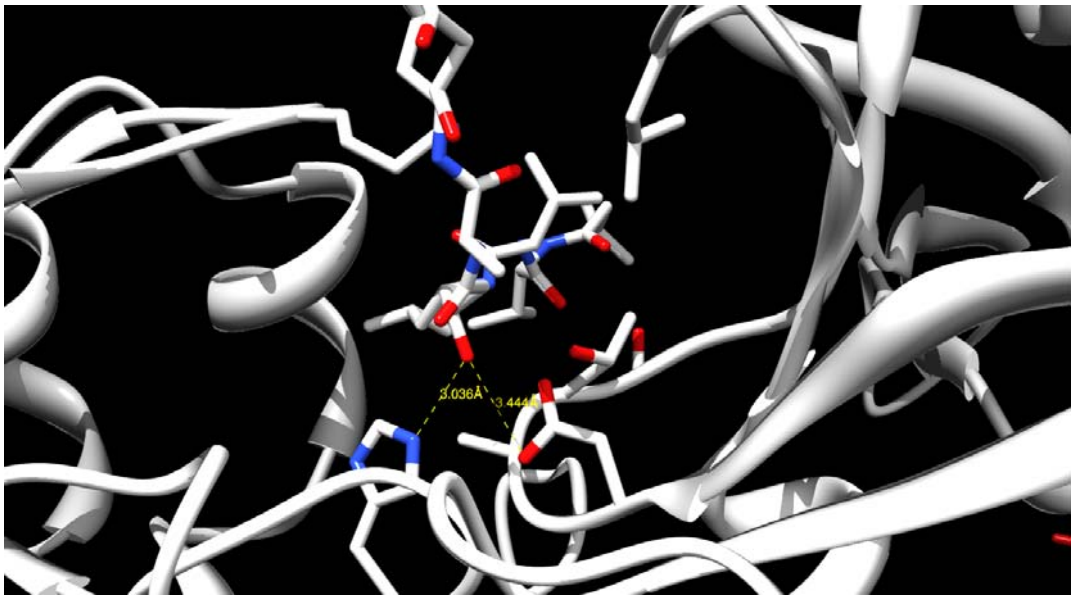

Fig. 4.6 Illustrates the position of central hydroxyl group of Pepstatin-A from the His32 and Asp215 of HAP structure.

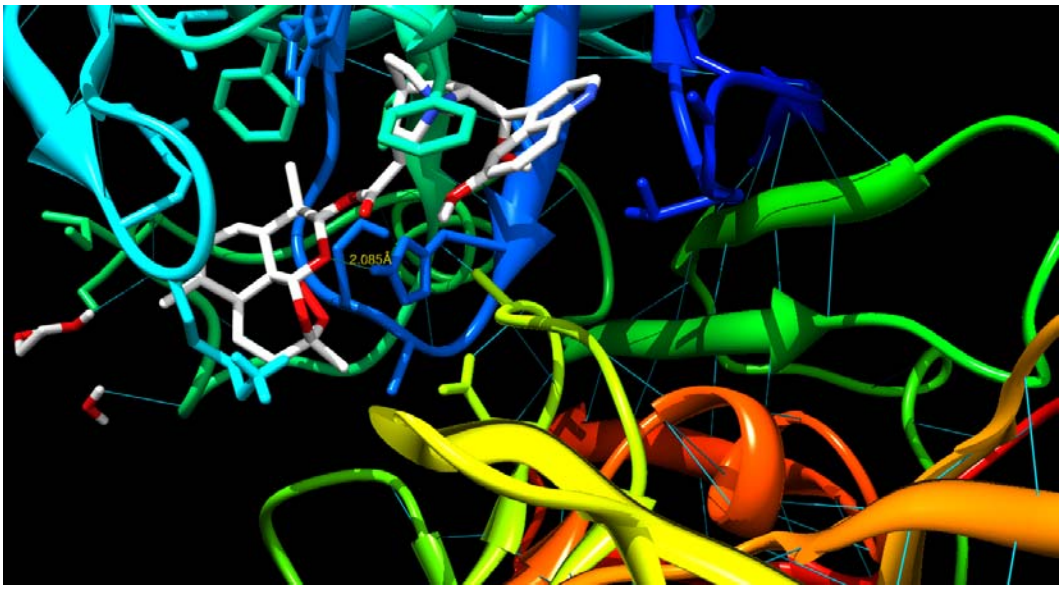

Fig. 4.7 Illustrates the H-bond interaction of His32 and O11 atom of Art-Qui-OH

4.15.3 Validation of the docking method by reproducing the crystallized HAP-KNI10006 and HAP-Pepstatin-A complex

The original crystal structure of HAP-Pepstain-A complex (PDB ID: 3FNT) & HAP-KNI-10006(PDB ID: 3FNU) complex were used to validate the Glide-XP docking protocol. This was done by moving the crystallized ligand outside of active site and then docking it back into the active site. The top 6 configurations after docking were taken into consideration to validate the result. The root mean square deviation (RMSD) for each configuration in comparison to the co-crystal of KNI-10006 was 0.000-1.384 Å. Whereas the RMSD value calculated from Pepstatin-A of each configuration was 0.000-1.248 Å. This revealed that the docked configurations have similar binding positions and orientations within the binding site and are similar to the crystal structure. The best docked structures, which are the configurations with the lowest G_{score}, were compared with the crystal structure as shown in the table .These docking results illustrate that the best docked KNI-10006 and Pepstatin-A complex agrees well with its crystal structure.

Table 4.4 The RMSD and docking score from the docking simulation of 6 lowest configurations of co-crystal Pepstatin-A with Histo-Aspartic Protease (3FNT)

Configuration	Glide Score	ΔG Score [a]	RMSD [b] (Å)
1	-8.758	0	1.132
2	-8.405	0.35	0.000
3	-8.369	0.38	1.217
4	-7.970	0.78	0.000
5	-7.922	0.83	1.112
6	-7.773	0.9	1.248

[a] $\Delta G\ Score = E_i - E_{lowest}$

[b] RMSD, RMSD between docked and co-crystal structure Pepstatin-A

Table 4.5 The RMSD and docking score from the docking simulation of 6 lowest configurations of co-crystal KNI-10006 with Histo-Aspartic Protease (3FNU)

Configuration	Glide Score	ΔG Score [a]	RMSD [b] (Å)
1	-8.777	0	1.384
2	-8.527	0.25	0.000
3	-8.079	0.69	0.433
4	-7.956	0.82	1.304
5	-7.917	0.86	0.589
6	-7.383	1.39	0.000

[a] ΔG Score= $E_i - E_{lowest}$

[b] RMSD, RMSD between docked and co-crystal structure KNI-10006

4.15.4 Calculation of Ki value

The Ki value of Art-Qui-OH complex with HAP enzyme has been calculated as follows.

$\Delta G^{calc}_{bind} = 2.303\ RT \log (Ki)$

$\text{Log Ki} = \Delta G^{calc}_{bind} / 2.303RT$

$= -10.66 / 2.303 * 0.001986 * 298$

$= -7.821$

$\text{Ki} = \text{antilog}(-7.821) = 15.10\ \text{nM}$

4.16. Discussion

4.16.1 Glide docking and rescoring using MM-GB/SA of ligands

Molecular docking methods are widely used by academic institutes and pharmaceutical industries to study drug-target interactions in order to understand the basic electronic/steric features required for therapeutic action and to design new drug candidates with improved activities. These docking calculations provide insight into

interactions of ligands with amino acids in the binding pocket of a target and to predict the corresponding binding affinities of ligands [Krovat *et al.*, 2005]. Table 4.2 presents the Glide XP docking results of KNI-10006, Pepstatin-A, and Art-Qui-OH. Their Glide score values range from -7.397 to -8.777 kcal/mol. The relative docking scores (ΔG_{score}) of Art-Qui-OH with reference to HAP-Pepstatin A complex is 1.29 kcal/mole where as it is estimated to be 1.38 kcal/mol HAP-KNI-10006 complex (Table 4.2). These results demonstrate that binding mode of Art-Qui-OH resembles to Pepstatin-A in compare to KNI-10006 in HAP active site (Fig.4.3). Although more computationally demanding, the MM-GB/SA scoring generally yields far superior correlations with experimentally scoring functions [Bernacki *et al.*, 2005, Huang *et al.*, 2006, Lyne *et al.*, 2006]. The docked complexes were rescored with MM-GB/SA and the relative binding energy ($\Delta\Delta G_{bind\text{-}cald}$) of Art-Qui-OH was calculated using Pepstatin-A and KNI-10006 as reference. The binding mode of KNI-10006 is drastically different from the Pepstain-A binding in HAP binding site. The predominant interactions of KNI-10006 are within the flap; the flap is closed in the structure of the Pepstatin-A complex, whereas it is open in the complex with KNI-10006. The drop in calculated relative binding energy ($\Delta\Delta G_{\ bind\text{-}cald}$) for Art-Qui-OH revealed strong binding (2.43 kcal/mol); with a similar conformation to Pepstatin-A binding (Fig.4.4) in compare to KNI-10006 conformation (Fig.4.5) having a $\Delta\Delta G_{\ bind\text{-}cald}$ value of 3.44 kcal/mol (Table 4.3). From the binding energy, the Ki value of the hybrid compound is calculated to be 10.15nM.

4.16.2 Inhibitor (Art-Qui-OH) binding to HAP

Pepstatin-A was noted to bind in an extended conformation, with the statine hydroxyl positioned between Asp215 and His32 (Fig.4.6). The binding mode of Pepstatin-A in the active site of HAP indicates that Asp215 and His32 are very likely involved in the catalytic reaction. The KNI-10006 inhibitor predominantly interacts within the enzyme in the flap area. Unlike KNI-10006, the mode of binding of Art-Qui-OH hybrid drastically different and the hybrid interacts in the active site of the enzyme with O11 atom of Artemisinin moiety forming H-bond with His32 (Fig.4.7). The O11 atom of Artemisinin and His 32 $N^{\varepsilon}2$ H-bond distance is 2.085 Å (Fig.4.8). The H-bond distance is less than the H-bond diatance (3.036 Å) formed between statine hydroxyl group and His32 residue (Fig.4.6) in the active site of HAP. This revealed a strong

binding affinity between ligand and binding site residue. No interaction has been observed in the binding pose of Art-Qui-OH with the functionally important flexible loop called the "flap" (residue 70-83), which changes its conformation upon ligand binding. The replacement of Asp by a His residue in the enzyme active site and some other replacements indicate the possibility of a catalytic mechanism differing from that of aspartic proteases. However, up to now, there are no available data on HAP specificity, which could confirm its catalytic activity. Experimental study revealed the stabilizing role of His 32 residue in the substrate catalytic reaction of HAP enzyme. Bjelic and Aquist (2008) have suggested that the positive charge on His32 provides a critical stabilization (by a factor of ~10, 000) to the water/hydroxide nucleophile as well as developing negative charge on the substrate during catalysis. There is also supportive evidence that mutation of His 32 to alanine disrupt a hydrogen bonding network that is critical for proper positioning of the Asp 215 residue [Parr *et al.*, 2008]. On the basis of recent crystal structure of HAP-KNI-10395 complex (3QVI) it has also been postulated that His32 might be directly involved in providing the electrophillic component for the catalytic mechanism [Bhumik P *et al.*, 2011].

4.17 Conclusion

The *in vitro* experimental result of artemisinin-quinine hybrid against *Plasmodium falciparum* at IC_{50}(s) and $IC_{50(R)}$ were 8.95nM (48hrs) and 10.4nM (72hrs) respectively. The study further revealed the corresponding drug resistance value as 9.59 nM (48 hrs) and 10.2nM (72 hrs) respectively. Thus it was conclusively proved that artemisinin-quinine hybrid can act as a potent inhibitor against multi drug resistant malaria parasite. The study as outlined in the chapter, also provides three lines of evidences about the antimalarial activity of Art-Qui-OH, which can be summarized as (1) Art-Qui-OH binds near the Pepstatin-A binding site of Histo-Aspartic Protease (HAP) (ii) The relative binding affinity ($\Delta\Delta G_{\text{bind-cald}}$) of Art-Qui-OH is 2.43 kcal/mol against Pepstatin-A in compare to $\Delta\Delta G_{\text{bind-cald}}$ value of 3.44 kcal/mol against KNI-10006 (iii) The Ki value of the compound is computed to be 10.15nM.

Chapter-5

Computer-aided drug design for inhibition of a family of *Plasmodium falciparum* aspartic proteases by a designed adaptive inhibitor

5.1 Introduction

With regard to the enzymology of haemoglobin degradation in *P.falciparum,* two families of proteases play prominent roles. Four aspartic proteases called plasmepsins and three cysteine proteases called falcipains are found in the food vacuole [Sijwali *et al.*, 2001]. All of them are capable of degrading haemoglobin or globin in biochemical assays using recombinant enzyme, although their order of action is unclear [Rosenthal *et al.*, 2001]. Inhibitors of aspartic and cysteine proteases kill parasites in culture and animal models, although their specificity is not strict [Bailly *et al.*, 1992]. Knockouts of Plasmepsins individually or in combination (Plasmepsins IV/I double knockout) give parasites with only slightly impaired growth [Liu *et al.*, 2005, Omara-Opyene *et al.*, 2004] and a falcipain-2 knockout shows normal growth [Sijwali *et al.,* 2004]. The effect of aspartic protease inhibitors is potentiated when combined with cysteine protease inhibitors or used in falcipain-2 knockout parasites [Sijwali *et al.,* 2004]. Therefore the evidence suggests that there is overlap in and between the food vacuole proteolytic families; their relative roles remain unclear.

5.2 Functional redundancy of vacuolar plasmepsins

Data from Bozdech *et al.*, (2003) and Le Roch *et al.,* (2003) indicate that PfPM1 and PfPM4 are transcribed early in the asexual cycle and the steady-state level of the mRNA falls during the latter half of the cycle, whereas for PfPM2 and PfHAP, the amount of transcript present is low in the first half of the cycle and rises prominently in the second half. This suggests that perhaps PfPM1 and PfPM4 could complement for each other, whereas PfPM2 and HAP could functionally complement as the other pair.

5.3 Adaptive inhibitor for plasmepsins family

Drug molecules with the ability to inhibit several members of a protein family with high affinity have been termed adaptive drugs [Velazquez-Campoy *et al.*, 2001, Nezami *et al.*, 2002].Usually, one member of the family is considered the primary target (e.g., the wild type, the most abundant, the most active, etc.). Rational anti-Plasmepsins drug design strategies therefore must be revised to include approaches to identify compounds capable of inhibiting at least two if not all four of these enzymes,

without toxicity to the host. The practicality of this approach requires that the primary target and the remaining members of the family share a common three-dimensional structure and a high degree of sequence similarity within the binding cavity.

The sequences of the plasmepsins are 60-70% identical [Banerjee *et al.*, 2001] and they have similar tertiary structures. The two adaptive inhibitor so far been reported to inhibit Plasmepsins are the general aspartic protease inhibitor Pepstatin-A and the allophenylnorstatine bases inhibitor KNI-10006 [Banerjee *et al*, 2001, Hidaka *et al.,* 2003]

5.4 Plasmepsins II as a drug target

Two aspartic proteases of *P. falciparum* have been implicated in the initial steps of the haemoglobin degradation process [Francis *et al.*, 1994, Gluzman *et al.,* 1994, Dame *et al.,* 1994]. The first protease, Plasmepsins I (Plm I), appears to make a strategic initial cleavage that presumably leads to an unravelling of the native haemoglobin structure such that further proteolysis can rapidly proceed. Plasmepsins II (Plm II), the second aspartic protease, is capable of cleaving native haemoglobin but is more active against denatured or fragmented globin, such as that produced by the action of Plm I. Among the plasmepsins, Plm I & Plm II has the highest catalytic efficiency among Plasmepsins with substrates that mimic the initial cleavage site of the natural substrate, haemoglobin [Banerjee et *al.*, 2001]. In addition, it has been shown that Plm II from *P. falciparum* has unique specificity and binding characteristics compared to the same enzyme from other *Plasmodium* species [Westling *et al.*, 1997].

5.4.1 Structural features of plasmepsins II

The structure of Plm II has the typical bilobal shape and topology of eukaryotic aspartic proteases [Davies *et al.*, 1990]. The single chain of 329 amino acids is folded into two topologically similar N- and C-terminal domains related by a pseudo 2-fold rotation axis. The domains contact each other along the bottom of the binding cleft that contains the catalytic dyad, Asp-34 and Asp-214. A β-hairpin structure, known as the "flap," lies perpendicular over the binding cleft and interacts with substrates and inhibitors. The N and C ends of the polypeptide chain of Plm II are assembled into the

characteristic six-stranded inter domain β-sheet. Plm II contains two disulfide bridges, Cys47-Cys52 and Cys249-Cys285. The latter is conserved among all eukaryotic aspartic proteases, whereas the N-terminal disulfide is conserved only among mammalian enzymes, suggesting a closer evolutionary relationship of the malarial enzymes to their mammalian rather than fungal counterparts. A unique feature of Plm II is the substitution of Ser for Thr at residue 215 in the Asp-Thr-Gly signature sequence for the C domain. Ser has also been observed at this position in some retroviral aspartic proteases that are homodimeric enzymes; however, its functional significance is unclear.

5.4.2 Inhibitors of plasmepsins-II

Pepstatin-A, a general inhibitor of aspartic proteases of microbial origin [Umezawa *et al*, 1970] was reported to inhibit haemoglobin degradation by extracts of digestive vacuoles of *P. falciparum.* Inhibition studies on the recombinant PMII showed that Pepstatin-A is a picomolar (Ki=0.006 nM) inhibitor for this enzyme [Silva *et al*, 1996] this inhibitor was used in the initial crystallographic studies [Silva *et al*, 1996]. Pepstatin-A was reported to bind in the active site of PMII in an extended conformation [Asojo *et al,* 2003]. The central hydroxyl group of the inhibitor is inserted in between the carboxylate groups of Asp32 and Asp215. KNI-10006, reported by Hidaka *et al.,* (2003), a norstatine-based lead structure, possesses nanomolar inhibition against all four plasmepsins in the DV of Pf, and is remarkably potent in the case of PfPM2. The Ki value for PfPM2 was determined to be in the 0.5 ± 1 nM range. However, having a good activity towards several of aspartic proteases, KNI-10006 was also found to be an efficacious inhibitor (Ki = 2 nM) of the most closely related human aspartic protease, cathepsin D (hCatD). Another disadvantage with this compound was the low capacity to reduce parasite growth in Pf-infected erythrocyte cultures (IC_{50} = 6.8 μM), a shortcoming which partly might be explained by insufficient cell / vacuole membrane permeability.

5.5 Plasmepsins-I as a drug target

It has been postulated that the process of haemoglobin degradation is initiated by PMI cleaving the Phe33–Leu34 bond in the globin chain of native haemoglobin

(Moon *et al.*, 1997). The first crystal structures of PMI, for the apoenzyme and for a complex KNI-10006, have been determined only very recently [Bhaumik *et al.*, 2011]. PMI shares overall 73% sequence identity and 84% active site identity with PMII [Ersmark *et al.*, 2006].

5.5.1 Structural features of plasmepsins I

The mature molecule of PMI (329 residues) is folded into two topologically similar N- and C-terminal domains. A large substrate-binding cleft is located between them, delineating an active site with two catalytic aspartates, Asp32 and Asp215 (pepsin numbering) and nucleophilic water molecule bound between them. The N-terminal domain contains the ‘‘flap’’, another important structural element of the catalytic machinery. The amino and carboxyl ends of the two domains of PMI are assembled into a characteristic six-stranded inter domain β-sheet which serves to link the two domains together and is conserved in the aspartic protease family.

In the apo-PMI crystals, forming a non-crystallographic dimer, two molecules (A & B) are present in the asymmetric unit. In the active site of molecule A, the nucleophilic water molecule (Wat103) is present and located between Asp32 and Asp215, together with another water molecule, Wat179, found close to Asp32 [Bhaumik *et al.*, 2011].

5.5.2 Inhibitors of plasmepsins-I

The first crystal structures of PMI, for the apoenzyme and for a complex KNI-10006, have been determined only very recently The IC_{50} value of KNI-10006 for Plm-I is 0.28 μM [Nezami *et al.*, 2003]. In the PMI–KNI-10006 complex, the hydroxyl group of the Apns moiety of the inhibitor is placed in between the two catalytic aspartates. This central hydroxyl group of the inhibitor forms hydrogen bonds with the $O^{\delta 2}$ atoms Asp32 and Asp215. The phenyl group of the Apns moiety of KNI-10006 makes additional hydrophobic interactions with Val76 which is present at the tip of the flap in PMI. The 2, 6-dimethylphenyloxymethyl group of the inhibitor is placed in a hydrophobic pocket of the active site, making apolar contacts with Met73, Tyr75, Leu128, Ile130, and Tyr189. The 2-aminoindanol moiety is positioned by forming a

hydrogen bond between its hydroxyl group and the main chain NH group of Ser219 [Bhaumik *et al*., 2011].

5.6 Plasmepsins IV as a drug target

The interest in Plm IV is motivated by the fact that it is the only plasmepsins located in the food vacuole of *P. falciparum* which has ortholog in the other three Plasmodium species infecting humans [Dame *et al.*, 2003]. The crystal structure of Plasmepsins IV (1LS5) reveals dimers with extensive buried surface areas [Asojo *et al.,* 2003]

5.6.1 Structure feature of plasmepsins IV

The mode of binding of Pepstatin-A in the PMIV active site (structure 1LS5) is similar to the one observed in the PMII–Pepstatin A complexes, despite the differences between some amino acids located in the binding site pockets. Met73 and Val76 of the flap in PMII are replaced in PMIV by the less bulky Ile73 and Gly76, respectively. Other significant differences include Phe109A, Thr111, Ile287, Leu289 and Phe291 in PMII being substituted by Leu109A, Ile111, Leu287, Val289 and Ile291 in PMIV, respectively. Because of these substitutions, the binding pocket of PMIV is more open compared to its counterpart in PMII [Asojo *et al.,* 2003]

Crystal structure of pmPMIV complexed with KNI-764 from *P.malariae* [Clemente *et al.*, 2006] shows an unexpected orientation of the compound in the active site. The inhibitor is bound in the active site by several hydrogen bonded interactions which include the hydrogen bonds between the central hydroxyl group of the inhibitor and the two catalytic aspartic acid residues. The allophenylnorstatine moiety makes hydrophobic interactions with Phe189, Ile291 and Ile300.

5.6.2 Inhibitor of plasmepsins IV

Pepstatin-A is a canonical peptide mimetic inhibitor of all aspartic proteases. Its binding constant for Plm IV has been reported to (Ki) 20 pM [Li et al., 2004]. KNI-764 is also reported to be a potent inhibitor of Plasmepsins-IV with ΔGexpbind value of -9.6 kcal/mol [Clemente *et al.,* 2006]. Although KNI-764 is a peptidomimetic inhibitor,

its chain direction is opposite to the direction of a natural substrate or of any other peptidomimetic inhibitors, such as Pepstatin-A [Silva *et al.,* 1996].

5.7 Comparative study of structural information of plasmepsins

In the feasibility of finding or designing an inhibitor capable of targeting several proteins with high affinity requires the specification of a composite target site containing a precise description of the location of conserved and variable regions. This composite site becomes the template for drug design. The four plasmepsins share a high degree of sequence homology. Taking Plasmepsins II as reference, Plasmepsins I shows 73% sequence identity and Plasmepsins IV reveals 69% identity. In contrast to that, mature enzyme of HAP exhibits 80% homology and 60% overall sequence identity compared to PMII, but only 39% identity in the active site region. However, even in this case most amino acid polymorphisms within the binding site are rather conservative (55% similarity).So the most conserved regions should be targeted with a constrained molecular moiety capable of establishing strong and highly specific interactions [Nezami *et al.,* 2003].

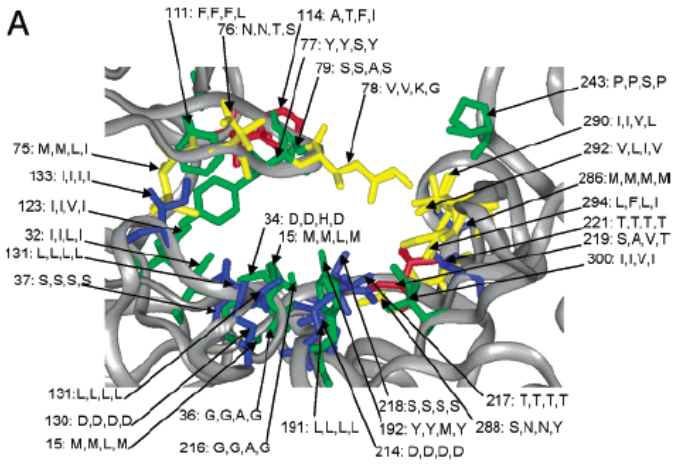

Figure 5.1 Distribution of amino acid heterogeneity within the binding site of the plasmepsins.

Table 5.1 Polymorphisms in the binding site of Plm I, Plm II, Plm III and HAP

Protein	Binding site residue number										
	15	32	34	36	37	75	76	77	78	79	
Plm I	M	I	D	G	S	M	N	Y	V	S	
Plm II	M	I	D	G	S	M	N	Y	V	S	
HAP	L	L	H	A	S	L	T	S	K	A	
Plm IV	M	I	D	G	S	I	S	Y	G	S	
	111	114	123	130	131	133	191	192	214	216	
Plm I	F	A	I	D	L	I	L	Y	D	G	
Plm II	F	T	I	D	L	I	L	Y	D	G	
HAP	F	F	V	D	L	I	L	M	D	A	
Plm IV	L	I	I	D	L	I	L	Y	D	G	
	217	218	219	221	243	286	288	290	292	294	300
Plm I	T	S	S	T	P	M	S	I	V	L	I
Plm II	T	S	A	T	P	M	N	I	L	F	I
HAP	T	S	V	T	S	M	N	V	I	L	V
Plm IV	T	S	T	T	P	M	Y	L	V	I	I

5.8 Artemisnin-Quinine hybrid-A putative inhibitor of plasmepsins family

Now-a-days an emerging strategy within medicinal chemistry and drug discovery is the combination of two distinct pharmacophores into a single hybrid molecule. Hybrid molecules offer a simpler and more effective way to deliver these agents, especially when difference like elimination times occurs. The experimental study revealed that antimalaria drug artemisinin-quinine hybrid compound inhibited the growth of live malaria parasite *P.falciparum*. Walsh *et al.* (2007) showed that a hybrid artemisinin covalently linked to quinine via an ester linkage, revealed superior activity to that of artemisinin alone, quinine alone, or a 1:1 mixture of artemisinin and quinine. Since it is well-established that basic antimalarial like quinine accumulate in the acidic food vacuole of the parasite, we have decided to make plasmepsins inhibitors containing quinine with basic nitrogen hybridized to artemisinin moiety.

5.9 Objective of the study

The specific objectives of this study were: (1) To identify adaptive inhibitors which are active against at least two digestive vacuolar plasmepsins from *Plasmodium falciparum*. (2) To design potent inhibitor with low Ki value.

5.10 Materials & Methods

5.10.1 Preparation of protein

We have used the 3-D structure of Plasmepsins-I-KNI-10006 complex (PDB ID: 3QSV), Plasmepsins II-Pepstatin-A complex (1SME) and Plasmepsins IV-Pepstatin A complex (1LS5) as the initial structure for the preparation of the artemisinin-quinine binding site. Hydrogen's were added to the model automatically via the Maestro interface leaving no lone pair and using an explicit all-atom model. The multi-step Schrodinger's protein preparation tool (PPrep) was used for final preparation of receptor model. The complex structures were energy minimised using the OPLS-2005 force field and the conjugate gradient algorithm, keeping all atoms except hydrogen fixed. The minimization was stopped either after 5000 steps of minimizations or after the energy gradient converged below 0.001 kcal/mol.

5.10.2 Preparation of ligands

The two dimensional structure of artemisinin-quinine hybrid was collected from published data [Walsh *et al.*, 2009]. We used ISIS Draw 2.3 software for sketching structure and converting it its 3D representation by using Chem sketch 3D viewer of ACDLABS 12.0. LigPrep was used for final preparation of ligand for docking. LigPrep is a utility of Schrodinger software suit that combines tools for generating 3D structures from 1D (Smiles) and 2D (SDF) representation, searching for tatutomers and steric isomers and perform a geometry minimization of ligand. Ligprep utility produces a number of structures from each input structure with various ionization states, tautomers, stereochemistry, and ring conformations. The program automatically generated all possible stereoisomer's (default value of 32 was used) for each ligand. Furthermore, a unique low-energy ring conformation for each stereoisomer with correct chirality was generated with the help of Ligprep. All structures were subsequently subjected to molecular mechanics energy minimization using Impact (version 5.6, Schrodinger Inc.) with default settings: maximum cycles 100, conjugate gradient minimizer, initial step size 0.05, maximum step size 1.0, gradient criteria 0.01. Partial atomic charges were assigned to the molecular structures using the 2005 implementation of the OPLS-AA force field. These energy minimized structures were used for Glide (grid-based ligand docking with energetic) docking.

5.10.3 Molecular docking and MM-GBSA scoring

All docking calculations were performed using the "Extra Precision" (XP) mode of Glide docking (version 4.5, Schrodinger Inc.) with the 2005 implementation of the OPLS-AA force field. Briefly, Glide approximates a systematic search of positions, orientations, and conformations of the ligand in the receptor binding site using a series of hierarchical filters.

In this work the bounding box of size 10 Å ×10 Å ×10 Å was defined in Plasmepsins I, II and IV and centred on the mass center of the crystallographic KNI-10006 or Pepstatin-A to confine the mass center of the docked ligand. The scale factor of 0.4 for van der Waals radii was applied to atoms of protein with absolute partial charges less than or equal to 0.25. Five thousand poses per ligand were generated during the initial phase of the docking calculation, out of which best 1000 poses per ligand were chosen for energy minimization. Energy minimization protocol included dielectric constant of 4.0 and 1000 steps of conjugate gradient minimizations. Upon completion of each docking calculation, 100 poses per ligand were generated and the best docked structure was chosen using a Glide Score (Gscore) function.

For each ligand, the pose with the lowest Glide score was rescored using Prime/MM-GBSA approach. This approach is used to predict the free energy of binding for set of ligands to receptor. The docked poses were minimized using the local optimization feature in Prime and the energies of complex were calculated using the OPLS-AA force field and generalized-Born/surface area (GB/SA) continuum solvent model. The binding free energy (ΔG_{bind}) is then estimated using equation:

$$\Delta G_{bind} = E_{R:L} - (E_{R+}E_L) + \Delta G_{solv+} \Delta G_{SA} \quad (1)$$

Where $E_{R:L}$ is energy of the complex, E_R+E_L is sum of the energies of the ligand and unliganded receptor, using the OPLS-AA force field, ΔG_{solv} (ΔG_{SA}) is the difference between GBSA solvation energy (surface area energy) of complex and sum of the corresponding energies for the ligand and unliganded protein. Corrections for entropic changes were not applied in this type of free energy calculation.

5.11 Results

5.11.1 Calculation of experimental binding energy (ΔG^{bind}_{exp})

Table 5.2 $\Delta G_{bind\ (Expt)}$ of Pepstatin-A-Plasmepsins I/II/IV complex

Receptor	Ligand	Ki value in nM	$\Delta G_{bind\ (Expt.)}$
Plasmepsin-I	Pepstain-A	0.001 [a]	-16.35
Plasmepsin-II	-do-	0.006 [b]	-15.29
Plasmepsin-IV	-do-	0.02 [c]	-14.58

Table 5.3 $\Delta G_{bind\ (Expt)}$ of KNI-10006-Plasmepsins I/II/IV complex

Receptor	Ligand	Ki value in nM	$\Delta G_{bind\ (Expt.)}$
Plasmepsin-I	KNI-10006	0.07 [d]	-13.84
Plasmepsin-II	-do-	0.5 [d]	-12.67
Plasmepsin-IV	-do-	1.25 [d]	-12.13

The ΔG_{bind} of the ligand were obtained using relationship $\Delta G^{bind}_{exp} = 2.303\ RT \log Ki$

[a] *Value from reference [Xiao H et al., 2007]*

[b] *Value from reference [Silva AM et al., 1996]*

[c] *Value from reference [Li T et al, 2004]*

[d] *Value from reference [Nezami et al, 2003]*

5.11.2 Calculation of calculated binding energy ($\Delta G^{bind}_{cald.}$) & Ki value

The docked complexes were rescored with MM-GBSA and the binding energy $\Delta G_{bind\ (Cald.)}$ of Artemisinin-Quinine against Plasmepsins I, II and IV has been calculated. The Ki value of the hybrid compound is calculated using the relationship as follows:

$$\Delta G_{bind\ (Cald.)} = 2.303RT \log Ki \qquad (1)$$

5.11.2.1 Inhibitor binding to Plasmepsins I

Plm I-KNI-10006 complex $\Delta G_{bind\ (Expt.)}$ = -13.84 kcal/mol

Plm I-Art-Qui-OH complex $\Delta G_{bind\ (Cald.)}$ = -22.45 kcal/mol

Using the above relationship in Eq. (1) the Ki value of the compound is calculated to $3.91*10^{-8}$ nM

5.11.2.2 Inhibitor binding to Plasmepsins II

PlmII-Pepstatin-A complex $\Delta G_{bind\ (Expt.)}$ = -15.29 kcal/mol

Plm II-Art-Qui-OH complex $\Delta G_{bind\ (Cald.)}$ = -16.13 kcal/mol

The Ki value of Art-Qui-OH against Plasmepsins II is calculated using the Eq. (1) as 0.001nM.

5.11.2.3 Inhibitor binding to Plasmepsins IV

PlmIV-Pepstatin-A complex $\Delta G_{bind\ (Expt.)}$ = -14.58 kcal/mol

Plm IV-Art-Qui-OH complex $\Delta G_{bind\ (Cald.)}$ = -19.43 kcal/mol

The Ki value of Art-Qui-OH against Plasmepsins IV is calculated as $6.3*10^{-6}$ nM.

Table 5.4 XP score, ΔG_{bind} & Ki value of Art-Qui-OH-Plm I/II & Plm IV complex

Complex	XP Score	$\Delta G_{bind\ (Cald.)}$	Ki in nM
PlmI-Art-Qui-OH	-8.880	-22.45	$3.91*10^{-8}$
PlmII-Art-Qui-OH	-8.289	-16.13	0.001
PlmIV-Art-Qui-OH	-9.432	-19.43	$6.3*10^{-6}$

5.12 Discussion

A required property of adaptive inhibitors is an extremely high affinity against the primary target and only a mild response to target heterogeneities. Unlike standard inhibitors, adaptive inhibitors do not rely on conformational constraints to achieve high binding affinity.

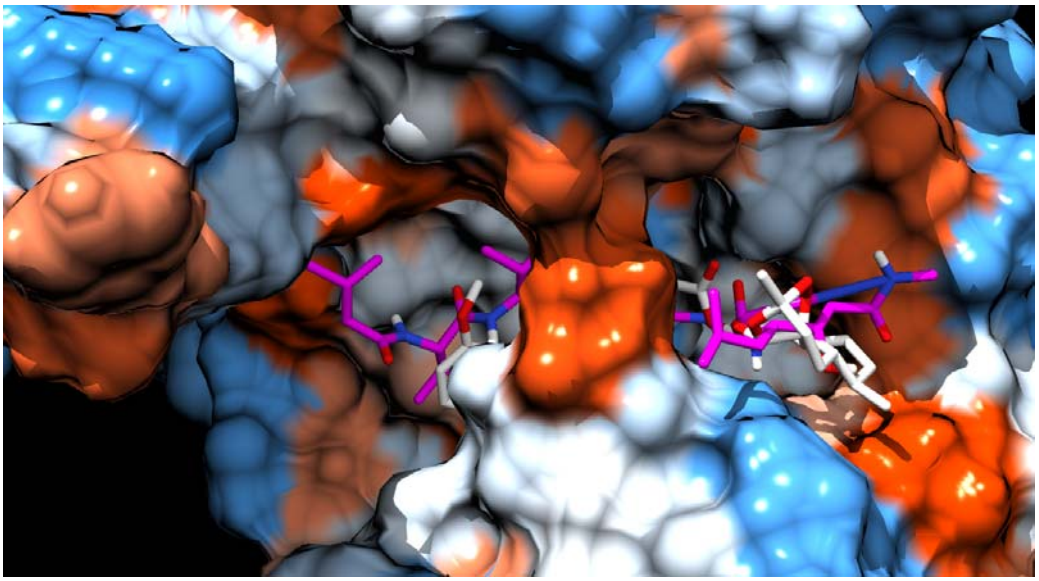

Fig 5.2 Overlapped docking poses of Pepstatin-A and Art-Qui-OH obtained from Glide docking in the binding site of Plasmepsins-II (Magenta= Pepstatin-A, Silver= Art-Qui-OH

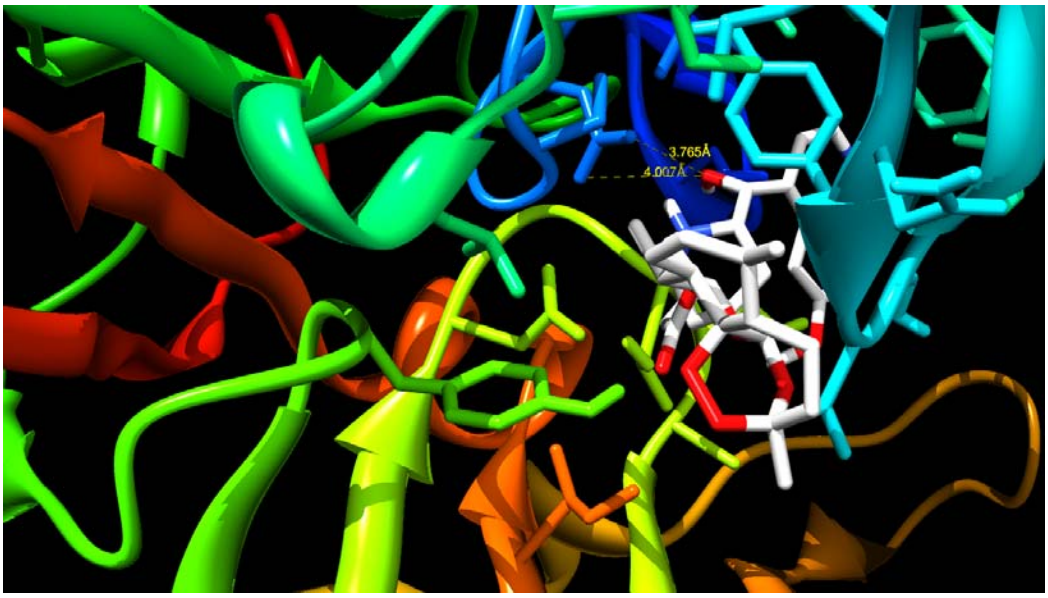

Fig 5.3 Illustrates the representative docking pose of Art-Qui-OH in Plasmepsins-II binding site. The central OH group is shown to be oriented towards the Asp34 residue having $O^{\delta 1}$ and $O^{\delta 2}$ distances are 4.007 Å and 3.765 Å respectively.

Art-Qui-OH exhibits a nanomolar binding affinity against Histo-Aspartic Protease with a Ki value of 10.15nM. For that reason, the inhibitory activity of the hybrid was measured against the entire Plasmepsins family. The Ki value of Art-Qui-OH complex is determined with molecular modelling analysis which indicates that that the value is 0.001 nM against Plasmepsins II in compare to $3.91*10^{-8}$ nM for Plasmepsins I and $6.3*10^{-6}$ nM for Plasmepsins IV. The Ki values of the hybrid against Plm-I and Plm-IV are relatively insignificant. However the significantly low Ki value of Art-Qui-OH against Plasmepsins II raises a new possibility of designing an adaptive inhibitor. The binding mode of Art-Qui-OH resemble to that of Pepstatin-A binding in Plasmepsins II (Fig.5.2). Interesting the central OH of the hybrid molecule is involved in the interaction with one of the catalytic Asp 34 residue (Fig.5.3). Therefore this novel inhibitor may fortuitously cross-reacts with at least two Plasmepsins (Plm II and HAP) if not all four of these, without toxicity to the host. However we suggest here that the molecular interaction proposed here for the binding mode of Art-Qui-OH hybrid with plasmepsins family enzymes should be considered for further structure based drug design efforts.

5.13 Conclusion

The plasmepsins are key enzymes in the life cycle of the *Plasmodium* parasites responsible for malaria. In this chapter we have used the structural information of plasmepsins as well as computer aided drug design to a study the binding affinity a potent antimalarial compound. From our computational analysis it revealed that Art-Qui-OH can be consided as a pan-Plasmepsins inhibitor for at least two plasmepsins playing crucial role in the pathogenesis of malaria.

CONCLUSION

Experimental study revealed that artemisinin-quinine hybrid was a superior antimalarial specifically against *P.falciparum.* The hybrid compound was observed to be a potent antimalarial drug with an $IC_{50\ (S)}$ value of 8.95nM and $IC_{50\ (R)}$ value of 9.59nM for chloroquine sensitive (3D7) and resistant (FcB1) strain.

Prompted by the experimental study, molecular modeling methods such as docking molecular mechanics based on generalized Born/surface area (MM-GBSA) solvation model was implemented in this work. The purpose of the study was to analyze the binding mode and affinity of artemisinin-quinine hybrid and its congeners with Fe-Protoporphyrin-IX as a putative receptor. A set of artemisinin-quinine hybrid with 34 analogous structures were computationally analyzed by molecular docking using Glide 4.0 software. The purpose was to identify new analogues that could have a similar mechanism of action yet superior activity. The XP score of experimental structure dihydroartemisinin-quinine compound was computed to be -7.485 kcal/mol and a ΔG_{bind} value of -32.35 kcal/mol. Seven ligands from the library were identified with a favourable G_{score} and ΔG_{bind} value in comparison to the experimental structure. The docking solvation model showed that the configuration of the hybrid had the peroxide oxygen O1 and O2 close to the haeme iron with Fe-O2 as the shortest haeme-artemisinin distance and Fe-O1 as the second shortest distance. The selectivity of artemisinin for infected erythrocyte, where the necessary haeme-iron is available, was noted to be responsible for peroxide functionality. The endoperoxide bridge (1, 2, 4-trioxane-ring) as revealed from the study played an essential role in antimalarial activity than the non peroxide oxygen. In the interaction of artemisinin-quinine hybrid with haeme (haemoglobin derived) Fe (II)-PPIX, a series of oxygen and carbon radicals were produced through the electron transfer from Fe (II) to peroxide bridge.

Histo-aspartic protease (HAP) is one of the most divergent vacuolar plasmepsins and is directly involved in the process of haemoglobin degradation making them potential targets for novel antimalarial therapy. As a proof-of-concept, it was conceptualized to evaluate *in silico* the binding mode and relative binding affinity of

Art-Qui-OH with the Histo-Aspartic Protease (HAP) of *P.falciparum.* The MM-GB/SA scoring resulted the relative binding energy ($\Delta\Delta G_{\text{bind-cald}}$) of the hybrid molecule with respect to Pepstatin-A as 2.43 kcal/mol and 3.44 kcal/mol against KNI-10006 respectively. The relative docking scores (ΔG score) of Art-Qui-OH with reference to Pepstatin-A and KNI-10006 were obtained to be 1.298 kcal/mole and 1.317 kcal/mol respectively. These results demonstrate that a strong binding affinity of Art-Qui-OH (binding mode resembles to Pepstatin-A) in HAP binding site. Art-Qui-OH hybrid was shown to interact in the active site of the enzyme with O11 atom of artemisinin moiety forming strong H-bond with His32. His32 is postulated to be play a crucial role in providing the electrophilic component and critical stabilization (by a factor of ~10, 000) in the substrate catalytic reaction of HAP enzyme. The Ki value of Art-Qui-OH was computed to 10.15nM. The study suggested that the Ki value & proposed binding mode of the Art-Qui-OH for HAP enzyme should be considered for further structure-based drug design efforts.

Art-Qui-OH exhibited a nanomolar binding affinity against Histo-Aspartic Protease. For that reason, the inhibitory activity of the hybrid was measured against the entire plasmepsins. The antimalaria activity of Art-Qui-OH was determined by molecular modeling analysis and indicated that the Ki value was 0.001 nM against Plasmepsins II in comparison to relatively insignificant value $3.91*10^{-8}$ nM for Plasmepsins I and $6.3*10^{-6}$ nM for Plasmepsins IV. The significantly low Ki value of Art-Qui-OH against Plasmepsins II as revealed from the study raises a new possibility of designing an adaptive inhibitor.

There is no doubt that the hybrid molecules shows potent and novel anti malarial drug. The next major steps, therefore, is to experimentally analyze the antimalarial activity of the hybrid compound against the drug target i.e. vacuolar Plasmepsins and haemoglobin derived Fe-Protoporphyrin IX, before it is promoted for the first clinical trial against malaria.

Bibliography

1. Acton N, Karle JM, Miller RE, (1993). Synthesis and antimalarial activity of some 9- substituted artemisinin derivatives. *J. Med. Chem*. 36:2552-2557.

2. Andreeva N, Bogdanovich P, Kashparov I, Popov M, Stengach M,(2004). Is histoaspartic protease a serine protease with a pepsin-like fold? Proteins 55:705–710.

3. Angus Bell, (2005).Antimalarial drug synergism and antagonism: Mechanistic and clinical significance. *FEMS Microbiology Letters.* 253: 171–184

4. Asawamahasakda W, Benakis A, Meshnick SR, (1994). The interaction of artemisinin with red cell membranes. *J Lab Clin Med.* 123: 757-62.

5. Ashley EA, White NJ, (2005). Artemisinin based combinations. *Curr. Opin. Infect. Dis.* 18(6): 531-536.

6. Asojo OA, Gulnik SV, Afonina E, Yu B, Ellman JA, Haque TS, Silva AM, (2003). Novel uncomplexed and complexed structures of Plasmepsins II, an aspartic protease from *Plasmodium falciparum. J Mol Biol.* 327(1):173-81.

7. Augustijns P, D'Hulst A, Van Daele J, Kinget R, (1996). Transport of artemisinin and sodium artesunate in Caco-2 intestinal epithelial cells. *J Pharm. Sci.* 85:577-9.

8. Avery MA, Alvin-Gaston M, Rodrigues CR, Barreiro EJ, Cohen FE, Sabnis YA, Woolfrey J, (2002). Structure activity relationships of the antimalarial agent artemisinin. The development of predictive *in vitro* potency models using CoMFA and HQSAR methodologies. *J Med.Chem*. 45:292-303.

9. Avery MA, Bonk JD, Chong WKM, Mehrotra S, Miller R. et al. (1995) Structure-Activity Relationships of the Antimalarial Agent Artemisinin. 2. Effect of heteroatom Substitution at O-11: Synthesis and Bioassay of N-Alkyl-11-aza-9- desmethylartemisinins. *J. of Med. Chem*. 38: 5038-5044.

10. Avery MA, Mehrotra S, Bonk JD, Vroman JA, Goins DK. et al. (1996) Structure-Activity Relationships of the Antimalarial Agent Artemisinin. 4. Effect of substitution at C-3. *J. of. Med. Chem*. 39: 2900-2906.

11. Bailly E, Jambou R, Savel J, Jaureguiberry G, (1992). *Plasmodium falciparum*: differential sensitivity in vitro to E-64 (cysteine protease inhibitor) and Pepstatin A (aspartyl protease inhibitor) *J Protozool.*39(5):593-9.

12. Bailly E., Jambou R., Savel J, Jaureguiberry G, (1992) *J. Protozool.* 39:593–599.

13. Banerjee R, Liu J, Beatty W, Pelosof L, Klemba M., Goldberg DE, (2002).Four plasmepsins are active in the *Plasmodium falciparum* food vacuole, including a protease with an active-site histidine. *Proc. Natl. Acad. Sci* 99: 990–995.

14. Bannister LH, Hopkins JM, Fowler RE, Krishna S, Mitchell GH, (2000). A brief ultra structural guide to asexual blood stages of Plasmodium falciparum. *Parasitol Today* 16: 427-433.

15. Benoit-Vical F, Lelievre J, Berry A, Deymier C, Dechy-Cabaret O, Cazelles J, Loup C, Robert A, Magnaval JF, Meunier B,(2007). Trioxaquines are new antimalarial agents active on all eryhrocytic forms, including gametocytes. *Antimicrobial Agents Chemother*. 51:1463–1472.

16. Bernacki K, Kalyanaraman C, Jacobson MP, (2005), Virtual ligand screening against *Escherichia coli* dihydrofolate reductase: improving docking enrichment physics-based methods, *J. Biomol. Screen*. 10:675−681.

17. Bhaumik P, Gustchina A, Wlodawer A (2011).Structural studies of vacuolar Plasmepsins. Biochimica. Biophysica Acta.

18. Bhaumik P, Xiao H, Hidaka K, Gustchina A, Kiso Y, Yada RY, Wlodawer A, (2011).Structural insights into the activation and inhibition of Histo-Aspartic Protease from *Plasmodium falciparum*. 50: 8862−8879.

19. Bhaumik P, Xiao H, Parr CL, Kiso Y, Gustchina A, Yada RY, Wlodawer A, (2009).Crystal structures of the Histo-aspartic protease (HAP) from *Plasmodium falciparum*. *J. Mol. Biol.* 388:520–540.

20. Bjelic S, Aqvist J (2004). Computational prediction of structure, substrate binding mode, mechanism, and rate for a malaria protease with a novel type of active site Biochemistry 43: 14521–14528.

21. Bohm HJ, (1994). The Development of a Simple Empirical Scoring Function to Estimate the Binding Constant for a Protein-Ligand Complex of Known 3-Dimensional Structure. *J. Comput.-Aided Mol. Des*. 8, 243–256.

22. Bosman A, Mendis KN, (2007). A major transition in the malaria treatment: the adsorption and deployment of artemisinin-based combination therapies. *Am. J.Trop.Med.Hyg.*77: 193-197

23. Bozdech Z, LLinas M, Pulliam BL, Wong ED, Zhu JC, Derisi JL,(2003).The transcriptome of the intraerythrocytic developmental cycle of *Plasmodium falciparum.* Brossi A, Venugopalan B, Dominguez Gerpe L, Yeh HJ, Flippen-Anderson JL, Buchs P, Luo XD, Milhous W, Peters W, (1988). Arteether, a new antimalarial drug: synthesis and antimalarial properties. *J Med Chem.* 31:645-50.

25. Chawira AN, Warhurst DC, (1987). The effect of artemisinin combined with standard antimalarials against chloroquine-sensitive and chloroquine-resistant strains of *Plasmodium falciparum* in vitro. *J Trop Med Hyg.* 90: 1-8

26. Chen PQ, Li GQ, Guo XB, (1994). The infectivity of gametocytes of *Plasmodium falciparum* from patient treated with artemisinin. *Chin.Med.J.* 107(9):709-711

27. Cheng F, Shen J, Luo X, Zhu W, Gu J, Ji R, Jiang H, Chen K, (2002). Molecular docking and 3-D-QSAR studies on the possible antimalarial mechanism of artemisinin analogues. *Bioorg. Med. Chem.* 10: 2883-2891.

28. Cherkasov A, Ban F, Li Y, Fallahi M, Hammond GL, (2006). Progressive docking: a hybrid QSAR/docking approach for accelerating *in silico* high throughput screening. *Journal of medicinal chemistry* 49: 7466-7478.

29. Chou AC, Chevli R, Fitch CD, (1980). Ferriprotoporphyrin IX fulfils the criteria for identification as the chloroquine receptor of malaria parasites. *Biochemistry.* 19: 1543–1549.

30. Chou AC, Fitch CD, (1993). Control of haeme polymerase by chloroquine and other quinoline derivatives. *Biochem. Biophys.Res. Commun.* 195: 422–427.

31. Clemente JC, Govindasamy L, Madabushi A, Fisher SZ, Moose RE, Yowell CA, Hidaka K., Kimura T, Hayashi Y, Kiso Y., Agbandje-McKenna M., Dame J.B, Dunn BM, McKenna R, (2006). Structure of the aspartic protease Plasmepsins 4 from the malarial parasite Plasmodium malariae bound to an allophenylnorstatine-based inhibitor, Acta Crystallography. D62:246–252.

32. Cleves AE, Jain AN, (2006). Robust ligand-based modeling of the biological targets of known drugs. *Journal of medicinal chemistry* 49:2921-2938.

33. Coombs GH, Goldberg DE, Klemba M, Berry C, Kay J, Mottram JC, (2001).Aspartic proteases of *Plasmodium falciparum* and other parasitic protozoa as drug targets. *Trends Parasitol*. 17:532–537.

34. Cosle´dan F, Fraisse L, Pellet A, Guillou F, Mordmuller B, Kremsner PG, Moreno A, Mazier D, Maffrand JP, Meunier B, (2008). Selection of a trioxaquine as an antimalarial drug candidate. *Proc Natl Acad Sci.* USA 105:17579–17584

35. Cumming JN, Ploypradith P, Posner GH, (1997). Antimalarial activity of artemisinin (quinghaosu) and related trioxanes: mechanism(s) of action. *Adv. Pharmacol*. 37: 253–297.

36. CW Jefford, (2001). Why artemisinin and certain synthetic peroxides are potent antimalarial. Implication for the mode of action. *Curr. Med. Chem*. 8:1803−1826.

37. Dame JB, Reddy GRG, CA,Yowell, Dunn BM, J Kay, Berry C, (1994). Sequence, expression and modelled structure of an aspartic proteinase from the human malaria parasite *Plasmodium falciparum*. 64 (2):177-90.

38. Dame JB, Yowell CA, Omara-Opyene L, Carlton J.M, Cooper RA, Li T, (2003). Plasmepsins 4, the food vacuole aspartic proteinase found in all Plasmodium spp.infecting man. *Mol. Biochem. Parasitol.* 130:1–12.

39. Dame JB, Yowell CA, Omara-Opyene L, Carlton JM, Cooper RA, Li T, (2003). Plasmepsins 4, the food vacuole aspartic proteinase found in all Plasmodium spp. infecting man. *Molecular & Biochemical Parasitology* 130 :1–12.

40. David A. Fidock et al. (2004). Antimalarial Drug Discovery: Efficacy Models for Compound Screening. *Nature Review Drug Discovery*. Vol.4. 509-520.

41. Davidson's Principles and Practice of Medicine by John Macleod.

42. Davies D, (1990). The Structure and Function of the Aspartic Proteinases. *Annu. Rev. Biophys. Biophys. Chem.* 19:189-215.

43. Davis TM, Karunajeewa HA, Ilett KF, (2005).Artemisinin-based combination therapies for uncomplicated malaria. *Med J. Aust.*182:181-185

44. De Villiers KA, Helder M, Marques, Egan TJ, (2008): The crystal structure of halofantrine–Ferriprotoporphyrin IX and the mechanism of action of aryl methanol antimalarial. *Journal of Inorganic Biochemistry*: 102:1660–1667

45. Desneves J., Thorn G, Berman A., Galatis D, La Greca N, Sinding J, Foley M, Deady LW, Cowman A, Tilley L (1996). Photo affinity labelling of mefloquine-binding proteins in human serum, uninfected erythrocytes and Plasmodium falciparum-infected erythrocytes. *Mol. Biochem. Parasitol*. 82:181–194.

46. Egan TJ, (2006). Interactions of quinoline antimalarial with haematin in solution: *Journal of Inorganic Biochemistry* 100:916–926

47. Egan TJ, (2008). Recent advances in understanding the mechanism of haemozoin (malaria pigment) formation: *Journal of Inorganic Biochemistry*. 102:1288–1299.

48. Eldridge MD, Murray CW, Auton TR, Paolini GV, Mee RP, (1997). Empirical scoring functions: I. The development of a fast empirical scoring function to estimate the binding affinity of ligands in receptor complexes. *J. Comput.-Aided Mol. Des.* 11: 425–445.

49. Ersmark K., Samuelsson B, Hallberg A, (2006).Plasmepsins as potential targets for new antimalarial therapy. *Med. Res. Rev*. 26:626–666.

50. Esposito A, Tiffert, T, Mauritz JM, Schlachter S, Bannister LH, Kaminski CF, Lew VL, (2008). FRET imaging of haemoglobin concentration in *Plasmodium falciparum* infected red cells. *PLoS One*. 3(11):e3780

51. Fitch CD, (1970). *Plasmodium falciparum* in owl monkeys: drug resistance and chloroquine binding capacity. *Science.*169:289-90.

52. Foote SJ, Cowman AF, (1994) The mode of action and the mechanism of resistance to antimalarial drugs. *Acta Trop* 56: 157-71.

53. Francis SE, Gluzman IY, Oksman, Knickerbocker A, Mueller R, Bryant M, Sherman DR, DG Russell, DE Goldberg, (1994) Molecular characterization and inhibition of a Plasmodium falciparum aspartic haemoglobinase *EMBO J.* 13: 306-317.

54. Francis SE, Sullivan Jr. DJ, and Goldberg DE, (1997). Haemoglobin metabolism in the malaria parasite *Plasmodium falciparum. Annu Rev Microbiol* 51: 97-123.

55. Francis SE., Sullivan Jr. DJ, Goldberg DE, (1997).Haemoglobin metabolism in the malaria parasite *Plasmodium falciparum*. *Annu. Rev. Microbiol.* 51:97–123.

56. Gluzman IY, Francis SE, Oksman A, Smith CE, Duffin K, Goldberg DE, (1994).Order and specificity of the *Plasmodium falciparum* haemoglobin degradation pathway. *J. Clin. Invest.* 93:1602-1608.

57. Gohlke H, Hendlich M, Klebe G, (2000). Knowledge-based scoring function to predict protein-ligand interactions. *J. Mol. Biol.*295, 337–356.

58. Gohlke H, Klebe G, (2002). Approaches to the description and prediction of the binding affinity of small-molecule ligands to macromolecular receptors. *Angew. Chem., Int. Ed.* 41, 2645–2676.

59. Goldberg DE, (2005) in Malaria: Drugs, Disease, and Post-Genomic Biology, eds. Sullivan, D. & Krishna, S. (Springer, Berlin), pp. 275–291.

60. Gomes M, Ribeiro I, Warsame M, Karunajeewa HA, Petzold M, (2008). Rectal artemisinins for malaria: a review of efficacy and safety from individual patient data in clinical studies. *BMC Infect. Dis*. 8(39)

61. Grace JM, Augliar AJ, Trotman KM, Peggins JO, Brewer TG, (1998). Metabolism of β-arteether to dihyroqinghaosou by human liver microsomes and recombinant cytochrome P 450. *Drug Metab.Dispos*.26(4):313-317

62. Hamedi Y, Safa O, Zare S, Tan-ariya P, Kojima S, Looareesuwan S,(2004).Therapeutics efficacy of artesunate in *Plasmodium vivax* malaria in Thailand. *Southeast Asian J. Trop:Med.Public Health* 35(3):570-574

63. Haynes RK et *al.* (2004). Artemisinin: activities and actions, *Microbes Infect*. 460:1339−1346.

64. Hidaka K, Kimura T, Ruben AJ, Uemura T, Kamiya M, Kiso A, Okamoto T, Tsuchiya Y, Hayashi Y, Freire E, Kiso Y (2008). Antimalarial activity enhancement in hydroxymethylcarbonyl (HMC) isostere-based dipeptidomimetics targeting malarial aspartic protease Plasmepsins. *Bioorg. & Med. Chem.* 16 :10049–10060

65. Holland KP, Elford HL, Bracchi V, Annis CG, Schuster SM, Chakrabarti D, (1998). Antimalarial activities of polyhydroxyphenyl and hydroxamic acid derivatives. *Antimicrobial. Agents Chemother*. 42, 2456–2458.

66. Homewood CA, Warhurst DC, Peters W, Baggaley VC, (1972) Lysosomes, pH and the antimalarial action of chloroquine. *Nature.* 235: 50–52.

67. Hong YL, Yang YZ, Meshnick SR, (1994). The interaction of artemisinin with malarial haemozoin. *Mol. Biochem. Parasitol*. 63: 121–128.

68. Huang N, Kalyanaraman C, Bernacki MP, Jacobson K (2006).Molecular mechanics methods for predicting protein−ligand binding, Phys. Chem. Chem. Phys. 8:5166−5177.

69. Huang N, Kalyanaraman C, Irwin JJ, Jacobson MP (2006). Physics-based scoring of protein−ligand complexes: enrichment of known inhibitors in large-scale virtual screening *J. Chem. Inf. Model*. 46:243−253.

70. Janse CJ, Waters AP, Kos J, Lugt CB, (1994). Comparison of in vivo and in vitro antimalarial activity of artemisinin, dihydroartemisinin and sodium artesunate in the *Plasmodium berghei* -rodent model. *Int. J Parasitol.* 24: 589-94.

71. John J. Walsh et al. (2007). A novel artemisinin–quinine hybrid with potent antimalarial activity: *Bioorganic & Medicinal Chemistry Letters.* 17:3599–3602

72. Kamchonwongpaisan S, Samoff E, Meshnick SR, (1997). Identification of haemoglobin degradation products in *Plasmodium falciparum*. *Mol. Biol. Parasitol.*86: 179-186.

73. Karunajeewa HA, Manning L, Muller I, Ilett KF, Davis TM, (2007). Rectal administration of artemisinin derivatives for the treatment of malaria. *JAMA* 297(21):2381-2390.

74. Karunajeewa HA, Mueller I, Senn M et al.(2008).A trial of combination antimalarials therapies in children from Papua New Guinea. *N. Engl. J. Med.* 359(24):2545-2557.

75. Kitchen DB, Decornez H, Furr JR, Bajorath J, (2004). Docking and scoring in virtual screening for drug discovery: methods and applications. *Nat. Rev. Drug Discov.* 3:935-949

76. Klayman DL, (1985). Qinghaosu (artemisinin): an antimalarial drug from China. *Science.* 228: 1049-1055.

77. Klebe G, (2006). Virtual ligand screening: strategies, perspectives and limitations. *Drug Discovery. Today* 11: 580-594.

78. Kokwaro G, Mwai L, Nzila A, (2007). Artemether/lumifantrine is the treatment of uncomplicated falciparum malaria. *Exp.Opin.Phramacotherapy.* 8:75-94.

79. Kouznetsova VV, Gómez-Barriob A,(2009).Recent developments in the design and synthesis of hybrid molecules based on aminoquinoline ring and their antiplsmodial evaluation. *European Journal of Medicinal Chemistry.*44(8):3091-3113.

80. Kremsner PG, Krishna S, (2004). Anti malaria combinations. *Lancet.* 364:285-294

81. Krovat EM, Steindl T, Langer T, (2005). Recent advances in docking and scoring, *Curr. Comput. Aided Drug Des*. 1:93−102.

82. Le Roch KG., Zhou Y, Blair PL, Grainger M, Moch J K., Haynes J D, De La Vega P, Holder AA, Batalov S, Carucci DJ, Winzeler EA.(2003) Discovery of gene function by expression profiling of the malaria parasite life cycle. *Science.* 301:1503–1508.

83. Lee IS, Hufford CD, (1990). Metabolism of antimalarial sesquiterpene lactones. *Pharmacol Ther.* 48: 345-55.

84. Li GQ, Guo XB, Fu LC, Jian HX, Wang XH, (1994). Clinical trials of artemisinin and its derivatives in the treatment of malaria in China. *Trans R Soc Trop Med Hyg* 88 Supple 1:S5-6.

85. Li T, Yowell CA, Beyer BB, Hung S.H, Westling, J, Lam MT, Dunn BM, Dame JB, (2004). Recombinant expression and enzymatic subsite characterization of Plasmepsins 4 from the four Plasmodium species infecting man, *Mol. Biochem. Parasitol.* 135:101-9.

86. Lin AJ, Lee M, Klayman DL, (1989). Antimalarial Activity of New Water-Soluble Dihydroartemisinin Derivatives, *J. Med. Chem*. 32: 1249-1252.

87. Lipinski CA et al. (2001).Experimental and computational approaches to estimate solubility and permeability in drug discovery and development settings. *Advanced Drug Delivery Reviews.* 46:3–26

88. Liu JM, (1979). Structure and reaction of arteannuin. *Acta Chim. Sin.* 37:129.

89. Loria P, Miller S, Foley M, Tilley L, (1999) Inhibition of the peroxidative degradation of haeme as the basis of action of chloroquine and other quinoline antimalarial. Biochem. J. 339:363–370.

90. Luksch T, Blum A, Klee N, Diederich WE, Sotriffer CA, Klebe G, (2010). Pyrrolidine derivatives as Plasmepsins inhibitors: binding mode analysis assisted by molecular dynamics simulations of a highly flexible protein. *ChemMedChem.* 5(3):443-54.

91. Luo XD, Shen CC, (1987). The chemistry, pharmacology, and clinical applications of Qinghaosu (artemisinin) and its derivatives. *Med Res Rev.* 7: 29-52.

92. Lyne PD, Lamb ML, Saeh JC, (2006) Accurate prediction of the relative potencies of members of a series of kinase inhibitors using molecular docking and MM-GBSA scoring. *J. Med. Chem.* 49: 4805−4808.

93. Macomber PB, Sprinz H, (1967). Morphological effects of chloroquine on *Plasmodium berghei* in mice. *Nature.* 214:937-9.

94. Maeno Y, Toyoshima T, Fujioka H, Ito Y, Meshnick SR, Benakis A, Milhous WK, Aikawa M, (1993). Morphologic effects of artemisinin in *Plasmodium falciparum. Am J Trop Med Hyg* 49:485-91

95. Meshnick SR, (2002). Artemisinin: mechanisms of action, resistance and toxicity. *Int. J. Parasitol*. 32:1655−1660.

96. Meshnick SR, Yang YZ, Lima V, Kuypers F, Kamchonwongpaisan S, Yuthavong Y, (1993) Iron-dependent free radical generation from the antimalarial agent artemisinin (qinghaosu). *Antimicrob Agents Chemother* 37: 1108-14.

97. Meshnick, SR, Thomas A, Ranz A, Xu CM, Pan HZ, (1991). Artemisinin (qinghaosu): the role of intracellular haemin in its mechanism of antimalarial action. *Mol. Biochem. Parasitol.* 49(2): 181–189.

98. Milhous WK, Kyle DE, Sherman IW, (1998). ed. Malaria Parasite Biology, 33. Pathogenesis and Protection. Washington, D.C. *ASM Press*: 303-316.

99. Moon RP, Tyas L, Certa U, Rupp K, Bur D, Jacquet C, Matile HH. Grueninger-Leitch LF, Kay J, Dunn BM, Berry C, Ridley RG, (1997).Expression and characterisation of Plasmepsins I from *Plasmodium falciparum*. *Eur. J. Biochem*. 244:552–560.

100. Morphy R et al. (2005). Designed multiple ligands. An emerging drug discovery paradigm. *J Med Chem*. 48:6523–6543.

101. Mu JY, Israili ZH, Dayton PG, (1975). Studies of the disposition and metabolism of mefloquine HCl (WR 142, 490), a quinolinemethanol antimalarial, in the rat. Limited studies with an analogue, WR 30,090. *Drug Metab. Dispos*. 3: 198–210.

102. Muegge I, Martin YC, (1999). A general and fast scoring function for protein-ligand interactions: A simplified potential approach. *J. Med.Chem.*42:791–804.

103. Muregi FW, Ishih A, (2010) Next-Generation antimalarial rugs: hybrid molecule as a new strategy in drug design. *Drug Dev. Res.* 71: 20–32.

104. Myint HY, Tipmanee P, Nosten F, Day NP, Pukrittayakamee S, Looareesuwan S, White NJ, (2004). A systematic overview of published antimalarial drug trials. *Trans R Soc Trop Med Hyg.* 98(2):73-81.

105. Nezami A, Freire E, (2002). The integration of genomic and structural information in the development of high affinity plasmepsins inhibitors. *International Journal for Parasitology*.32 :1669–1676

106. Nezami A, Kimura T, Hidaka K, Kiso A, Liu J, Kiso Y, Goldberg DE, Freire E, (2003). High-affinity inhibition of a family of *Plasmodium falciparum* proteases by a designed adaptive inhibitor. *Biochemistry.*42:8459–8464.

107. Nezami A, Kimura T, Hidaka K., Kiso A, Liu J, Kiso Y, Goldberg DE, Freire E, (2003). High-affinity inhibition of a family of *Plasmodium falciparum* proteases by a designed adaptive inhibitor. Biochemistry.42:8459–8464.

108. Norsten F, White NJ, (2007). Artemisinin-based combination treatment for falciparum malaria. *Am J. Trop.Med.Hyg.*77:181-192

109. Olliaro P, (2005). Drug resistance hampers our capacity to roll back malaria. *Clinic. Infect. Dis. 41,* S244-257

110. Olliaro P, Wells TN, (2009). The global portfolio of new antimalarial medicines under development. Clin Pharmacol Ther. 85:584–595.

111. Olliaro PL, Trigg PI, (1995). Status of antimalarial drugs under development. *Bull World Health Organ.* 73: 565-71

112. Olson JE, Lee GK., Semenov A, Rosenthal PJ, (1999). Antimalarial effects in mice of orally administered peptidyl cysteine protease inhibitors. *Bioorg. Med.Chem*. 7: 633–638.

113. Omara-Opyene AL, Moura PA, Sulsona CR., Bonilla JA, Yowell CA, Fujioka H, Fidock David A, Dame John B, (2004). Genetic disruption of the *Plasmodium falciparum* digestive vacuole plasmepsins demonstrates their functional redundancy. *The Journal of Biological Chemistry*. 279(52): 54088–54096.

114. Oprea TI, Matter H, (2004). Integrating virtual screening in lead discovery. *Curr. Opin. Chem. Biol.* 8: 349-358.

115. Orrling KM, Marzahn M, Gutierrez-de-Teran Hugo, Aqvist Johan, Dunn BM, Larhed M(2009). α-substituted norstatines as the transition-state mimic in inhibitors of multiple digestive vacuole malaria aspartic proteases. *Bioorganic & Medicinal Chemistry.* doi: 10.1016/j.bmc.2009.06.065

116. Padmanaban G, Rangarajan PN, (2001). Emerging targets for antimalarial drugs *Expert Opin. Ther. Targets* 5: 423-441.

117. Pagola S, Stephens PW, Bohle DS, Kosar AD, Madsen SK, (2000). The structure of malaria pigment beta-haematin. Nature, 404:307-10.

118. Parr CL, Tanaka T, Xiao H, Yada RY, (2008). The catalytic significance of the proposed active site residues in *Plasmodium falciparum* histoaspartic protease. *FEBS Journal.* 275:1698–1707

119. Perrin DD, (1965). Dissociation constants of organic bases in aqueous solution. Butterworth & Co., London.

120. Peter B. Madrid et al. (2005). Synthesis of ring-substituted 4-aminoquinolines and evaluation of their antimalarial activities. *Bioorganic & Medicinal Chemistry Letter.* 15:1015–1018.

121. Peters W, (1982). Antimalarial drug resistance: an increasing problem. *Br Med Bull.* 38 (2):187-192.

122. Phan GT, de Vries PJ, Tran BQ et al. (2002). Artemisinin or chloroquine for blood stage for *Plasmodium vivax* malaria in Vietnam. *Trop.Med.Int.Health.* 7(10):858-64.

123. *PLoS Biol.* 1(1): e5. doi:10.1371/journal.pbio.0000005

124. Popov ME, Stengach MA, Andreeva NS (2008). Modelling of Substrate and Inhibitory Complexes of Histidine-Aspartic Protease *Russian J. Biorg. Med. Chem*. 34:3380-386.

125. Posner GH, Oh CH, Gerena L, Milhous WK, (1992). Extraordinarily Potent Antimalarial Compounds: New, Structurally Simple, Easily Synthesizes, Tricyclic 1, 2, 4-Trioxanes.*J. Med. Chem*. 35: 2459-2467.

126. Ribeiro M. C. de A, Augusto O, Ferreira A. M. da C, (1997). Influence of quinoline-containing antimalarials in the catalase activity of ferriprotoporphyrin IX. *J. Inorg. Biochem*.65: 15–23.

127. Richard T. Eastman and David A. Fidock, (2009). Artemisinin-based combination therapies: a vital tool in efforts to eliminate malaria. *Nat Rev Microbiol.* 7(12): 864–874.

128. Ridley RG, (2002). Medical need, scientific opportunity and the drive for antimalarial drugs. *Nature.* 415: 686-93.

129. Ronn AM, Msangeni HA, Mhina J, Wernsdorfer WH, and Bygbjerg IC, (1996). High level of resistance of *Plasmodium falciparum* to sulfadoxine-pyrimethamine in children in Tanzania. *Trans R Soc Trop Med Hyg.* 90: 179-81.

130. Rosenthal PJ (2001). Antimalarial Chemotherapy, Mechanisms of Action, Resistance, and New Directions in Drug Discovery, ed. Rosenthal, P. J. (Humana, Totowa, NJ), pp. 325–345.

131. Rosenthal PJ, (2003).Antimalarial drug discovery: old & new approaches. *J. Expt. Biol.*206:3735-3744

132. Sachs J, Malaney P, (2002). The economic and social burden of malaria. *Nature.* 415: 680-685.

133. Salako LA, Sowunmi A, (1992). Disposition of quinine in plasma, red blood cells and saliva after oral and intravenous administration to healthy adult Africans. *Eur. J Clin. Pharmacol.* 42(2):171-174.

134. Shenai BR., Sijwali PS., Singh A, Rosenthal PJ. (2000) Characterization of native and recombinant falcipain-2, a principal trophozoite cysteine protease and essential hemoglobinase of *Plasmodium falciparum J. Biol. Chem*.275: 29000–29010.

135. Sherman IW, (1998). (Ed.) In Malaria. *Am Soc Microbiol Press, Washington, DC.* :1-556.

136. Sherman IW, Tanigoshi L, (1970). Incorporation of 14C-amino-acids by malaria (plasmodium lophurae) IV. In vivo utilization of host cell haemoglobin, *Int. J.Biochem*. 1:635–637.

137. Sijwali PS, Rosenthal PJ, (2004). Gene disruption confirms a critical role for the cysteine protease falcipain-2 in haemoglobin hydrolysis by *Plasmodium falciparum. Proc.Nat.Acd.Sci*: 101(13):4384-9.

138. Sijwali PS., Shenai BR., Gut J, Singh A. Rosenthal PJ. (2001) Expression and characterization of the *Plasmodium falciparum* haemoglobinase falcipain-3. Biochem.J. 360, 481–489.

139. Silva A.M et al. (1996). Structure and inhibition of Plasmepsins II, a haemoglobin-degrading enzyme from *Plasmodium falciparum. Proc. Natl. Acad. Sci*.93:10034-10039.

140. Skinner TS, Manning LS, Johnston WA, Davis TM, (1996). *In-vitro* stage specific sensitivity of *Plasmodium falciparum* to quinine and artemisinin drugs. *Int.J.Parasitol.*26:519-525.

141. Slater AFG, Cerami A, (1992). Inhibition by chloroquine of a novel haeme polymerase enzyme activity in malaria trophozoites. *Nature.* 355: 167–169.

142. Sousa SF, Fernandes PA, Ramos MJ, (2006). Protein-ligand docking: current status and future challenges. *Proteins* 65: 15-26.

143. Sowunmi A, Oduola AM, Ogundahunsi OA, Salako LA, (1998). Comparative efficacy of chloroquine plus chlorpheniramine and pyrimethamine/sulfadoxine in acute uncomplicated falciparum malaria in Nigerian children. *Trans R Soc Trop Med Hyg.* 92: 77-81

144. Stahura FL, Bajorath J, (2004). Virtual screening methods that complement HTS. *Comb. Chem. High Throughput Screen.* 7: 259-269.

145. Umezawa H, Aoyagi, T, Morishima H, Matsuzaki M., Hamada M, Takeuchi T, (1970) *J. Antibiot.* (Tokyo) 23:259-262.

146. Van Agtmael MA, Eggelte TA, van Boxtel CJ, (1999). Artemisinin drugs in the treatment of malaria: from medicinal herb to registered medication. *Trends Pharmacol Sci.* 20: 199-205.

147. Veber DF et al. (2002).Molecular properties that influence the oral bioavailability of drug candidates. *J. Med. Chem.,* 45:2615-2623.

148. Velazquez-Campoy A, Freire E, (2001). Incorporating target heterogeneity in drug design. *J. Cell. Biochem.*S37:82-88.

149. Velazquez-Campoy, Kiso A, Y Freire E, (2001a). The binding energetic of first and second generation HIV-1 protease inhibitors: implications for drug design. *Arch. Biochim. Biophys*. 390:169–75.

150. Walsh JJ, Bell A, (2009). Hybrid Drugs for Malaria. *Current Pharmaceutical Design.* 15: 2970-2985

151. Warhurst DC, (1981). The Quinine-Haemin interaction and its relationship to antimalaria activity. Biochemical Pharmacology.30 (24):3323-3327

152. Warhurst DC, Craig JC , Adagu IS, Meyer DJ , Lee SY (2003).The relationship of physico-chemical properties and structure to the differential antiplasmodial activity of the cinchona alkaloids: *Malaria Journal* 2:26

153. Warhurst DC, Craig JC, Adagu IS, Guy RK, Madrid PB, Fivelman QL (2007). Activity of piperaquine and other 4-aminoquinoline antiplasmodial drugs against chloroquine-sensitive and resistant blood-stages of Plasmodium falciparum. Role of β-haematin inhibition and drug concentration in vacuolar water- and lipid-phases. *Biochemical pharmacology.* 7 3:1 91 0 – 19 2 6.

154. Wernsdorfer WH, Payne D, (1991). The dynamics of drug resistance in *Plasmodium falciparum*. *Pharmacol Ther.* 50: 95-121.

155. Westling J, Yowell CA, Majer P, Erickson JW, Dame JB, Dunn BM,(1997). *Plasmodium falciparum*, *P. vivax* and *P. malariae*: a comparison of the active site properties of Plasmepsins cloned and expressed from three different species of the malaria parasite. 87(3):185-93.

156. White N, (1999).Anti malaria drug resistance and combination chemotherapy. *Phil.Trans.R.Soc.London.*354:739-749

157. White N, (1999a). Antimalarial drug resistance and combination chemotherapy. *Philos Trans R Soc Lond B Biol Sci.* 354: 739-49.

158. White NJ, (1998) Drug resistance in malaria. *Br Med Bull* 54: 703-15.

159. White NJ, (2008) Qinghaosau (artemisinin): The price of success. *Science* 320:330-334

160. White NJ, Chanthavanich P, Krishna S, Bunch C, Silamut K, (1983). Quinine disposition kinetics. *Br J Clin Pharmacol* .16(4):399-403.

161. WHO malaria report, 2010.

162. Woodrow CJ, Haynes RK, Krishna S, (2005). Artemisinin. *Postgtad.Med.J. 81:71-78*

163. Wu WM, (1998). Unified mechanistic framework for the Fe (II)-induced cleavage of qinghaosu and derivatives/analogues. The first spin-trapping evidence for the previously postulated secondary C-4 radical. *J. Am. Chem. Soc.* 120:316−3325.

164. Wu Y, (2002). How might qinghaosu (artemisinin) and related compounds kill the intra-erythrocytic malaria parasite? A chemist's view. *Acc Chem Res.* 35: 255-9.

165. Xiao H, Briere LA, Dunn SD, Yada RY, (2010). Characterization of the monomer-dimer equilibrium of recombinant Histo-aspartic protease from *Plasmodium falciparum*. *Mol. Biochem. Parasitol*. 173: 17–24.

166. Yoon S, Smellie A, Hartsough D, Filikov A, (2005a). Computational identification of proteins for selectivity assays. Proteins 59: 434-443.

167. Yoon S, Smellie A, Hartsough D, Filikov A, (2005b). Surrogate docking: structure-based virtual screening at high throughput speed. *Journal of computer aided molecular design* 19: 483-497.

Appendix

Publications from the thesis work

- **Rajani Kanta Mahapatra**, Niranjan Behera, Pradeep Kumar Naik **(2012).** Molecular modeling and evaluation of binding mode and affinity of Artemisinin-Quinine hybrid and its congeners with Fe-protoporphyrin-IX as a putative receptor. ***Bioinformation.*** **8(8):369-380**

- **Rajani Kanta Mahapatra**, Niranjan Behera, Pradeep Kumar Naik **(2012)**. Molecular modeling and determination of binding mode & relative binding affinity of artemisinin-quinine hybrid onto Histo-aspartic Protease (HAP).***Communicated to Genomics, Proteomics & Bioinformatics.***

Ancillary publication from the research work

- Alok Pani, **Rajani Kanta Mahapatra,** Niranjan Behera, Pradeep Kumar Naik **(2011)** Computational identification of Sweet Wormwood (*Artemisia annua)* miRNA and their m-RNA targets. ***Genomics, Proteomics & Bioinformatics.*** **9(6): 200-210**.

BIOINFORMATION
Discovery at the interface of physical and biological sciences

open access www.bioinformation.net Hypothesis

Volume 8(8)

Molecular modeling and evaluation of binding mode and affinity of artemisinin-quinine hybrid and its congeners with Fe-protoporphyrin-IX as a putative receptor

Rajani Kanta Mahapatra[1, 2]*, Niranjan Behera[1] & Pradeep Kumar Naik[3]

[1]School of Life Sciences, Sambalpur University, Burla, Odisha-768019, India; [2]School of Biotechnology, KIIT University, Bhubaneswar, Odisha-751024, India; [3]Department of Biotechnology & Bioinformatics, JUIT, Solan, Himachal Pradesh-173 215, India; Rajani Kanta Mahapatra – Email: rmohapatra@kiitbiotech.ac.in; *Corresponding author

Received April 10, 2012; Accepted April 16, 2012; Published April 30, 2012

Abstract:
A recent rational approach to anti-malarial drug design is characterized as ''covalent biotherapy'' involves linking of two molecules with individual intrinsic activity into a single agent, thus packaging dual activity into a single hybrid molecule. In view of this background and reported anti malaria synergism between artemisinin and quinine; we describe the computer-assisted docking to predict molecular interaction and binding affinity of Artemisinin-Quinine hybrid and its derivatives with the intra-parasitic haeme group of human haemoglobin. Starting from a crystallographic structure of Fe-protoporphyrin-IX, binding modes, orientation of peroxide bridge (Fe-O distance), docking score and interaction energy are predicted using the docking molecular mechanics based on generalized Born/surface area (MM-GBSA) solvation model. Seven new ligands were identified with a favourable glide score (XP score) and binding free energy (ΔG) with reference to the experimental structure from a data set of thirty four hybrid derivatives. The result shows the conformational property of the drug-receptor interaction and may lead to rational design and synthesis of improved potent artemisinin based hybrid antimalarial that target haemozoin formation.

Keywords: Artemisinin-Quinine Hybrid, Molecular Docking, Fe-O Distance, Binding Affinity

Background:
Malaria is a non-contagious disease of chronic evolution that manifests in acute episodes **[1]**. Currently, millions of people in the tropical and subtropical zones of the world are affected by malaria **[1]**. The malaria parasite manifests disease condition only during its blood stage in its lifecycle. This part occurs largely within the red blood cell of the human host **[1],** where it digests a major proportion of the red cell haemoglobin **[2].** It has been demonstrated that *Plasmodium falciparum*, the causative agent of almost all fatal cases of malaria, detoxifies host haemoglobin-derived ferriprotoporphyrin IX (Fe (III) PPIX) in an acidic digestive vacuole (DV) mainly by converting it to haemozoin **[2].** Fe (III) PPIX produced by autoxidation of haeme (Fe (II) PPIX) released from haemoglobin is known to be capable of causing lipid peroxidation **[2]** and to destabilize membranes through a colloid osmotic mechanism **[2]**. Packaging Fe (III) PPIX into compact and highly insoluble haemozoin crystals decreases its pro-oxidant capacity **[3]** and likely also avoids colloid osmotic effects. Haemozoin is now known to be a crystalline cyclic dimer of Fe(III)PPIX in which the propionate group of one porphyrin moiety coordinates to the Fe(III) center of its partner and vice versa, while the second

propionic acid group of each Fe(III)PPIX hydrogen bonds to a neighbouring dimer in the crystal **[3]**.

The widely used quinoline drugs chloroquine, quinine, and mefloquine, as well as amodiaquine and the nonquinoline drugs such as halofantrine and lumefantrine are known to act against the blood stages of the infection by inhibiting detoxification of Fe (III) PPIX into haemozoin, resulting in a build-up of toxic Fe (III) PPIX **[2, 4]** and artemisinin cause a similar effect by reacting with haeme (FeII-protoporphyrin IX) to give free radicals and adducts **[5, 6]**. The artemisinins are the most effective antimalarial drugs with a remarkable therapeutic index **[6]**. As a fact World Health Organisation (WHO) has advocated the policy of Artemisinin-based combination therapy (ACTs) for treating *P.falciparum* malaria **[6]**. The rationale for this combination is that the artemisinin derivative rapidly clears 95% of the parasites and the remaining 5% are cleared by the longer half-life partner drug and thus the risk of recrudescence is minimized. Because of the paucity of promising novel antimalarial drugs under development and fear of loss of the artemisinin to resistance, in malaria drug combination therapy, the current trend is to co-formulate two or more agents into a single tablet, as a multicomponent drug **[7].** However, based on the wide interest in the hybrid molecules as well as numerous encouraging efficacy and toxicity reports, the next generation antimalarial may well be hybrid drugs as opposed to multicomponent ones. There are numerous advantages of employing hybrid molecules over multicomponent drugs in malaria therapy. Compared to the latter, hybrid drugs may be less expensive since, in principle, the risks and costs involved may not be different from any other single entity. Another advantage is that of the lower risk of drug–drug adverse interactions compared to multicomponent drugs **[7]**.

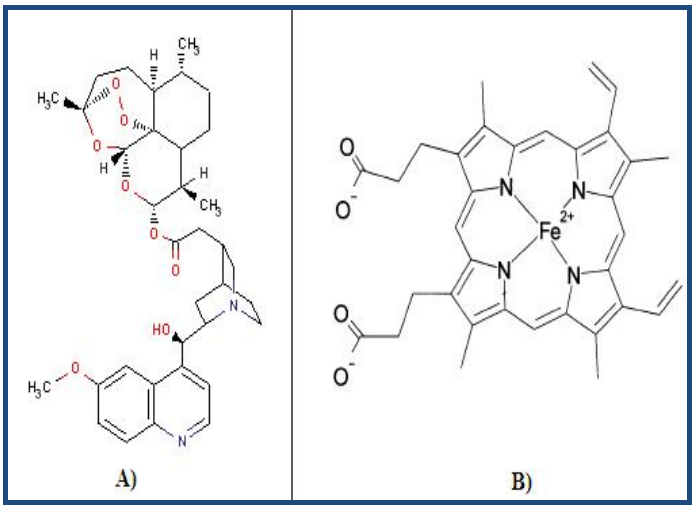

Figure 1: A) 2D molecular structure of Dihydroartemisinin-Quinine hybrid; **B)** 2D structure of Haeme

The mechanism of action of any drug is very important in drug development. Generally, the drug compound binds with a specific target, a receptor, to mediate its effects. Therefore, suitable drug–receptor interactions are required for high activity. Understanding the nature of these interactions is very significant and theoretical calculations, in particular the molecular docking method, seem to be a proper tool for gaining such understanding. The docking results obtained will give information on how the chemical structure of the drug should be modified to achieve of new and more effective drugs. As a proof-of-concept and the reported antimalarial synergism between artemisinin/other endoperoxides and quinine, we conceptualize to evaluate *in silico* the molecular interaction and binding affinity of a covalently linked artemisinin–quinine hybrid in which the vinyl functionality of quinine was modified to allow for the attachment of dihydroartemisinin **(Figure 1A)** with intra-parasite prosthetic haeme group of human haemoglobin **[8]**.The rationale behind the design was to address the fact that artemisinin is lipophilic, fast-acting but quickly eliminated drugs that is associated with high rates of recrudescence when used in monotherapy **[9]**. It was suggested that coupling of the slow-acting, relatively polar quinine derivative might increase the half-life of the artemisinin moiety. Current research in this field seems to endorse hybrid molecules as the next-generation antimalarial drugs **[10].**

Methodology:

Preparation of protein

Studies on the mode of action of artemisinin and its derivatives have shown that free haeme could be the molecule targeted by artemisinin in biological systems **[11-15].**Similarity spectrophotometric study revealed that quinine and related antimalaria drugs interact with Ferriprotoporphyrin-IX **[16]**.

So the X-ray structure of halofantrine-Ferriprotoporphyrin-IX (CCDC_659633) from the Cambridge Crystallographic Data Centre is used as initial structure in the preparation receptor binding site **[17].** Ferriprotoporphyrin-IX is a planar molecule with a strong positive charge on its central iron atom **(Figure 1B)**. After removal of halofantrine structure, the charge on the iron was assigned as +2 but the structure was kept the same. Hydrogen's were added to the model automatically via the Maestro interface **[18]** leaving no lone pair and using an explicit all-atom model. The multi-step Schrödinger's protein preparation tool (PPrep) was used for final preparation of receptor model. The complex structure was energy minimised using the OPLS-2005 force field and the conjugate gradient algorithm, keeping all atoms except hydrogen fixed. The minimisation was stopped either after 1000 steps or after the energy gradient converged below 0.01 KJ/mol.

Virtual library design

The virtual library of Artemisinin-Quinine hybrid analogues contain 34 compounds divided into nine sub libraries. All these compounds are taken from various sources belonging to different derivatives of Artemisinin and Quinine **[19-26]**.The following physiochemical parameters are considered for design of Artemisinin -Quinine hybrid derivatives. **(Table 1a-1h, see supplementary material)**.

Log P (partition coefficient)

The logP value of Artemisinin-Quinine-OH hybrid is estimated to be 5.57. In view of background; the logP value is set to be in the range of 4.5-6.10 **[27]**.

Molecular weight

The molecular weight of the hybrid molecule is estimated to be 622.74 g/mol. So the molecular weight kept below 650 g/mol to enhance the membrane permeability **[28].**

H-bond donor and acceptor
In designing inhibitor with reference to hydrogen bond donor and acceptor we have refereed to 'Lipinski rule of 5' which state that hydrogen bond donor and acceptor should not be more than 5 and 10 respectively **[29, 30].**

Sub lib-I:
Dihydroartemisinin-Quinine Hybrid-This library consist of only of one ligand. The structure is designed experimentally in which the vinyl functionality of quinine was modified to allow for the attachment of dihydroartemisinin.

Sub lib-II:
Artemisinin-Quinine Hybrid - This library consists of five ligands which are designed by attachment of Quinine moiety to the Artemisinin molecule at O-14.

Sub lib-III:
C9 Artemisinin-Quinine Hybrid- This library consists of two ligands in which the C9 substituted Artemisinin entity is attached to Quinine at O-14 position.

Sub lib-IV:
C3 Artemisinin-Quinine Hybrid- C3 substituted Artemisinin derivatives are attached to Quinine moiety and two hybrids are present in this sub library.

Sub lib-V:
C10 Artemisinin-Quinine Hybrid- This library consist of five ligands in which the C10 carbon atom of Artemisinin is modified and Quinine molecule is attached to it at C9 carbon atom.

Sub lib-VI:
Seco Artemisinin-Quinine Hybrid-This library is having three ligands (16-18) with logP in the range from 5.22 to 5.79.The Quinine molecule is attached to the seco artemisinin entity at C9 carbon atom.

***Sub lib-VII*:**
Miscellaneous Artemisinin-Quinine Hybrid- This library consists of four ligand in which various substitution in different carbon atom of Artemisinin molecule are attached to the Quinine entity.

Sub lib-IX:
Quinoline-Artemisinin Hybrid-Quinoline-Artemisinin sub library is having twelve ligands in which the various substitutions at quinoline ring of the Quinine molecule is attached to artemisinin phramacophore.

We used ISIS Draw 2.3 software for sketching structure and converting it its 3D representation by using ChemSketch 3D viewer of ACDLABS 12.0. LigPrep was used for final preparation of ligands from libraries for docking. LigPrep is a utility of Schrodinger software suit that combines tools for generating 3D structures from 1D (Smiles) and 2D (SDF) representation, searching for tatutomers and steric isomers and perform a geometry minimization of ligands. The ligands were minimized by means of Molecular Mechanics Force Fields (OPLS-2005) with default setting.

Docking procedure
It is quite important to have an accurate model for the haeme-Art-Qui-OH complex, because this knowledge can be used to design better and more potent antimalarial. The Schrodinger Glide program version 4.0 has been used for docking. After ensuring that receptor and ligand are in the correct form for docking, the receptor-grid file was generated using a grid-receptor generation program. The default size was used for the bounding and enclosing boxes. The grid box was generated at the centroid of the haeme. The ligands were docked initially using the 'standard precision' method. The best 10 poses and corresponding scores have been evaluated using Glide in single precision mode (Glide SP) .The pose with the lowest Glide SP score has been taken as the input for the Glide calculation in extra precision mode (Glide XP). To soften the potential for non-polar parts of the receptor, we scaled van der Waals radii of receptor atoms by 1.00 with partial atomic charge 0.25.

The docked poses were minimized using the local optimization feature in Prime and the energies of complex were calculated using the OPLS-AA force field and generalized-Born/surface area (GB/SA) continuum solvent model. The binding free energy (ΔG_{bind}) is then estimated using equation **[31]**.

$$\Delta G_{bind} = E_{R:L} - (E_R + E_L) + \Delta G_{solv} + \Delta G_{SA} \quad (1)$$

Where $E_{R:L}$ is energy of the complex, $E_R + E_L$ is sum of the energies of the ligand and unliganded receptor, using the OPLS-AA force field, ΔG_{solv} (ΔG_{SA}) is the difference between GBSA solvation energy (surface area energy) of complex and sum of the corresponding energies for the ligand and unliganded protein. Corrections for entropic changes were not applied in this type of free energy calculation.

Discussion:
Early reports have revealed that *P. falciparum* 3D7 strain growth was inhibited by much lower concentrations of the hybrid than that of quinine or artemisinin alone. This suggested that the actions of both quinine and artemisinin moieties were preserved. Moreover, when the activity of the hybrid was compared with that of a 1:1 mixture of quinine and artemisinin (on a mol quinine/mol artemisinin basis), the hybrid was about 3 fold superior. Similar results were obtained with the chloroquine-resistant strain FcB1 **Table 2 (see supplementary material**).

Prompted by the experimental study; a set of Artemisinin-Quinine hybrid with its 34 analogous structures have been computationally analyzed by molecular docking simulation to identify new analogues that have a similar mechanism of action yet superior activity. Glide 4.0 **[32]** in XP mode has been used to dock the library (I–IX) of Art-Qui-OH with the putative receptor Fe-PPIX. Interaction of Art-Qui-OH and its derivatives with Fe (II) PPIX (Iron (II)) involves binding between the endoperoxide bridges (O1 and O2) bridge of the hybrid to the front of the iron bridge of protoporphyrin-IX shown in **(Figure 2).**

The XP score of the experimental structure; dihydroartemisinin-quinine compound is computed to -7.485 kcal/mol. Out of 34 derivatives; seven novel ligands among the library; two from C3-Artemisinin-Quinine hybrid, three from C10-Artemisinin-Quinine hybrid and two from Miscellaneous Artemisinin-

Quinine hybrid have better Glide score. Previous studies showed that interactions between peroxide linkage in artemisinin compounds and haeme iron play major role in the binding mode, therefore, distances between haeme iron and two peroxide oxygen's; O1, O2 as well as O11 and O13 and ΔG_{bind} of these seven derivatives were monitored.

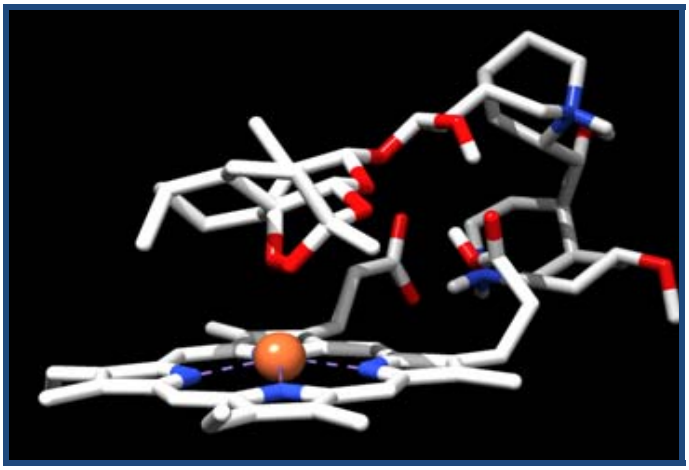

Figure 2: Representative docking Fe-(O1-O2) interaction of Dihydroartemisinin-Quinine hybrid with Fe-(II) PPIX as a putative receptor

For each of the seven ligands, the pose with the lowest Glide score was rescored using Prime/MM-GBSA approach. This approach is used to predict the free energy of binding for set of ligands to receptor. The ΔG_{bind} energies among the ligands vary in between -49.00 to-32.35 kcal/mol. The calculated relative binding energy ($\Delta\Delta G_{bind\text{-}cald}$) of the ligands was also obtained by using Art-Qui-OH as reference. The drop in calculated relative binding energy of the ligand provides a favourable energetic evaluation of the binding affinity **Table 3 (see supplementary material**).

In any binding energy calculation, the correct binding structure of each ligand has to be determined first prior to binding energy estimation. Excluding only one structure from C10 Artemisnin-Quinine hybrid; in other docking configuration it was observed that artemisinin moiety of the hybrid prefers to dock at endoperoxide oxygen's (O1 and O2), with O2–Fe as the shortest haeme–artemisinin distance and O1–Fe as the second shortest distance. Configuration of dihydroartemisinin-quinine hybrid had the peroxide oxygen O1 and O2 close to the haeme iron (3.273 Å & 2.817 Å) with O11 and O13 atom further removed (5.071 Å & 5.149 Å). The ΔG_{bind} value of the structure is -32.35 kcal/mol. Configuration of ligand 9 and 10 of C3-Artemisnin-Quinine hybrid series were almost identical. In both the cases O1 (3.281 and 3.282 Å) and O2 (2.817 and 2.825 Å) were closest, with other oxygen atom being further away: O11 (4.867 and 4.951 Å) and O13 (5.125 and 5.172 Å). The docked configuration of ligand 11 of C10 Artemisinin-Quinine hybrid the binding with the endoperoxide moiety of artemisinin is in a different configuration, and a stronger O11–Fe attraction is resulted (3.812 Å) than O1, O2 and O13 (6.487 Å, 6.176 Å and 5.325 Å). The relative binding energy ($\Delta\Delta G_{bind\text{-}cald}$) of the ligand is calculated to be -10.13 kcal/mol. Such deviation may be explained on the basis of stereochemistry of artemisinin analogues that is controlled by steric hindrance. The analogues which approach the haeme-iron as close as possible will have better interaction and thus a good glide score. However, owing to the planar structure of the Ferriprotoporphyrin-IX, the repulsion between artemisinin and the protoporphyrin ring prevents artemisinin from approaching haeme-iron. Ligand 12 and 14 of this group produce final orientation with a relative binding energy $\Delta\Delta G_{bind\text{-}cald}$ of -11.76 Kcal/mol and -5.08 kcal/mol. Both the configuration involved interaction of the peroxide-derived oxygen with the Fe atom of protoporphyrin-IX. In the most favourable configuration between haeme and miscellaneous Artemisinin-Quinine hybrid with a Gscore of -8.913 kcal/mol (the lowest), the iron is between 3.317 and 2.817 Å from each of the oxygen in the endoperoxide bridge (O1 & O2). This structure has the lowest (ΔG_{bind}) score of -49.00 kcal/mol. From the docking simulation study it revealed that the structure as well as orientation of Artemisnin-Quinine hybrid with respect to haeme has a significant effect on drug action. It could then be concluded that iron in haeme interacts with O2 more preferably than O1, a preference which might arise from the more negative charge at O2 and the steric hindrance at O1. This observation is in agreement with docking results reported by Shukla *et al.* **[33]**.

Artemisinin-Quinine hybrid molecule is novel due to its modified structure and has potent anti malaria activities with presence of artemisinin consisting of endo-peroxide Bridge. Studies suggest that the antimalarial activity of artemisinin is due to the interaction of its peroxide group with the prosthetic haeme group of human haemoglobin. Reduction of the peroxide group may lead to cytotoxic free radicals and electrophilic intermediates, which may be able to react which may be able to react with specific *P.falciparum* membrane associated proteins, leading to the parasite's death. As shown by Walsh *et al.*, 2007 their hybrid was highly active in vitro against the strains of *P. falciparum* 3D7 (with IC_{50} value 8.95 nM) and Chloroquine resistant strain *P.falciparum* FcB1 (IC_{50} value 9.59 nM).The reported results demonstrate a proof to the concept that linkage of artemisinin and quinine is being retained in a single molecule and possibly enhances the antimalarial activity of the parent compounds. It is likely that the hybrid can interact with haeme or its oxidation product haematin as a common target since these are both present in the eryhrocytic parasite.

There is no doubt that the hybrid molecules show potent and novel anti malarial activity. The next major steps, therefore, is to experimentally analyze the antimalaria activity by determining the IC_{50} value of Art-Qui-OH and its structural derivatives by BHIA (β-haematin inhibitory assay). Though the analogues ranged from poor to good binding affinity; the structures are yet to be synthesized. The information that we have obtained in this study may lead to the design and hopefully (synthesis) of more potent hybrid derivatives with receptor as haematin.

Conclusion:

We propose a model for the binding mode and binding affinity of Art-Qui-OH and its derivatives with a putative receptor. This model will help the rational design of new artemisinin based hybrid anti-malarial that target haemozoin formation.

Competing interests:

The authors have declared that no competing interests exist.

Acknowledgment:
The authors acknowledge R. Raghu, Schrödinger Inc. for providing trial license software for preparation of the manuscript.

References:

[1] ArauJo JQ *et al. Bioorg Med Chem*. 2008 **16** : 5021 [PMID: 18375130]
[2] Egan TJ, *J Inorg Biochem.* 2006 **100** : 916 [PMID: 16384600]
[3] Egan TJ, *J Inorg Biochemy*. 2008 **102**: 1288 [PMID: 18226838]
[4] Warhust DC *et al. Malar J*. 2003 **2**: 26 [PMID:14505493]
[5] Meshnick SR *et al. Antimicrobial Agents Chemother*. 1993 **37**: 1108 [PMID: 8517699]
[6] Cui L & Su XZ, *Expert Rev Anti Infect Ther*. 2009 **7**: 999 [PMID: 19803708]
[7] Morphy R & Rankovic Z, *J Med Chem*. 2005 **48**: 6523 [PMID: 16220969]
[8] Walsh JJ *et al. Bioorg Med Chem Lett*. 2007 **17**: 3599 [PMID: 17482816]
[9] Walsh JJ & Bell A, *Curr Pharm Des*. 2009 **15**: 2970 [PMID: 19754373]
[10] Muregi FW & Ishih A, *Drug Dev Res*. 2010 **71**: 20 [PMID: 21399701]
[11] Cheng F *et al. Bioorg Med Chem*. 2002 **10:** 2883 [PMID: 12110308]
[12] Jefford CW, *Curr Med Chem*. 2001 **8**: 1803 [PMID: 11772352]
[13] Wu WM *et al. J Am Chem Soc*. 1998 **120**: 3316
[14] Meshnick SR, *Int J Parasitol*. 2002 **32**: 1655 [PMID: 12435450]
[15] Haynes RK & Krishna S, *Microbes Infect*. 2004 **6**: 1339 [PMID: 15555542]
[16] Warhurst DC, *Biochem Pharmacol*. 1981 **24**: 3323 [PMID:7326041]
[17] De Villiers KA, *J Inorg Biochem*. 2008 **102**: 1660 [PMID:18508124]
[18] http://www.schrodinger.com.
[19] Woolfrey R *et al. J Comput Aided Mol Des*. 1998 **12**: 165 [PMID: 9690175]
[20] Acton N *et al. J Med Chem*. 1993 **36**: 2552 [PMID: 8355254]
[21] Lin AJ *et al. J Med Chem*. 1989 **32**: 1249 [PMID: 2657065]
[22] Posner GH *et al. J Med Chem*. 1992 **35:** 2459 [PMID:1619620]
[23] Avery MA *et al. J of Med Chem*. 1995 **38**: 5038 [PMID: 8544180]
[24] Avery MA *et al. J Med Chem*. 1993 **36**: 4264 [PMID: 8277509]
[25] Avery MA *et al. J of Med Chem*. 1996 **39**: 2900 [PMID: 8709124]
[26] Peter B, *Bioorganic & Medicinal Chemistry Letter*. 2005 **15**: 1015 [PMID: 15686903]
[27] Warhurst C *et al. Biochem Pharmacol*. 2007 **73**: 1910 [PMID: 17466277]
[28] Kristina M *et al. Bioorganic & Medicinal Chemistry*. 2009 doi: 10.1016/j.bmc.2009.06.065
[29] Veber DF, *J Med Chem*. 2002 **45**: 2615 [PMID:12036371]
[30] Lipinski CA, *Adv Drug Deliv Rev*. 2001 **46**: 3 [PMID: 11259830]
[31] Lyne PD *et al. J Med Chem*. 2006 **49**: 4805 [PMID: 16884290]
[32] Friesner RA *et al. J Med Chem*. 2004 **47**: 1739 [PMID: 17034125]
[33] Shukla KL *et al. J Mol Graph*. 1995 **13**: 215 [PMID: 8527414]

Edited by P Kangueane
Citation: **Mahapatra *et al.*** Bioinformation 8(8): 369-380 (2012)

BIOINFORMATION

open access

Supplementary material:

Table 1a: Dihydroartemisinin-Quinine hybrid

Sl. No	Structure	LogP	Molecular	Weight(g/mol)	XP Score (Kcal/mol)
1.	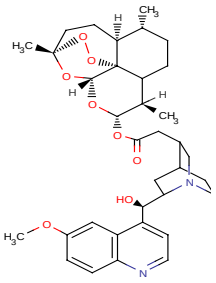	5.57	622.68		-7.485

Table 1b: Artemisinin-Quinine Analogous

Sl.No.	Structure	LogP	Molecular	Weight(g/mol)	XP Score (Kcal/mol)
2.	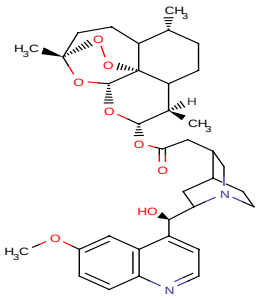	5.57	622.78		-6.802
3.	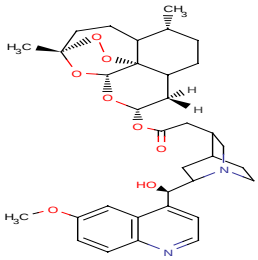	5.08	608.72		-6.914
4.	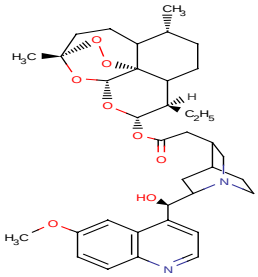	6.10	636.77		-6.950
5.	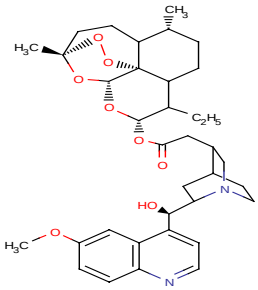	6.10	636.77		-6.932

6.	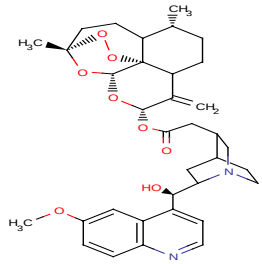	5.75	620.73		-7.241

Table 1c: C9 Artemisinin-Quinine Hybrid

Sl. No	Structure	LogP	Molecular	Weight(g/mol)	XP Score (Kcal/mol)
7.	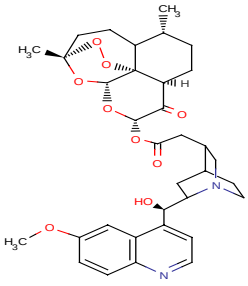	5.18	622.70		-5.310
8.	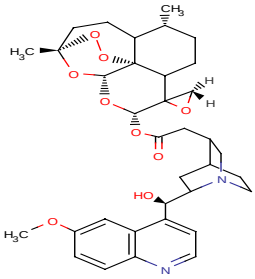	4.92	636.73		-5.450

Table 1d: C3 Artemisinin-Quinine Hybrid

Sl. No.	Structure	LogP	Molecular	Weight(g/mol)	XP Score (Kcal/mol)
9.	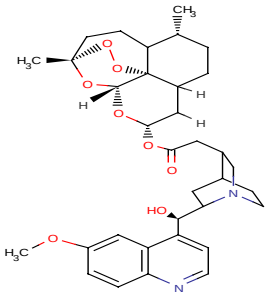	5.08	608.72		-7.673
10.	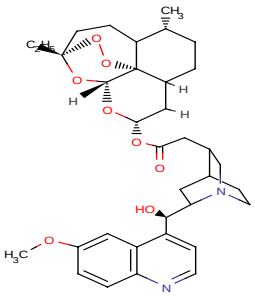	5.61	622.74		-7.620

Table 1e: C10 Artemisinin-Quinine hybrid

Sl. No.	Structure	LogP	Molecular Weight(g/mol)	XP Score(Kcal/mol)
11.	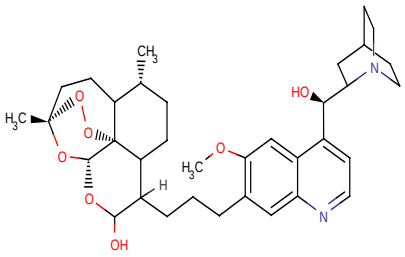	5.58	608.76	-7.722
12.	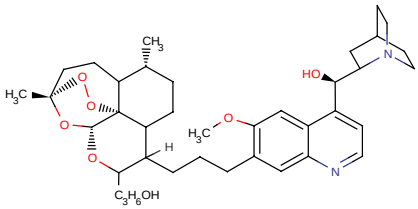	5.86	650.00	-7.815
13.	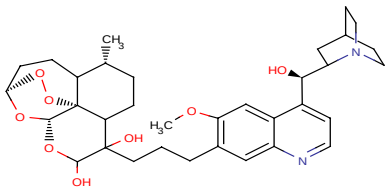	5.36	610.73	- 6.277
14.	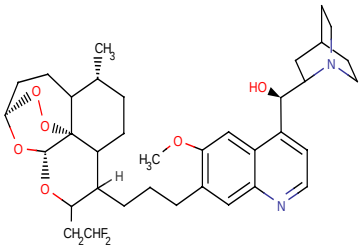	5.93	642.77	-7.622
15.	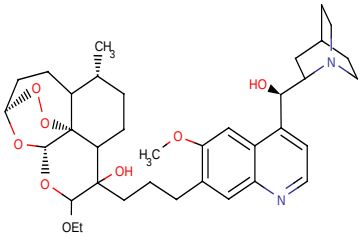	6.08	638.79	-6.283

Table 1f: Seco-Artemisinin-Quinine Hybrid

Sl. No.	Structure	LogP	Molecular Weight(g/mol)	XP Score (Kcal/mol)
16.	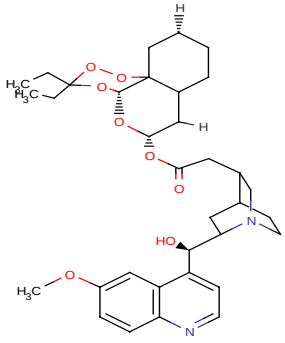	5.79	610.73	-7.070

ISSN 0973-2063 (online) 0973-8894 (print)
Bioinformation 8(8): 369-380 (2012)

17.	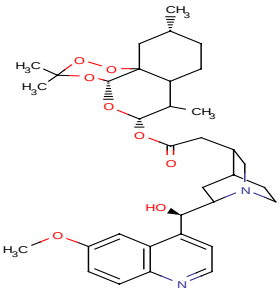	5.71	610.73	-5.586
18.	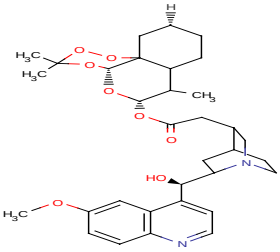	5.22	596.71	-6.914

Table 1g: Miscellaneous Artemisinin-Quinine Hybrid

Sl. No.	Structure	LogP	Molecular Weight(g/mol)	XP Score (Kcal/mol)
19.	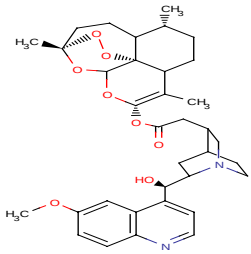	5.98	620.73	-7.600
20.	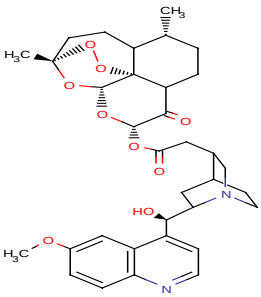	5.18	622.70	-6.768
21.	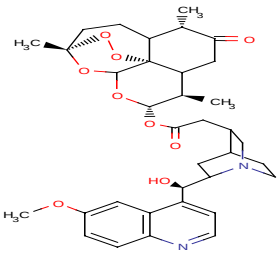	4.56	636.73	-8.913
22.	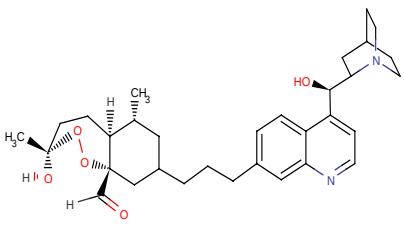	5.02	537.70	-6.671

Table 1h:Artemisinin-Quinoline Derivatives

Sl.No.	Structure	LogP	Molecular Weight(g/mol)	XP Score (Kcal/mol)
23.	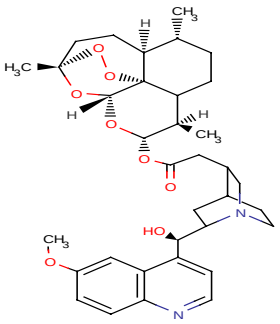	5.57	622.74	-5.83
24.	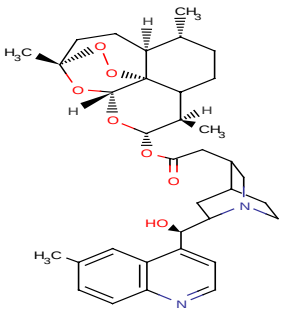	5.94	606.74	-7.02
25.	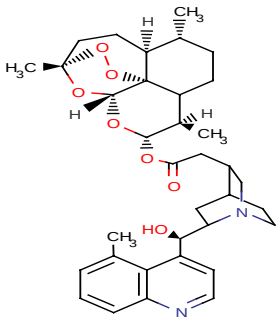	5.94	606.74	-7.30
26.	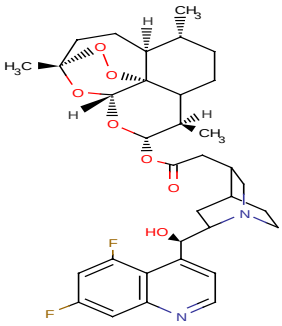	5.89	628.70	-5.79
27.	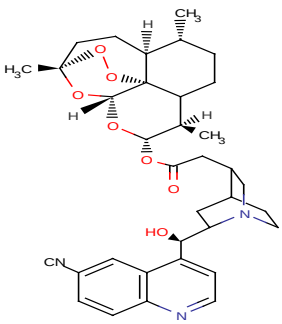	5.06	617.73	-6.64

28.	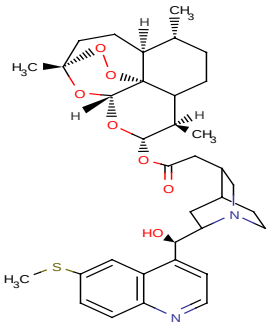	5.97	638.83	-6.77
29.	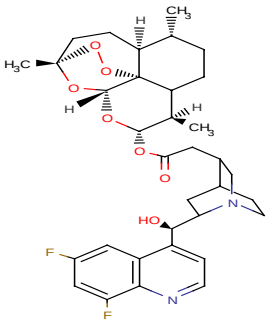	5.70	628.70	-6.56
30.	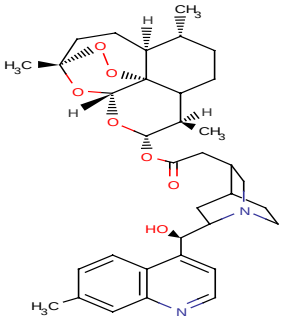	5.94	606.74	-6.69
31.	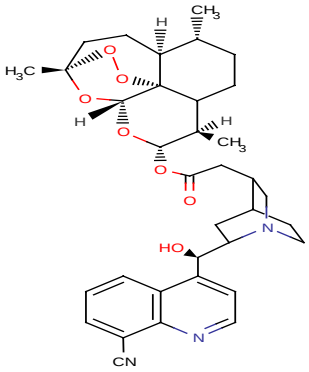	4.79	617.73	-6.53
32.	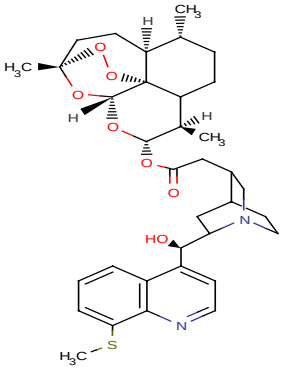	5.97	638.81	-6.58

33. 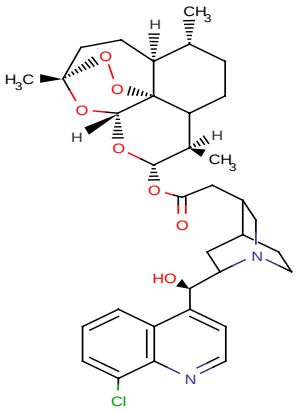	5.73	627.16	-6.54
34. 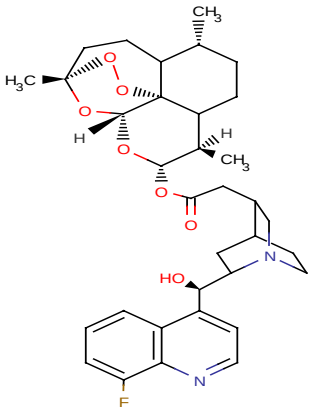	5.90	610.71	-6.54

Table 2: Fifty percent inhibitory concentration (IC_{50}) of the Artemisinin-Quinine hybrid compared with the individual drugs **[8].**

Compound	3D7 (48 hrs)	3D7 (72 hrs)	FcB1 (48 hrs)	FcB2 (72 hrs)
	IC_{50}/nM/Final/Initial	*IC_{50}/nM/Final/Initial*	*IC_{50}/nM/Final/Initial*	*IC_{50}/nM/Final/Initial*
	Geometric mean IC_{50}/nM (95% confidence limit)			
Quinine	149 (95.1, 232)	73.5 (57.0, 94.6)	96.8 (74.5, 126)	75.3(59.0, 96.1)
Artemisinin	89.4 (40.7, 60.0)	45.5 (35.3, 58.6)	50.0 (43.7, 57.3)	55.0(39.0, 77.4)
Art-Qui-OH	8.95 (6.59, 12.2)	10.4 (6.06, 17.9)	9.59 (7.06, 13.0)	10.2(4.73, 21.9)
Quinine+ Artemisinin [a]	31.8 (27.4, 37.0)	28.6 (21.5, 38.2)	27.9 (26.5, 29.5)	26.3(24.7, 28.0)

Activities against cultured, asynchronous, blood-stage P. falciparum strains 3D7 and FcB1 were determined after 48 and 72 h using the parasite lactate dehydrogenase assay. Dose–response curves were used to determine the IC_{50} and the results are expressed as geometric means of IC_{50} from three duplicate determinations.

[a] *Values represent concentrations of each of quinine and artemisinin in a 1:1 ratio, for example, a combination of 31.8 nM quinine + 31.8 nM artemisinin inhibited the growth of 3D7 by 50% after 48 h.*

Table 3: XP Score and Prime-MM-GBSA energy of Art-Qui-OH and its derivatives with Fe (II) PPIX

Ligand	G Score	ΔG_{bind}	$\Delta\Delta G_{bind\text{-}cald}$	Fe-O_1 (Å)	Fe-O_2 (Å)	Fe-O_{13} (Å)	Fe-O11 (Å)
1	-7.485	-32.35	0.00	3.273	2.817	5.149	5.149
19	-7.600	-34.38	-2.03	3.298	2.853	5.214	4.934
10	-7.620	-36.57	-4.22	3.282	2.825	5.172	4.951
14	-7.622	-37.43	-5.08	3.330	2.731	4.998	4.772
9	-7.673	-41.30	-8.95	3.281	2.817	5.125	4.867
11	-7.722	-42.48	-10.13	6.487	6.176	5.235	3.812
12	-7.815	-44.11	-11.76	3.276	2.833	5.083	4.639
21	- 8.913	-49.00	-16.65	3.317	2.817	5.120	4.786

All the energy parameters are expressed in kcal/mol

$\Delta\Delta G_{bind\text{-}cald} = \Delta G_{bind\text{-}ligand} - \Delta G_{Art\text{-}Qui\text{-}OH}$

Available online at www.sciencedirect.com
ScienceDirect
www.sciencedirect.com/science/journal/16720229
GENOMICS PROTEOMICS & BIOINFORMATICS

Article

Computational Identification of Sweet Wormwood (*Artemisia annua*) microRNA and Their mRNA Targets

Alok Pani[1], Rajani Kanta Mahapatra[1,2*], Niranjan Behera[2], and Pradeep Kumar Naik[3]

[1]*School of Biotechnology, Kalinga Institute of Industrial Technology (KIIT) University, Bhubaneswar, Odisha 751024, India;*
[2]*School of Life Sciences, Sambalpur University, Burla, Odisha 768019, India;*
[3]*Department of Biotechnology & Bioinformatics, Jaypee University of Information Technology, Solan, Himachal Pradesh 173215, India.*

Genomics Proteomics Bioinformatics 2011 Dec; 9(6): 200-210 DOI: 10.1016/S1672-0229(11)60023-5

Received: Jun 08, 2011; Accepted: Oct 28, 2011

Abstract

Despite its efficacy against malaria, the relatively low yield (0.01%-0.8%) of artemisinin in *Artemisia annua* is a serious limitation to the commercialization of the drug. A better understanding of the biosynthetic pathway of artemisinin and its regulation by both exogenous and endogenous factors is essential to improve artemisinin yield. Increasing evidence has shown that microRNAs (miRNAs) play multiple roles in various biological processes. In this study, we used previously known miRNAs from *Arabidopsis* and rice against expressed sequence tag (EST) database of *A. annua* to search for potential miRNAs and their targets in *A. annua*. A total of six potential miRNAs were predicted, which belong to the miR414 and miR1310 families. Furthermore, eight potential target genes were identified in this species. Among them, seven genes encode proteins that play important roles in artemisinin biosynthesis, including HMG-CoA reductase (HMGR), amorpha-4,11-diene synthase (ADS), farnesyl pyrophosphate synthase (FPS) and cytochrome P450. In addition, a gene coding for putative AINTEGUMENTA, which is involved in signal transduction and development, was also predicted as one of the targets. This is the first *in silico* study to indicate that miRNAs target genes encoding enzymes involved in artemisinin biosynthesis, which may help to understand the miRNA-mediated regulation of artemisinin biosynthesis in *A. annua*.

Key words: artemisinin, microRNA, EST, computational prediction, *Artemisia annua*

Introduction

Malaria is a global health problem with more than 1 billion people living in areas at a high risk of the disease. Artemisinin combination therapies (ACTs) are the recommended treatment regimen for uncomplicated malaria caused by the *Plasmodium falciparum* parasite (*1*). It has long been recognized that the problem of artemisinin resistance is best addressed by increasing access to ACTs (*2*). This approach receives strong support from the global health community. However, there is growing concern that the supply chain will be unable to consistently produce high-quality artemisinin in the quantities that will be required (*2*). ACT supply remains reliant on the agricultural production of artemisinin, which is a sesquiterpenoid synthesized in the glandular trichomes of the Chinese medicinal plant sweet wormwood (*Artemisia annua* L.) (*3*). However, artemisinin concentration in *A. annua* is low, (in the range of

*Corresponding author.
E-mail: rmohapatra@kiitbiotech.ac.in

0.01%-0.8% per dry weight of tissue), which seriously limits the commercialization of the drug (*4*). Therefore, improved varieties of *A. annua* for farmers in the developing countries would bring immediate benefits to the existing artemisinin supply chain by reducing production costs, stabilizing supplies, and improving growers' confidence in the crop (*2*).

Conventional breeding and genetic engineering approaches would allow construction of *A. annua* genotypes rich in artemisinin (*4*). A better understanding of the biochemical pathway leading to the artemisinin synthesis and regulation by both exogenous and endogenous factors is essential for facilitating yield increase (*5*). With the elucidation of the artemisinin biosynthetic pathway and identification of amorpha-4,11-diene synthase (ADS), which catalyses the first biosynthetic step in artemisinin biosynthesis, it is possible to explore unconventional alternate strategies that are economically viable for the commercial production of artemisinin. Two approaches appear promising. The first approach is to synthesize artemisinin from its simple precursor such as artemisinic acid via semi-synthetic route. Recently, scientific effort is being directed to develop a biological method to supply sufficient and reliable quantities of artemisinic acid, a direct precursor of artemisinin. For example, there was report on engineering of *Saccharomyces cerevisiae* to produce high titres (up to 100 mg/L) of artemisinic acid using an engineered mevalonate pathway, ADS, and a novel cytochrome P450 monooxygenase (CYP71AV1) from *A. annua* (*6*). The second approach is to regulate key enzymes leading to increased artemisinin biosynthesis with metabolic engineering. Certainly, the latter strategy has provided some exciting results and further efforts may accelerate commercialization of this crucial drug. Zhang *et al* showed that down-regulation of squalene synthase (SQS), a key enzyme of sterol pathway that is competitive with artemisinin biosynthetic pathway, by hairpin-RNA-mediated gene silencing in *A. annua* resulted in a 3-fold increase in artemisinin production (*7*). Furthermore, study on the expression of genes involved in the terpene metabolism also indicated that SQS may significantly compete for farnesyl diphosphate (FDP) in artemisinin-producing tissues of *A. annua* (*8*). In addition, higher artemisinin content was reported in induced tetraploid *A. annua*, which may result from the upregulated expression of some key enzyme genes related to artemisinin biosynthesis including ADS, farnesyl diphosphate synthase (FPS), HMG-CoA reductase (HMGR) and artemisinin metabolite-specific aldehyde hydrogenase 1 (*9*). Therefore, a better understanding of the molecular mechanisms involved in the artemisinin biosynthesis and regulation will provide better strategies to develop new varieties with a higher content of artemisinin.

miRNAs are a large family of endogenous small RNAs containing ~22 nucleotides, which are derived from large precursors that are transcribed from non-protein-coding genes (*10*). Plant miRNAs generally interact with their targets through perfect or near-perfect complementarity and repress translation (*11, 12*) or cleave targeted mRNAs (*13*), thus negatively regulate the expression of their target genes (*14*). Plant miRNAs target a large number of genes with functions in a range of development processes, including meristem cell identity (*15*), leaf organ morphogenesis (*11, 12*), polarity and floral differentiation and development (*16*). miRNAs are also reported to be involved in plant responses to biotic and environmental stresses (*17*). The metabolite biosynthesis is also regulated by miRNAs (*18*). A large number of miRNAs have so far been identified in various plant species. However, no miRNA from Asteraceae has been reported yet, reflecting a disparity between the important values of this plant family and insufficient molecular and genetic studies, including small RNA mediated gene regulation, in Asteraceae. To gain insight into miRNAs and their important regulatory functions in artemisinin biosynthetic pathway, we studied miRNA and their targets in *A.annua* using computational approach.

Computational or bioinformatics approach is one of the many approaches available for miRNA prediction (*19*), which can discover miRNAs not only from species with full genomic and sufficient EST database available, but also from those with incomplete genomic information while with sufficient EST sequences available (*20*). In addition, this approach is very useful for predicting miRNAs that usually cannot be detected by the direct cloning, particularly the low-abundance miRNAs. The computational approaches are based on homology search, gene search, neighbor stem-loop search, comparative genomic al-

gorithm or phylogenetic shadowing (*21*). Homology search, which can be further classified as genome-based search or EST-based search (*22*), is based on conserved sequences and secondary structures and identifies miRNA genes by searching nucleotide databases using BLAST. Using homology search, orthologues of known miRNAs were revealed in different species, supporting that miRNAs are conserved in different species (*23*). In addition, hundreds of new miRNAs were also identified using this method from the genomes of model species, such as *Arabidopsis* (*24*) and rice (*Oryza. sativa*) (*25*).

With the development of computational methods, several computer software programs have been developed to help identify plant potential miRNA target genes in mRNA sequences. Because almost all miRNAs show perfect or near-perfect complementarity with their targets in plants, it is much easier to predict miRNA targets using a BLAST search of mRNA database. More and more studies have shown the success of this powerful approach to select potential miRNA targets in mRNA sequences for experimental validation (*21*).

Results and Discussion

Identification of potential miRNAs in *A. annua*

Most mature miRNAs are evolutionarily conserved from species to species within the plant kingdom, which facilitates the prediction of the existence of new miRNA orthologs or homologs in other plant species. In this study, we applied the comprehensive strategy to identify potential miRNAs in *A. annua* by searching EST against known miRNAs of a dicotyledonous plant *Arabidopsis* and a monocotyledonous rice.

Following the procedure depicted in **Figure 1**, 94,724 ESTs from *A. annua* were searched against 584 mature sequences of miRNAs from *Arabidopsis* and rice after removal of redundant sequences. In total, six potential miRNAs were predicted from *A. annua* (**Figure 2**). The six identified *A. annua* candidate miRNAs belong to two miRNA families. miR1310 family has one miRNA. miR414 family has five homologs with two from *A. thaliana* and three from *O. sativa*, respectively (**Table 1**).

It is estimated that in plants, approximate 10,000 ESTs contain 1 miRNA. Therefore, the total of 94,724 ESTs in *A. annua* examined in this study may contain 9-10 miRNAs. However, in this study, only six miRNAs were predicted even with maximal 5-mismatches were allowed. The average length of ESTs is 654 nt and the longest is 795 nt, while most of miRNA precursors have 80-150 nt as identified by MirEval software (*26*), suggesting that the EST may contain other element sequences in addition to miRNA precursor sequence (*27*). The length of miRNA precursors in *A. annua* varied from 80 to 150 nt, with an average of 97 nt. The different sizes of the identified miRNAs within different families suggest that they may offer unique functions for regulation of miRNA biogenesis or gene expression (*28*). The diversity of the identified miRNAs could be also found in the location of mature miRNA sequences. It is shown that the sequences of miR1310 and two members of miR414 from *O. sativa* family were located at the 5' end of the miRNA precursors, while the other miR414 members were found at the 3' end. Minimal folding free energy (MFE) is an important characteristic that determines the secondary structure of nucleic acids (DNA and RNA). The lower the MFE is, the higher the thermodynamically stable secondary structure of the corresponding sequence is (*29*). The MFE index (MFEI) for each sequence was calculated as previously reported (*30*). In this study, the MEFI values ranged from 0.41 to 0.87. miRNA precursor sequences have significantly higher MFEI value than other non-coding or coding RNAs. To avoid false calling of other RNAs as miRNA candidates, MFEI was also considered when predicting secondary structures (*31*).

Identifying miRNAs using EST analysis (*32*) has some advantages over other methods (*33*). It has been suggested that most of the miRNAs predicted by EST analysis can be recovered by high-throughput deep sequencing (*34*).

Although we have computationally identified six miRNAs, the number of miRNAs discovered is relatively small. *A. annua* belongs to Asteraceae, which is the largest plant family of vascular plants on Earth; comprising more than 23,000 genetically diverse and

ecologically successful species (http://www.mobot.org/MOBOT/research/APweb/, Angiosperm Phylogeny Website, Version 9, 2011). Unfortunately, not a single miRNA from Asteraceae family has been deposited in the MiRbase (*35*). We expect that as more miRNAs of this family are publicly available, more miRNAs will be identified in *A. annua*. Interestingly, a recently published study reported that 151 potentially conserved miRNAs belonging to 26 miRNA families were successfully identified and characterized using qPCR in 11 genus of Asteraceae (*36*). In addition, another recent article reported 11 highly conserved miRNA precursors from 9 families using gene-oriented clusters of transcript sequences of *A. annua* with 88,174 UniGenes using a modified computational approach (*37*). However, no miRNA targets were found among genes encoding enzymes involved in artemisinin biosynthesis, maybe because the conserved miRNAs preform evolutionarily stable functions, or miRNA-mediated regulation of artemisinin synthesis could be exerted primarily by novel or clade-specific miRNAs.

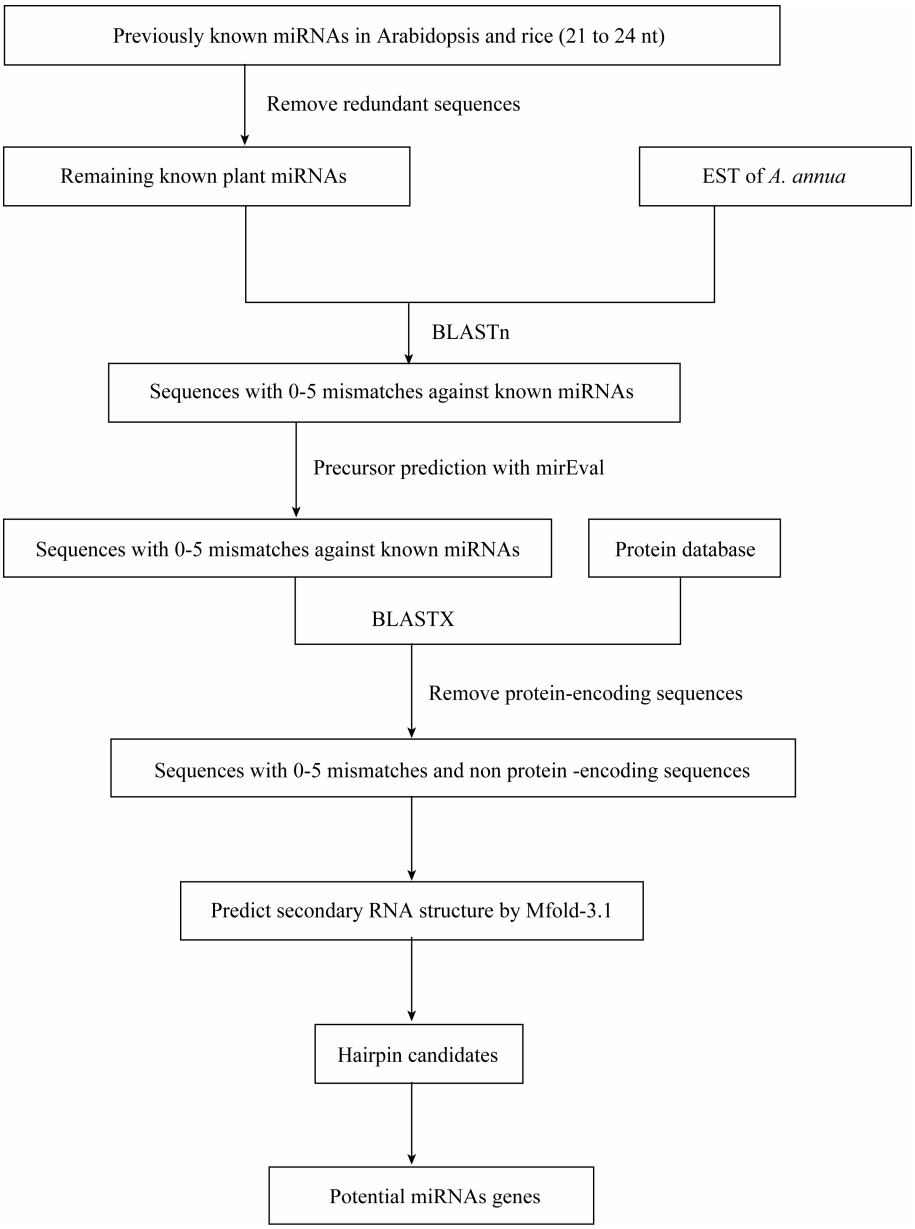

Figure 1 Schematic diagram for searching potential miRNA genes in *A. annua* by identifying homologs of previously known plant miRNAs.

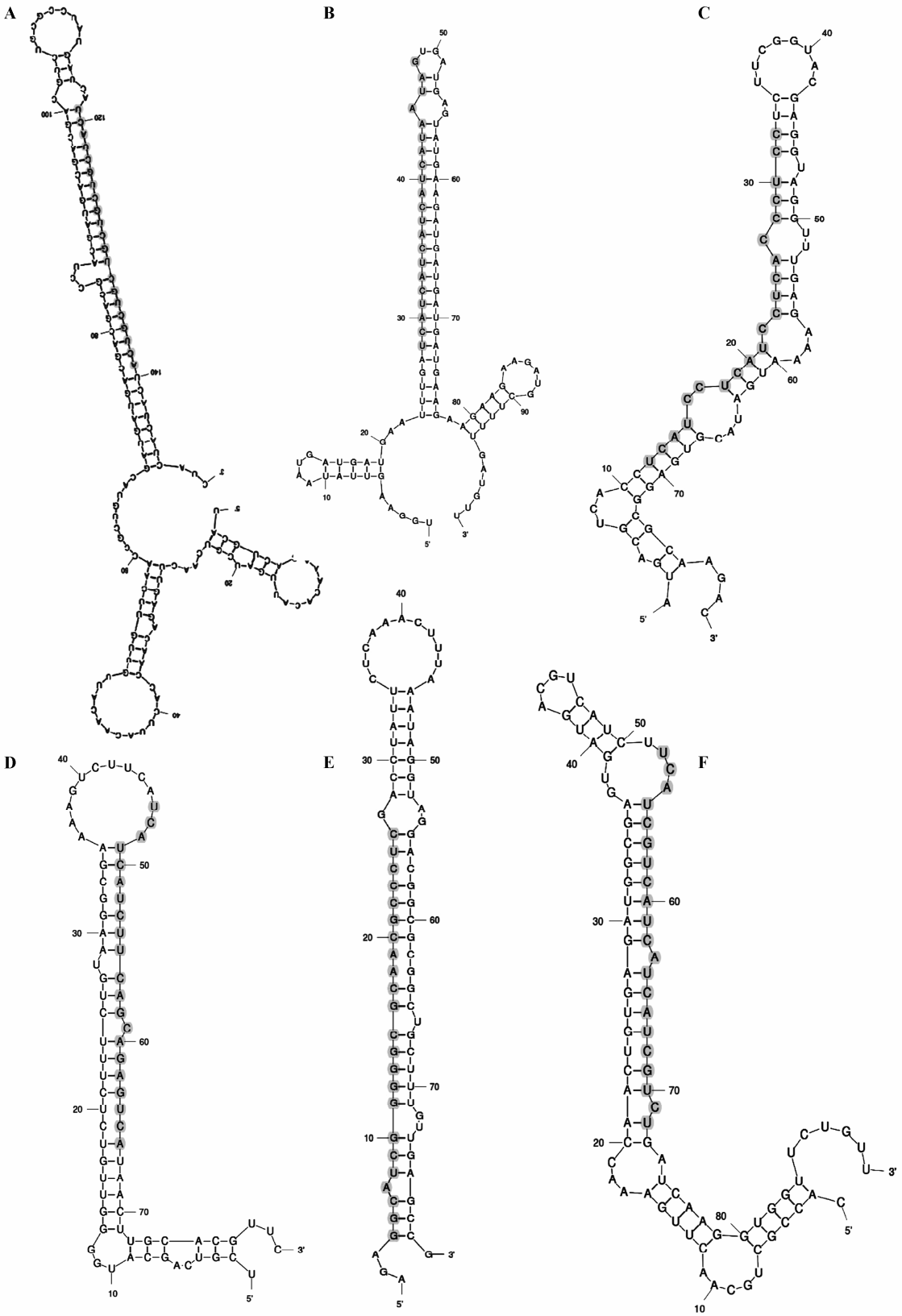

Figure 2 Mature and precursor sequences and the predicted stem and loop structures of newly identified miRNAs in *A. annua*. The mature miRNAs are highlighted in gray. **A.** miR414 (EY064998; homolog of *A. thaliana*); **B.** miR414 (EY057163; homolog of *O. sativa*); **C.** miR414 (EY082442; homolog of *O. sativa*); **D.** miR414 (EY107691; homolog of *A. thaliana*); **E.** miR1310 (EY057327; homolog of *O. sativa*); **F.** miR414 (EY083764; homolog of *O. sativa*).

Table 1 Newly identified miRNAs from ESTs of *A. annua*

miRNA	Reference Species	Gene ID	EST length (nt)	NM (nt)	LM (nt)	LP (nt)	Side	A + U (%)	MFE	MEFI
miR414	*A. thaliana*	EY107691	697	5	21	80	3'	55	14.7	0.41
	A. thaliana	EY064998	795	4	21	150	3'	52	46.1	0.64
miR414	*O. sativa*	EY057163	759	5	21	100	5'	70	26.2	0.87
	O. sativa	EY083764	678	2	21	90	3'	52.2	28.5	0.66
	O. sativa	EY082442	612	3	21	80	5'	48.8	22.5	0.55
miR1310	*O. sativa*	EY057327	381	3	23	80	5'	42.5	29.4	0.64

Note: NM, number of mismatch; LM, length of mature miRNAs; LP, length of precursor; MFE, minimal folding free energy; MFEI, minimal folding free energy index.

Prediction of potential targets of putative miRNAs in *A. annua*

Gaining insight into the miRNA targets will help us understand the spectrum of miRNA regulation and elucidate the functional importance of miRNAs. miRNAs may directly target transcription factors which affect plant development and specific genes which control metabolism as well (*38*). To identify potential regulatory targets, we first searched mRNA database in *A. annua* and screened for mRNAs complementary to the six miRNAs with less than 4 mismatches. Gaps, G-U and other non-canonical pairs were not allowed and considered as mismatches. By screening against mRNA sequences of *A. annua* using the six newly identified miRNAs, we found 8 target genes complementary with less than 4 mismatches. Interestingly, one miRNA can be complementary to more than one regulatory target (**Table 2**). For example, six sequences were detected as targets of miR414 of *A. annua*.

One target gene identified for rice miR414 homolog in *A. annua* (EY082442) is FPS (Table 2). FPS catalyzes two consecutive condensation reactions to produce FDP, which is the starting point of a large variety of essential isoprenoid end products, including artemisinin (*39, 40*). It is clear that the first dedicated step in the biosynthesis of artemisinin is the cyclization of FDP to form amorpha-4,11-diene catalyzed by ADS, one of the sesquiterpene cyclases (SQCs) (*41*). The cyclase reaction establishes an important stereochemical framework upon which all other chemical modifications take place (*43*). Interestingly, another rice miR414 homolog in *A. annua*, EY083764, is predicted to target ADS (Table 2). Modification of the amorpha-4,11-diene carbon skeleton to produce artemisinin acid was thought to involve a cytochrome P450 enzyme leading to the production of artemisinic alcohol, which could then be oxidized twice by either cytochrome P450 enzymes or dehydrogenases to yield artemisinic acid (*44*). In our study, we found that both EY082442 and another *Arabidopsis* miR414 homolog in *A. annua* (EY064998) were predicted to target putative flavonoid 3'-hydroxylase cytochrome P450 (DQ363131).

In addition, EY082442 was also predicted to target HMGR (U14625), which is a rate-limiting enzyme of the mevalonate pathway. Recently it has been shown that HMGR expression limits artemisinin formation in *A. annua* (*8*). Overexpression of ADS and HMGR led to significant increase in the artemisinin yield from the transgenic *A. annua* (*42*).

A third rice miR414 homolog of *A. annua*, EY 57163, targets a putative SQC (CAB56499), while epi-cedrol synthase (EPS, AJ001539), an identified SQC converting FDP to 8-epicedrol, is the only target of miR1310 homolog of *A. annua*, EY057327 (Table 2). A diagram depicting the involvement of miRNAs and their targets was shown in Figure S1.

Other than the enzymes involved in production of secondary metabolites, our computational result demonstrates that *A. annua* miR414 (EY107691) targets the mRNA encoding putative AINTEGUMENTA protein (GQ468547) (Table 2), which is a transcription activator that recognizes and binds to the DNA consensus sequence 5'-CAC[AG]N[AT]TNCCNAN G-3' (*45*). AINTEGUMENTA is required for the initiation and growth of ovules integumenta, and also involved in organ initiation and development, including floral organs (*46*). Interestingly, a positive correlation

Table 2 List of the potential targets of newly identified miRNAs in *A. annua*

miRNA	Gene ID	Target Gene ID	Target Protein	Target Function
miR414	EY107691	GQ468547	Putative AINTEGUMENTA	Transcription regulation
	EY064998	DQ363131	Putative flavonoid 3'-hydroxylase cytochrome P450	Oxidation-reduction process
miR1310	EY057327	AJ001539	EPS	Lyase activity
miR414	EY057163	CAB56499	Putative SQC	Lyase activity
	EY083764	FJ432667, AF327527	ADS	Biosynthesis of artemisinin
	EY082442	GQ420346	FPS	Biosynthesis of cholesterol, isoprene, lipid, steroid and sterol
		U14625	HMGR	Oxidation-reduction process
		DQ363131	Putative flavonoid 3'-hydroxylase cytochrome P450	Oxidation-reduction process

Note: EPS, epi-cedrol synthase; SQC, sesquiterpene cyclase; ADS, amorpha-4,11-diene synthase; FPS: farnesyl pyrophosphate synthase; HMGR, HMG-CoA reductase.

was noticed between the plant age and artemisinin yield (*47*). Furthermore, artemisinin is present in high concentration in either flowers or leaves but low or zero in stems and roots (*48*). For *A. annua*, the highest artemisinin concentration has been reported in leaves and flowers during full bloom stage, in comparison to the pre- and post-flowering stages (*49, 50*).

Conclusion

A. annua has received increasing attention due to its ability to produce artemisinin, which today is widely used for treatment of malaria. In addition to its anti-malarial properties, artemisinin is cytotoxic for cancer cells. Recent reports demonstrate that artemisinin inhibits the secretion and gene expression of tumor necrosis factor (TNF)-α, interleukin (IL)-1ß, and IL-6 in a dose-dependent manner (*51*). The unfortunately low yield of artemisinin and a worldwide shortage of the drug has led to intense research in order to increase the yield of this sesquiterpenoid. Our study is the first *in silico* study to identify miRNAs and their targets in *A. annua*, which we hope could help to better understand miRNA-mediated regulation of genes related to artemisinin biosynthesis.

In summary, in the present study, we predicted six miRNAs conserved in *A. annua*. Furthermore, eight potential target genes were predicted, with functions in a variety of biological processes, including artemisinin biosynthesis, signal transduction and development. Most of the targets are unique to *A. annua* genome, which encode the enzymes associated with the artemisinin biosynthesis pathway. Interestingly, we also identify one target coding for putative AINTEGUMENTA, a transcription factor involved in developmental process, especially for floral organs, which is coincident with the higher artemisinin content during flowering. The result from the computational prediction will be useful to guide experimental design for biological verification. The next major steps, therefore, are to experimentally analyze the functional categories suggested by our computational approach, determine the analogous molecular functions amongst divergent plant species, and further elucidate any significant correlations between the miRNAs and their target genes. Hopefully all these efforts would help make more artemisinin available at lower costs for more people in the Third World, so people who suffer most from malaria can benefit more from this valuable and effective drug.

Materials and Methods

Databases of miRNAs, ESTs, and mRNA sequences

To search potential miRNAs, a total of previously known 674 miRNAs and their precursor sequences from *A. thaliana* and *O. sativa* were obtained from miRNA Registry Database (Release 16.0, October

2010; http://www.mirbase.org/) (*52*). These miRNAs were defined as the reference set of miRNA sequences. We have referred to the previous work on computational prediction of miRNAs by Zhang *et al* (*53*). To avoid the redundant or overlapping miRNAs, the repeated sequences of miRNAs within the above species were removed and the remaining 584 sequences were used as query sequences for BLAST search. *A. annua* EST and mRNA databases were obtained from the National Center for Biotechnology Information (NCBI) GenBank nucleotide databases (http://ftp.ncbi.nlm.nih.gov).

Availability of software

Comparative software BLAST-2.2.14 was used from NCBI GenBank. MFOLD 3.1 from website (http://www.bioinfo.rpi.edu/applications/mfold/rna/form1.cgi) was used online to analyze secondary structure of RNAs. MirEval (http://tagc.univ-mrs.fr/mireval) was used to predict miRNA precursors (*26*). BLASTx from NCBI (http://www.ncbi.nlm.nih.gov) was used to analyze potential targets of miRNAs.

Prediction of miRNAs

Procedure for searching potential miRNAs in *A. annua* is shown in **Figure 2**. We used the method described by Zhang *et al* (*53*) with some modifications. Briefly, the previously known miRNAs in *A. thaliana* and *O. sativa* were screened out, and the redundant sequences were removed. The remaining miRNA sequences were subjected to BLAST search for *A. annua* miRNA homologs against EST databases.

The mature sequences of all miRNAs from A*rabidopsis* and rice were subjected to BLASTn search in the *A. annua* EST databases using BLASTn 2.2.9. The adjusted BLASTn parameter settings were as follows: expect values were set at 1,000; low complexity was chosen as the sequence filter; the number of descriptions and alignments was raised to 1,000. The default word-match size between the query and database sequences was 7. RNA sequences were considered as miRNA candidates only if they fit the following criteria: (1) at least 18 nt length were adopted between the predicted mature miRNAs and (2) allowed to have 0-5 nt mismatches in sequence with all previously known plant mature miRNAs (*53*). The ESTs that closely match the previously known plant mature miRNAs were included in the set of miRNA candidates and used for additional characterization based on the following criteria: (1) the entire EST sequence was selected to predict the secondary structures and to screen for miRNA precursor sequences; (2) the selected ESTs were further compared with each other to eliminate redundancies; and (3) these sequences were subjected to evaluation for miRNA precursor prediction properties using mirEval software (*26*). These precursor sequences were used for BLASTx analysis for removing the protein-coding sequences and retaining only the non-protein-coding sequences.

Prediction of secondary structure

Precursor sequences of these potential miRNA homologs were subjected to hairpin structure predictions using the Zuker folding algorithm with Mfold-3.1. The following parameters were used in predicting the secondary structures: (1) linear RNA sequence; (2) folding temperatures fixed at 37ºC; ionic conditions of 1 M NaCl without divalent ions; (3) percent suboptimality number of 5; (4) maximum interior/bulge loop size of 30; (5) the grid lines in energy dot plot turned on. All other parameters were set with default values. In brief, the following criteria were applied in designating the RNA sequence as an miRNA homolog as described by Wang *et al* (*54*): (1) the sequence could fold into an appropriate stem-loop hairpin secondary structure; (2) the small RNA sits in one arm of the hairpin structure; (3) no more than 6 mismatches are between the predicted mature miRNA sequence and its opposite miRNA (miRNA*) sequence in the secondary structure; (4) no loop or break is in the miRNA or miRNA* sequences, and (5) predicted secondary structure has higher MFEI and negative MFE.

The MFEI was calculated using the following equation (*54*):

MEFI= [(MEF/length of the RNA sequence)×100] / (G+C)%

MFE denotes the negative folding free energies (ΔG).

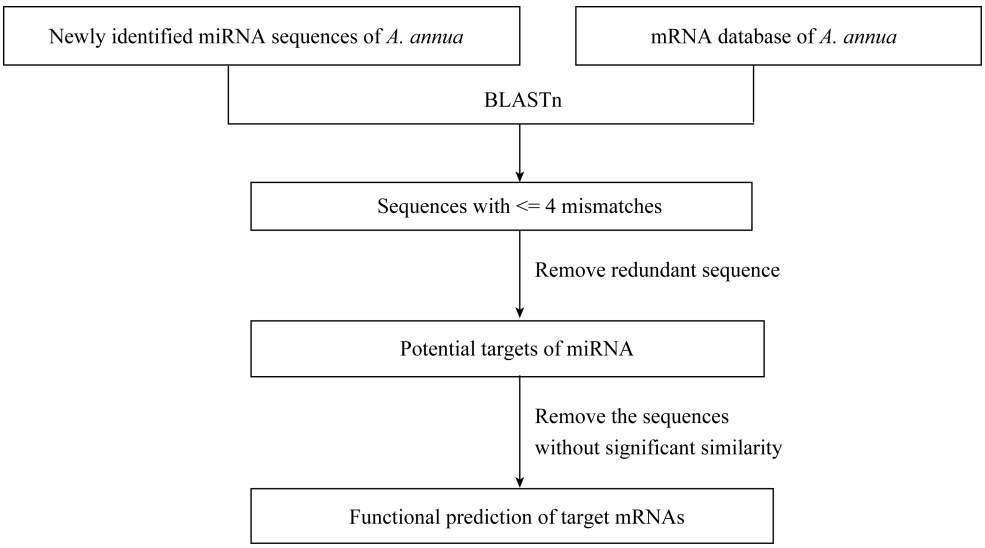

Figure 3 Schematic diagram for searching potential target mRNA of miRNAs by blasting mRNA database of *A. annua* with newly identified miRNA sequences.

Prediction of mRNA targets of miRNAs

Previous study has shown that most known plant miRNAs bind to the protein-coding region of their mRNA targets with perfect or nearly-perfect sequence complementarity, and degrade the target mRNA in a way similar to RNA interference (*10, 12*). This suggests a powerful approach to predict miRNA targets in plants by simply using homology search (**Figure 3**). In this study, we used homology search to predict miRNA targets in *A. annua.* The number of allowed mismatches at complementary sites between miRNA sequences and potential mRNA targets was no more than 4 and no gaps were allowed at the complementary sites.

Acknowledgements

AP and RKM thank Dr. Mrutyunjay Suar, Director of School of Biotechnology in KIIT University, for his encouragement and support during the course of study.

Authors' contributions

RKM conceived the project. AP and RKM collected the data and conducted the computational analysis. NB and PKN supervised the work. AP and RKM interpreted the data and RKM prepared the manuscript. All authors read and approved the final manuscript.

Competing interests

The authors have declared that no competing interests exist.

References

1 W.H.O. 2010. *World Malaria Report*. WHO Press, World Health Organization, Geneva, Switzerland.
2 Committee on the Economics of Antimalarial Drugs. 2004. Antimalaria drug and drug resistance. In *Saving Lives, Buying Time: Economics of Malaria Drugs in an Age of Resistance* (eds. Arrow, K.J., *et al.*), pp. 252-300. National Academies Press, Washington D.C., USA.
3 Klayman, D.L. 1985. Qinghaosu (artemisinin): an anti-malarial drug from China. *Science* 228: 1049-1055.
4 Abdin, M.Z., *et al*. 2003. Artemisinin, a novel antimalarial drug: biochemical and molecular approaches for enhanced production. *Planta Med*. 69: 289-299.
5 Weathers, P.J., *et al*. 2006. Artemisinin: the biosynthetic pathway and its regulation in *Artemisia annua*, a terpenoid-rich species. *In Vitro Cell. Dev. Bio. Plant* 42: 309-317.
6 Ro, D.K., *et al*. 2006. Production of the antimalarial drug precursor artemisinic acid in engineered yeast. *Nature* 440: 940-943.

7 Zhang, L., *et al*. 2009. Development of transgenic *Artemisia annua* (Chinese wormwood) plants with an enhanced content of artemisinin, an effective anti-malarial drug, by hairpin-RNA-mediated gene silencing. *Biotechnol. Appl. Biochem.* 52: 199-207.

8 Olofsson, L., *et al*. 2011. Relative expression of genes of terpene metabolism in different tissues of *Artemisia annua* L. *BMC Plant Biol*. 11:45

9 Lin, X., *et al.* 2011. Enhancement of artemisinin content in tetraploid *Artemisia annua* plants by modulating the expression of genes in artemisinin biosynthetic pathway. *Biotechnol. Appl. Biochem.* 58: 50-57.

10 Bartel, D.P. 2004. MicroRNAs: genomics, biogenesis, mechanism, and function. *Cell* 116: 281-297.

11 Aukerman, M.J. and Sakai, H. 2003. Regulation of flowering time and floral organ identity by a microRNAs and its APETALA2-like target genes. *Plant Cell* 15: 2730-2741

12 Chen, X. 2004. A microRNA as a translational repressor of APETALA2 in Arabidopsis flower development. *Science* 303: 2022-2025.

13 Schwab, R., *et al.* 2005. Specific effects of microRNAs on the plant transcriptome. *Dev. Cell* 8: 517-527.

14 Allen, E., *et al*. 2005. MicroRNA-directed phasing during trans-acting siRNA biogenesis in plants. *Cell* 121: 207-221.

15 Mallory, A.C., *et al*. 2005. MicroRNA-directed regulation of Arabidopsis AUXIN RESPONSE FACTOR17 is essential for proper development and modulates expression of early auxin response genes. *Plant Cell* 17: 1360-1375.

16 Juarez, M.T., *et al*. 2004. MicroRNA-mediated repression of rolled leaf1 specifies maize leaf polarity. *Nature* 428: 84-88.

17 Kasschau, K.D., *et al*. 2003. P1/HC-Pro, a viral suppressor of RNA silencing, interferes with Arabidopsis development and miRNA function. *Dev. Cell* 4: 205-217.

18 Robert-Seilaniantz, A., *et al.* 2009. A biotic or abiotic stress? In *Abiotic Stress Adaptation in Plants, Physiological, Molecular and Genomic Foundation* (eds. Pareek, A., *et al.*), pp. 113-116. Springer, Dordrecht, Netherlands.

19 Xie, F.L., *et al*. 2007. Computational identification of novel microRNAs and targets in *Brassica napus*. *FEBS Letters*. 581: 1464-1474.

20 Zhang, B.H., *et al*. 2005. Identification and characterization of new plant microRNAs using EST analysis. *Cell Res*. 15: 336-360.

21 Zhang, B.H., *et al*. 2006. Evidence that miRNAs are different from other RNAs. *Cell Mol. Life Sci.* 63: 246-254.

22 Jones-Rhoades, M.W. and Bartel, D.P. 2004. Computational identification of plant microRNAs and their targets, including a stress-induced miRNA. *Mol. Cell* 14: 787-799.

23 Adams, M.D, *et al*. 1991. Complementary DNA sequencing: expressed sequence tags and human genome project. *Science* 252: 1651-1656.

24 Wang, X.J., *et al*. 2004. Prediction and identification of *Arabidopsis thaliana* microRNAs and their mRNA targets. *Genome Biol.* 5: R65.

25 Li, Y., *et al*. 2005. Computational identification of novel family members of microRNA genes in *Arabidopsis thaliana* and *Oryza sativa*. *Acta Biochim. Biophys. Sin.* (Shanghai) 37: 75-87.

26 Ritchie, W., *et al*. 2008. Mireval: a web tool for simple micro-RNA prediction in genome sequences. *Bioinformatics* 24: 1394-1396.

27 Zhang, B., *et al*. 2006. Identification of 188 conserved maize microRNAs and their targets. *FEBS Lett*. 580: 3753-3762.

28 Zhang, B., *et al.* 2006. Conservation and divergence of plant microRNAs genes. *Plant J.* 46: 243-59.

29 Prabu, G.R. and Mandal, A.K.A. 2010. Computational identification of miRNAs and their target genes from expressed sequence tags of tea (*Camellia sinensis*). *Genomics Proteomics Bioinformatics* 8: 113-121.

30 Yin, Z., *et al*. 2008. Identification of conserved microRNAs and their target genes in tomato (*Lycopersicon esculentum*). *Gene* 414: 60-66.

31 Zhang, B.H., *et al.* 2007. Identification of cotton miRNA and their targets. *Gene* 397: 26-37.

32 Frazier, T.P., *et al*. 2011. Salt and drought stresses induce the aberrant expression of microRNA genes in tobacco. *Mol. Biotechnol*. doi:10.1007/s12033-011-9387-5.

33 Zhang, B.H., *et al.* 2008. Identification of soybean microRNAs and their targets. *Planta* 229: 161-182.

34 Kwak, P.B., *et al*. 2009. Enrichment of a set of microRNAs during the cotton fiber development. *BMC Genomics* 10: 457.

35 Griffiths-Jones, S., *et al*. 2008. miRBase: tools for microRNA genomics. *Nucleic Acids Res.* 36: D154-D158.

36 Monavar Feshani, A., *et al*. 2011. Identification and validation of Asteraceae miRNAs by the expressed sequence tag analysis. *Gene* doi:10.1016/j.gene.2011.11.024.

37 Pérez-Quintero, A.L., *et al.* 2011. Mining of miRNAs and potential targets from gene oriented clusters of transcripts sequences of the anti-malarial plant, *Artemisia annua*. *Biotechnol. Lett.* DOI 10.1007/s10529-011-0808-0.

38 Zhang, B.H., *et al.* 2006. Plant microRNAs: a small regulatory molecule with big impact. *Dev. Biol*. 289: 3-16.

39 Banyai, W., *et al*. 2010. Overexpression of farnesyl pyrophosphate synthase (FPS) gene affected artemisinin content and growth of *Artemisia annua* L. *Plant Cell Tissue Organ Cult.* 103: 255-265.

40 Newman, J.D. and Chappell, J. 1997. Isoprenoid biosynthesis in plants: carbon partitioning within the cytoplasmic pathway. *Crit. Rev. Biochem. Mol. Biol*. 34: 95-106.

41 Mercke, P., *et al*. 2000. Molecular cloning, expression, and characterization of amorpha-4,11-diene synthase, a

key enzyme of artemisinin biosynthesis in *Artemisia annua* L. *Arch. Biochem. Biophys.* 381: 173-180.

42 Alam, P. and Abdin, M.Z. 2011. Over-expression of HMG-CoA reductase and amorpha-4,11-diene synthase genes in *Artemisia annua* L. and its influence on artemisinin content. *Plant Cell Rep.* 30: 1919-1928.

43 Mercke, P., *et al*. 1999. Cloning, expression and characterization of epi-cedrol synthase, a sesquiterpene cyclase from *Artemisia annua* L. *Arch. Biochem. Biophys.* 369: 213-222.

44 Teoh, K.H., *et al*. 2006. *Artemisia annua* L. (Asteraceae) trichome-specific cDNAs reveal CYP71AV1, a cytochrome P450 with a key role in the biosynthesis of the antimalarial sesquiterpene lactone artemisinin. *FEBS Lett.* 580: 1411-1416.

45 Klucher, K.M., *et al*. 1996. The AINTEGUMENTA gene of Arabidopsis required for ovule and female gametophyte development is related to the floral homeotic gene APETALA2. *Plant Cell* 8: 137-153.

46 Elliott, R.C., *et al*. 1996. AINTEGUMENTA, an APETALA2-like gene of *Arabidopsis* with pleiotropic roles in ovule development and floral organ growth. *Plant Cell* 8: 155-68.

47 Singh, A., *et al.* 1988. Evaluation of *Artemisia annua* strains for higher artemisinin production. *Planta Med.* 54: 475-476.

48 Charles, D.J., *et al*. 1990. Germplasm variation in artemisinin content of *Artemisia annua* using an alternative method of artemisinin analysis from crude plant extracts. *J. Nat. Prod*. 53: 157-160.

49 Baraldi, R., *et al*. 2008. Distribution of artemisinin and bioactive flavonoids from *Artemisia annua* L. during plant growth. *Biochem. Syst. Ecol*. 36: 340-348.

50 Mannan, A., *et al*. 2011. Effects of vegetative and flowering stages on the biosynthesis of artemisinin in Artemisia species. *Arch. Pharm. Res.* 34: 1657-61.

51 Wang, Y., *et al*. 2011. The anti-malarial artemisinin inhibits pro-inflammatory cytokines via the NF-κB canonical signaling pathway in PMA-induced THP-1 monocytes. *Int. J. Mol. Med*. 27: 233-241.

52 Griffiths-Jones, S., *et al*. 2006. miRBase: microRNA sequences, targets and gene nomenclature. *Nucleic Acids Res*. 34: D140-D144.

53 Zhang, B., *et al*. 2007. Identification of cotton microRNAs and their targets. *Gene* 397: 26-37.

54 Wang, L., *et al*. 2011. Identification and characterization of maize microRNAs involved in the very early stage of seed germination. *BMC Genomics* 12: 154.

Supplementary Material

Figure S1

DOI: 10.1016/S1672-0229(11)60023-5